Sediment supply controls on sequence stratigraphy

Master thesis in petroleum geology/sedimentology

Kristian Smith-Hella

University of Bergen,

Department of Earth Science,

May 2012

Abstract:

A three-dimensional numerical model of deltaic deposition is used to study the influence of sediment supply changes on delta development. Sediment supply will have a cyclic variation under conditions of constant linear sea level rise and a combined cyclic sediment supply at cyclic relative sea-level.

Results illustrate the differences in 3D form of delta, cross-section stratal geometry, and delta evolution during cycles of sediment supply change.
During initial increase in sediment supply, stratal geometry is dominated by the progradational to aggraditional with progressively steepening of the break point trajectory. During decrease of sediment supply, stratal geometry is controlled by amount of sediment volume supplied. Low sediment supply lead to a stratal geometry change from progradational to aggraditional to aggraditional at a much earlier stage than deltas with high sediment supply. As a result, there is a delay on onset of aggradation is associate with an increase in sediment supply volume.

The delta evolution during combine sediment supply under condition of a sinusoidal sea-level cycle form incised channels with varying head ward lobes during sea level fall. At sea level rise, sediment supply fills the relict topography around the lobes, forming an apron. The delta morphology and internal geometry are strongly controlled by changes in sea-level, but variation in sediment affect strike variation, shoreline shifts and basinward expansion.

Acknowledgements

This thesis has been part of my master's degree in geology at the University of Bergen. I would like to express appreciation to my supervisor, Prof. Rob Gawthorpe which I have had many good and instructive discussions with in his office.

I would also like to thank my co-supervisor Dr. Emma Finch who has developed the 3D evolution model used in the thesis and introduced me to how I used the modeling program.

I am also very thankful for my wife, who has shown great understanding while I wrote this thesis, and has been an important support along the way.

Kristian Smith-Hella

Bergen, 2012

Table of Contents

Table of Figures

Tables

Chapter one – Introduction

1.1 Rationale

This thesis presents a sedimentological interpretation by using a three-dimensional numerical model of deltaic deposition to investigate the influence of sediment supply changes on delta development and sequence variability. In sequence stratigraphy, it is emphasized that both eustatic and tectonically controlled regional changes of sea level is the dominant control on sequence stratigraphy. The emphasis on changes in sea-level is despite general acknowledgement that sediment supply is also a fundamental control on facies stacking patterns and shoreline migration. For example, different systems tracts can be coeval along different parts of basin margins and key stratal surfaces defining and subdividing depositional sequences may be diachronous or absent (e.g., Posamentier and Allen 1993; Schlager 1993; Wehr 1993; Gawthorpe et al. 1994; Martinsen and Helland-Hansen 1995; Church and Gawthorpe 1997; Gawthorpe et. al 1997; Ritchie et al. 2004).

If we consider different situations in which sediment supply is either absent, highly variable or very high, it is not hard to think that the development of the systems tracts and sequences will have various appearances. If there is no sediment supply, there would be no deposition of new sediment, regardless of what relative sea-level is doing. Whether the relative sea-level rises or fall, the previous depositional surface will be eroded either by waves or subaerial erosion. This means that only the eroded products being deposited, a condensed sequence developed or simply an unconformity surface.

If sediment supply is very high, accommodation space will quickly be filled. This can result in too much sediment entering the basin, and aggradation and retrogradation could not occur.

In general, would the rate of sediment supply decrease during a relative sea-level rise, because flooding of the land reduces the potential for erosion closed to the shoreline. With a relative sea-level fall, the shoreline is more exposed to erosion and usually leads to an increase in sediment supply (A.Coe et al, 2005).

1.2 Aims and objective

The main aim for this thesis was to investigate role of sediment supply is controlling evolution of deltaic depositional system using 3D numerical model of sediment transport, deposition and erosion based on Ritchie et al. (1999). The study addresses two specific styles/interactions of sediment supply with relative sea level:

- Cyclic variation in sediment supply and constant relative sea-level rise
- Combined cyclic sediment supply at cyclic relative sea-level

The study focuses on how sediment supply impact on the following aspects of delta stratigraphy:

i) Stratal geometries
ii) 3D form of delta
iii) Break-point (topset-foreset transition) trajectory of sediment between topsets and foresets
iv) Development of incised channels and associated delta lobes

1.3 Approach and methodology

The project will utilize existing numerical models of deltaic deposition (e.g. Hardy and Gawthorpe 2002; Ritchie et al 2004). Models are using a simple system comprising a single drainage outlet supplying sediment with various rates to a ramp-like basin margin subject to sinusoidal sea-level cycles of different amplitude. This approach will allow the parameters controlling sediment supply to be isolated and changed, and the stratigraphic response to be documented quantitatively.

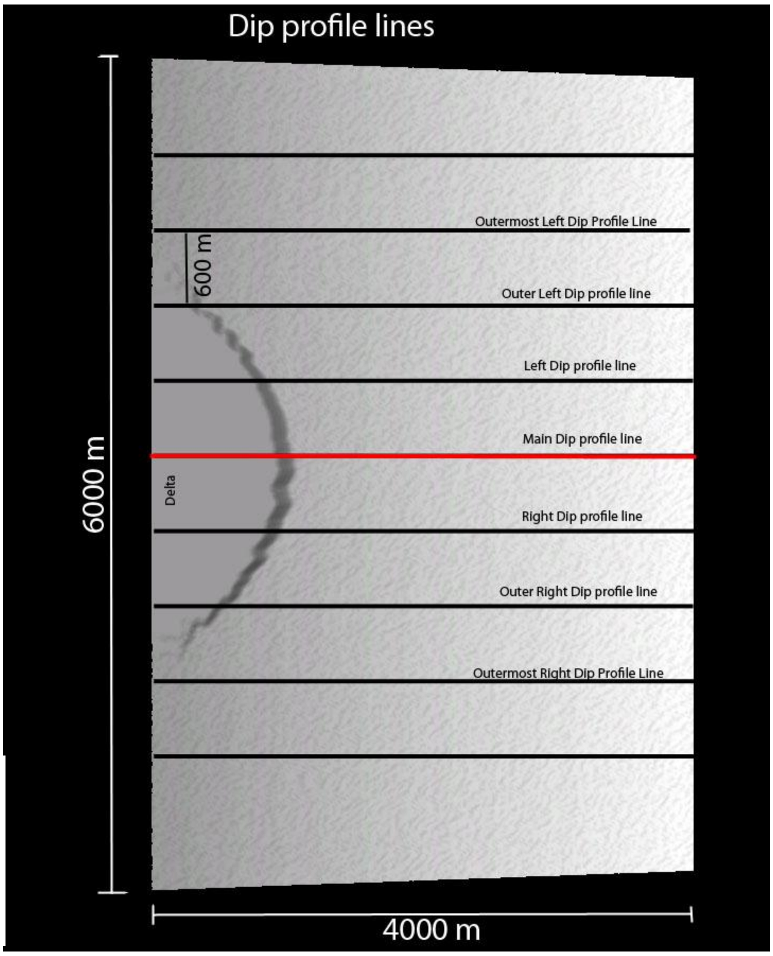

Fig. 1: Overview of the model program's output of dip lines across a delta. Red marked line is the main dip profile line, which will be used mostly during the study.

Initial experiments will examine how the amplitude and the rate of change of sediment supply affect the depositional environment sequence architecture. The following experiments (Chapter Four) will be focused on examining the impact of combinations in sediment supply and Chapter Five will focus on sinusoidal sea-level curve with different phase shifts in sediment supply.

It is used three-dimensional modeling software because it makes it easier to investigate than if one should studying rocks or used an analogue flume tank. The three-dimensional modeling software would provide figures showing the morphology and cross sections of the delta. View of the surface morphology is shown from up-dip angle and this will represent the direction in the description of the delta (right/left side). Output for cross sections provides ten dip lines and ten strike lines every 25 kyr. Dip lines are 600 m apart from each other, while the strike lines have a spacing of 200 m.

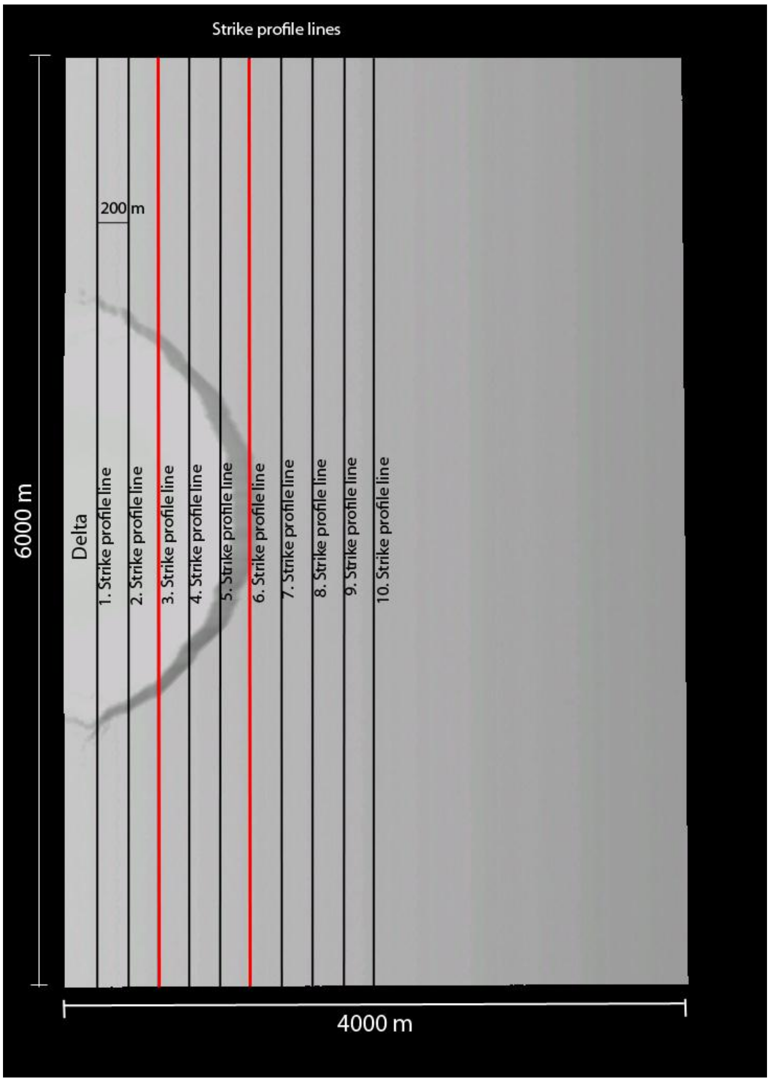

Fig. 2: Overview of the model program's output of strike lines across a delta. Red marked lines are the third and sixth strike profile line, which will be used during the experiments in Chapter Five.

Dip and strike lines provide data every 2500 years (marked as gray top and foresets) and a colored data line every 12.5 kyr (see figure 3 as an example of data lines in a dip profile). In chapter four, all of the figures of the cross section of the deltas display the mid cross section line of the delta (called the main dip profile line) going from proximal to distal parts of deltas. The main dip line profile is marked red in Fig. 1. In Appendix III, the left- and right dip profile line for models in chapter four is included, to compare the main dip line profile line, in order to see if the main dip line profile is representative of the deltas stratal geometry. In the experiments in chapter five, all of the figures would display main the dip profile line also, but since the experiments were more extensive, the right and left dip line profile was also displayed. Due to the comprehensiveness of the experiments in chapter five, cross section of the deltas left to right side were included. Also strike lines are represented in the chapter five, one is 600 m and the other 1200 m from the drainage outlet (sediment source). They are represented as the third and sixth strike line and are marked red in Fig. 2. At the dip lines that have been carried out measurements (Fig. 3). There was measured thickness of foresets (Fig. 3a), where the foresets were too thin to make accurate measurements, and it was therefore measured the average thickness. This was done by measuring with a ruler from one color to the next (12.5 kyr) and dividing it by five (since the dip profile provides four and a gray-colored line, a total of five foresets). Basinward expansion (Fig. 3b) was measure by ruler, from the start of deltaic deposits (sediment source) to the topset-foreset transition. Maximum thickness was also measure by a ruler, from the topset-foreset transition and down to the seabed (Fig. 3c). The topsets height (Fig. 3d) was measured from one color line to the next (12.5 kyr), while foresets height (Fig. 3e) was an average measurement from the foreset-topset transition in the middle (grey colored) foreset and down to the seabed.

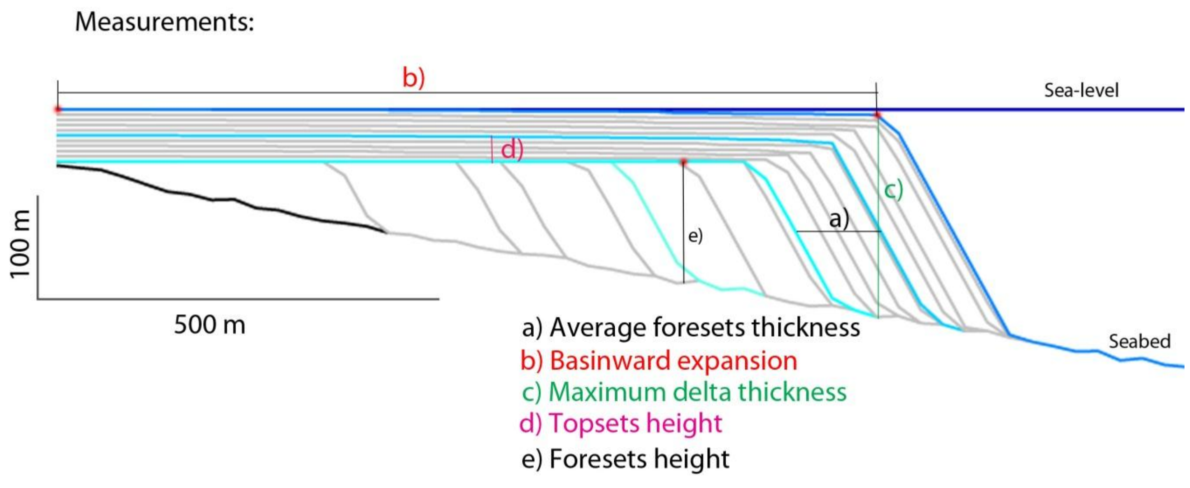

Fig. 3: Overview of how the measurements are carried out during this thesis. These measurements were made with a ruler.

Differences between the models									
Models:	Reference model	Low sediment supply	High sediment supply	Double Frequency	Highest Frequency	High sediment supply with double frequency	High sediment supply with highest frequency	Low sediment supply with double frequency	Low sediment supply with highest frequency
Time:									
Total run time (kyr)	150								
Sediment supply:									
Values (m3/yr)	8775	4388	17552			17552	17552	4388	4388
Amplitude (m3/yr)	2325	1163	4648			4648	4648	1163	1163
Wavelength (kyr) (Frequency)	50			25	12,5	25	12,5	25	12,5
Start time (yrs)	25 000				18 740		18740		18740
Sea-level:									
Amplitude (m/kyr)	7,5								
Start time (kyr)	25								

Green background = same value as constant sediment supply model

Table. 1: Overview of the parameters that were changed in the models compared to the reference model during the experiments in chapter four

Differences between the models			
Models:	Constant sediment supply	In-phase sediment supply	Out-phase sediment supply
Time:			
Total run time (kyr)	200		
Sediment supply:			
Values (m3/yr)	8775		
Amplitude (m3/yr)		2325	-2325
Wavelength (kyr)		50	50
Start time (yrs)	0	25	25
Sea-level:			
Amplitude (m)	25		
Start time (kyr)	25		
Wavelength (kyr)	50		

Green background = same value as constant sediment supply model
Black background = does not have this parameter

Table. 2: Overview of the parameters that were changed in the models compared to the constant sediment supply model during the experiments in chapter five.

During the study in chapter four, it was created nine different models with different parameters. The parameter was changed in each model and Table 1 shows an overview of what was changed relative to the reference model. The green color indicates that the parameter is the same as in the reference model. The parameter, value in sediment supply, provide the initial value of the sediment volume supplied to the model, while the amplitude of the sediment supply represents fluctuations (maximum / minimum) in sediment supply. Is it a positive value, then start sediments with an increase. Negative and sediment supply will start to decrease.

In the study in chapter five, it was made three different models in order to study the interplay between sediment supply and sea level changes. Table 2 shows an overview of which parameters were changed compared to the constant sediment supply model. Table 2 is constructed as Table 1, but in addition so has Table. 2, black bars that indicates that the parameter is not included in the model. This applies for the constant sediment supply model that has no amplitude and frequency as the sediment supply is constant.

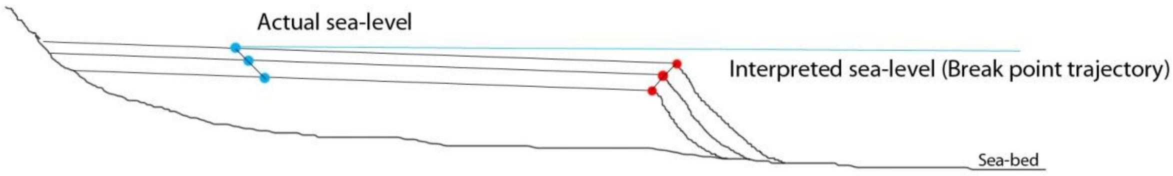

Fig. 4: Sketch that illustrates the difference between break-point trajectory and shoreline trajectory. In many cases break-point trajectory would be the shoreline, while in some cases where the delta is flooded, the actual shoreline will be located further landward.

During this thesis the topset-foreset transition would be referred to as break-point trajectory. This is because the deltas will be flooded and thus would shoreline trajectory have been further landward (Fig. 4). In many cases the break-point trajectory is the shoreline, but in some cases as Fig. 4 illustrate, the break-point trajectory would not be the shoreline. As the modification of the delta front by tide and wave processes is not included in the model, it would not have erosional truncation, if deltas had been seen by seismic and therefore would break-point trajectory been interpreted as the shoreline during this thesis.

1.4 Thesis overview

The first chapter in this thesis will provide a brief introduction of the background for the thesis and discusses the methods used during this study. Chapter Two will provide a basic introduction to sequence stratigraphy and terminology. Chapter Three will present a detailed description of the model's software that was used during the simulation and also provide a description of the different parameters used. Chapter Four describes and shows sequence stratigraphic responses to nine different scenarios of sediment supply under conditions of a constant linear sea-level rise. Chapter Five will give a description of the sequence stratigraphic response to three different scenarios of sediment supply in relation to a sinusoidal sea-level cycle. Chapter Six will provide a summary and conclude the study.

Chapter Two - Sequence stratigraphic review

Sequence stratigraphy was introduced in late 1970's and has been continuously developed to the present day (e.g. Mitchum, 1977; Posamentier et al.1988; Posamentier and Vail, 1988; Van Wagoner, 1990; Van Wagoner, 1995; Posamentier and Allen, 1999; Catuneanu, 2006). Concepts are used to identify changes in facies and the identification of key surfaces and facies stacking patterns within a chronostratigraphic framework (Catuneanu et al.2009).

"Sequence stratigraphy (Posamentier et al. 1988; Van Wagoner, 1995) : The study of rock relations within a time-stratigraphic framework of repetitive, genetically related strata bounded by surfaces of erosion or nondeposition, or their correlative conformities"

"Sequence stratigraphy (Posamentier and Allen, 1999) : the analysis of cyclic sedimentation patterns that are present In stratigraphic successions, as they develop in response to variations in sediment supply and space available for sediment to accumulate"

"Sequence stratigraphy(Catuneanu, 2006): the analysis of the sedimentary response to changes in sea-level, and the depositional trends that emerge from the interplay of accommodation and sedimentation"

Fig. 5: Several definitions of sequence stratigraphy (Figure derived from Catuneanu et al. 2009)

The tool has improved the understanding of facies analysis, identification and historical sea-level cycles, deposition and climate. An underlying principle in sequence stratigraphy is to explore where Walther's law is violated. Walther's Law states that "Facies adjacent to one another in a continuous vertical sequence also accumulated adjacent to one another laterally". Intervals where Walther's law works are in genetically-related vertical successions, whereas in key stratal surfaces where genetic relationships break down, the Walther's law does not work.

There have been many attempts to define sequence stratigraphy. Common to all definitions of sequence stratigraphy, is emphasis on the cyclicity, temporal framework, genetically related strata and the interplay of accommodation and sedimentation (Fig. 5) (Catuneanu et al. 2009).

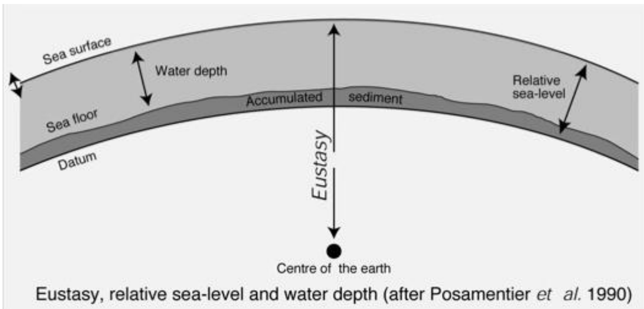

Fig. 6: Overview of different terms of a change in elevation in sea-level (Posamentier et al.1990).

Depositional sequence is more or less controlled by sea-level change, subsidence, uplift, climate, sediment supply, basin physiography and compaction (Catuneanu et al.2009). These main controls will have a dynamic interplay that influences bounding surfaces, 3-D form and internal character of depositional sequences. The following is a brief explanation of the different controls of sequence stratigraphy. Eustatic sea-level is change in sea-level relative to the stationary datum at the center of the earth (Fig. 6). There are two main components to eustatic sea-level change, these component have different rate and magnitude. The components are glacial (10s m/kyr) and tectonic (0.2m/ 100 000 yr). Subsidence and uplift rates vary depending on basin drive mechanisms as stretching and faulting of crust, cooling, and flexure. Compaction of previously deposited sediments leads to addition of accommodation space. Basin physiography has two main types of basin margin, shelf-break and ramp margins. Difference is that the shelf-break margins have abrupt change from gently dipping shelf (<0.5°) to steeper slope (3-6°). Ramp margins have uniform low angle dip (<1°).

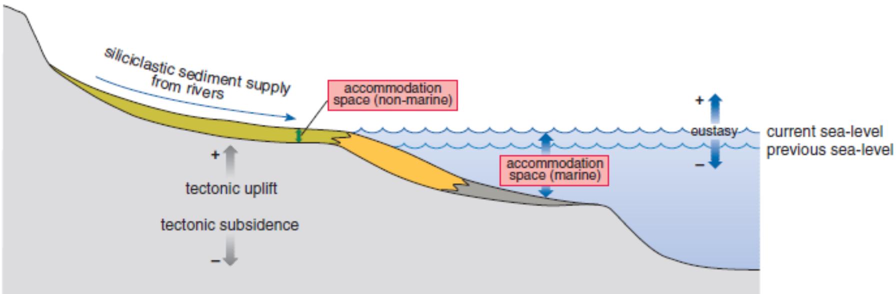

Fig. 7: Accommodation space is the space available in a basin so that sediment will be deposited. A rise in relative sea level (sea level relative to the sea floor) creates marine accommodation, while a fall in relative sea level destroys accommodation space for the sediment. (From A.Coe et al 2005)

The climatic conditions control the supply of sediment. The degree of precipitation affects the type and abundance of vegetation and, therefore, both the weathering and erosion rate of the hinterland and transportation of resultant products. The greater range in temperature either side of 0°C, the greater the degree of physical weathering because the extremes of temperature lead to frost shattering. Several

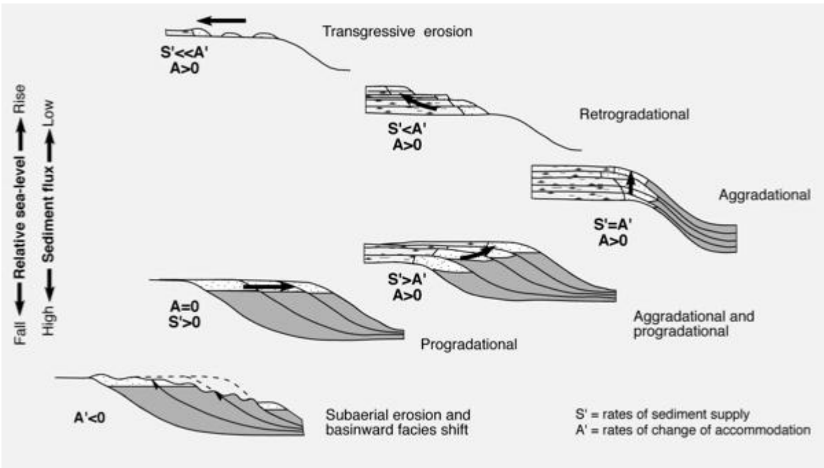

Fig. 8: Stratal geometries and stacking patterns as a result of interaction of relative sea-level and sediment supply (Galloway 1999; redrawn by R. Gawthorpe).

studies have found that during periods of climate change, more sediment tends to be produced than during stable climatic periods (A.Coe et al. 2005).

Over geologic time scales, relative sea-level changes are controlled primarily by allogenic mechanisms, including tectonism and sea-level change (eustasy) (Catuneanu et al. 2009). The area between datum (see Fig. 6) and sea surface is called accommodation space (Fig. 7). The amount of space that is available for sediment to fill up to the relative sea-level defines the concept of accommodation (Jervey, 1988; Catuneanu et al. 2009). A rise in relative sea-level creates accommodation space, whereas a fall in relative sea-level takes space away. Variation in rate of accommodation space combined with variations in the rate of sediment supply control the depositional architecture. For a given rate in relative sea-level change, depending on sediment supply, a shoreline may remain stationary or undergo regression or transgression. This interaction between accommodation and sediment supply leads to a number of predictable geometries (Fig. 8). Each stratal stacking pattern defines a particular genetic type of deposit (i.e. transgression, normal regression and force regression) with a distinct geometry and facies preservation style (Hunt and Tucker, 1992; Posamentier and Morris, 2000; Catuneanu et al. 2009). Genetic types of deposits are defined as a function of the ratio between the rates of relative sea –level changes, and the sedimentation rates at the shoreline (Plint, 1988, Posamentier et al.1992, Catuneanu et al, 2002).

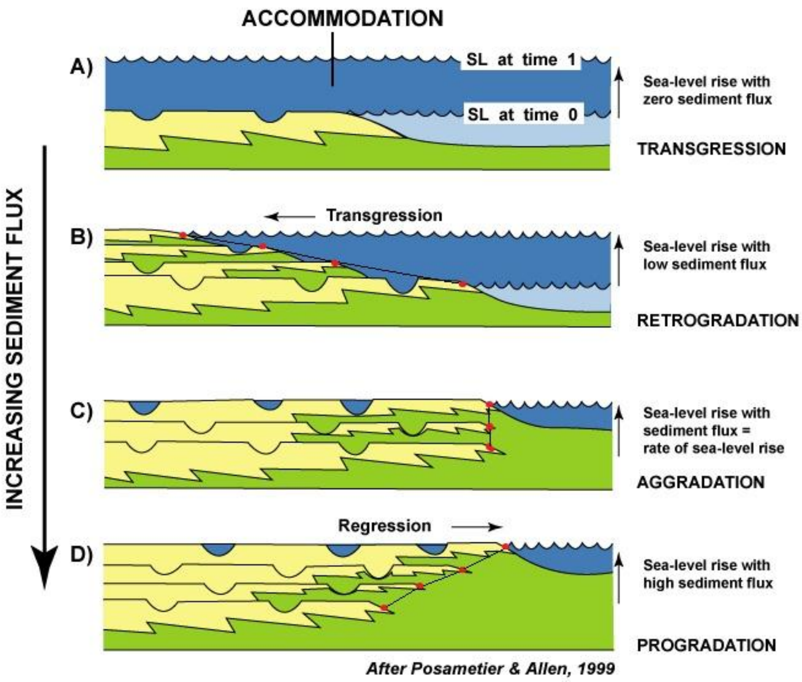

Fig. 9: Overview of the pattern of vertical stacking of parasequence sets with shoreline trajectories (marked with red bullet and black lines. After http://sepmstrata.org/terminology/coastaltraject.htm 2012

Transgression (landward migration) occur when the rate of increase in accommodation space outpace the rate of sediment supply at the shoreline which leads to the depositional trend is retrogradational. Usually by landward migration, retrogradation (i.e. facies shifting laterally landward) would likely occur with problems delivering sediments, because sediment is trapped in proximal area and there are no incision (A.Coe et al. 2005). This can lead to sediment starvation in distal areas.

In sequence stratigraphy, it is essential to distinguish between regression and forced regression. Both processes involve a decreasing accommodation space but with different mechanisms. A normal regression occurs when the amount of accommodation space gets consumed by the sediment supply. In this case, all the available accommodation space gets filled with sediments and the shoreline migrate basinward. Depositional trend in normal regression are progradation with aggradation.

Forced regression is where the relative sea-level is falling and the shoreline would move basinward (also drop down in the depositional profile) irrespective of the sediment supply. This leads to a deposition trend that is progradation with downstepping. These basinward and landward migration results that the facies belts also migrate and one can see it in terms of systematic stacking patterns and stratal geometry.

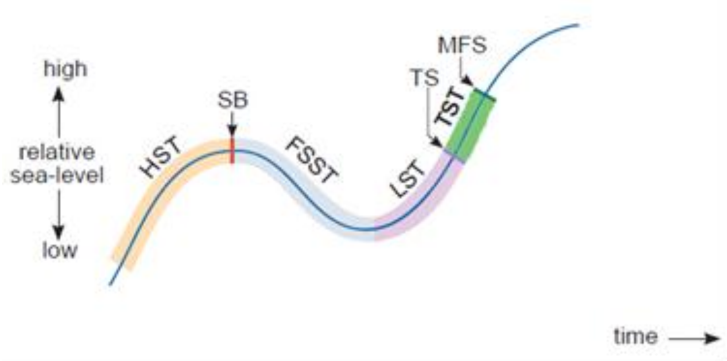

Fig. 10: An example of a relative sea-level cycle with foreshortenings like HST (represent highstand systems tract) and TS (represent transgressive surface) (A.Coe et al. 2005).

The study of the lateral and vertical migration is called trajectory analysis, which focuses on the paths and directions of migration. Usually break in slope at the shoreline or shelf edge used to measure the trajectory (In this thesis, the break of slope is used). Trajectory analysis is an aid in the determination of the depositional setting. A shoreline or shelf margin trajectory is the path taken by the shoreline or shallow shelf margin facies as they change position when a sedimentary basin fills (Helland-Hansen & Martinsen, 1996). The main controls for these trajectories are various rate of sediment accumulation, various change in accommodation space (eustatic sea-level change and tectonic activity) and basin physiography. These trajectories are the main event required for the pattern of vertical stacking of parasequence sets (Fig. 9) could be interpreted in terms of progradational, retrogradational and aggradational (defined by Van Wagoner, et al, 1990).

Stratal geometries can be used to determine key stratal surfaces and systems tracts, and also understand accommodation conditions at the time of deposition (Catuneanu et al. 2009). Systems tract represent a package of strata that have different genetic types of deposit that were deposited during specific phases of relative sea-level cycle (Fig. 10) (i.e. lowstand, highstand, forced regression, transgression, regression). The term systems tract was proposed by Brown and Fisher (1977), where their definition was “Systems tract: a linkage of contemporaneous depositional systems forming the subdivision of a sequence”. A sequence is composed of a succession of parasequence sets. Parasequence are building blocks of sequences. Each sequence represents one cycle of change in the balance between accommodation space and sediments (A.Coe et al. 2005). Every sequence is composed of up to four systems tracts each of which represents a specific part in the cyclic change in the balance between accommodation space and sediment supply. Different conditions may result in one or more of the systems tract not being developed and/or preserved (A.Coe et al. 2005). According to Van Wagoner et al (1987, 1990, 1995) can systems tract interpreted based on stratal geometry, facies stacking patterns, position within the sequence, and types of bounding surfaces.

Sequence stratigraphic surfaces are a result of the relative sea-level changes at the shoreline and the associated shoreline shifts (Catuneanu et al. 2002). A sequence boundary is an erosional or depositional surface that separates the relative sea-level cycles of deposition.

Here is a brief definition of surfaces of sequence stratigraphy:

- Transgressive surface: a surface that form due to a change in shoreline trajectory from lowstand normal regression to transgression. Characteristic of the transgressive surface is that it has the youngest marine clinoform, onlapped by transgressive strata, and it is possible to correlate surfaces in nonmarine and deep-water settings (Helland-Hansen and Martinsen, 1996).

- Maximum flooding surface: The change in shoreline trajectory from transgression to highstand normal regression is made up by this surface. Usually does it contain a downlap surface in shallow-water settings, where highstand coastlines prograde on top of transgressive condensed sections (Frazier, 1974; Posamentier et al, 1988; Van Wagoner et al. 1988; Galloway et al, 1989).

- Regressive surface of marine erosion: an erosional surface that has been formed under the relative sea-level by waves in regressive, wave-dominated lower shoreface to inner shelf settings. This surface is diachronous, its get younger the longer it comes basinward (Plint, 1988).

-Correlative conformitys: are stratigraphic surfaces that showing the change in stratal stacking patterns from highstand normal regression to forced regression. It is the oldest or youngest marine clinoform associated with offlap (Posamentier et al. 1988; Posamentier and Allen, 1999).

- Subaerial unconformity: an unconformity that forms over the relative sea-level by fluvial erosion or bypass, wind degradation or dissolution and kartification (Sloss et al. 1949, Catuneanu 2009). Subaerial unconformities can be formed through all or part of the relative sea-level fall during periods of transgression accompanied by coastal erosion (Lekie, 1994).

- Transgressive ravinement surfaces: erosional surfaces made by waves or tidal scouring during transgression in coastal to upper shoreface settings (Nummedal and Swift, 1987; Galloway et al. 2001b

The latter surfaces (Transgressive ravinement) will not have an impact on the models due to the modification of the delta front by tide and wave processes is not included in the model.

Chapter Three - Model Overview

The modeling properties is designed to characterize essential features of coarse-grained deltaic depositional system in order to provide a better understanding of influence by sediment supply on coarse-grained delta deposits over time intervals of 100 yrs to 150 kyr. The modeling approach does not try to simulate the detailed physics of every process involved in erosion, transport and deposition on a daily or monthly perspective. Rather, the model simulates the basic elements (of perspective of hundreds of years) of: i) transport of coarse sediment from a drainage basin discharge into a depositional basin, ii) deltaic deposition, and iii) fluvial incision along the sediment transport pathways.

The Earth's surface are in the models represented by a grid of cells, with the cell size, here 40 m by 40 m. The models are during temporal evolution updated for each time step (in this case every 20 years) and height of the cells is the result of erosional or depositional environment processes. To have the most stability on the erosional and deposition algorithms are used, the choice fell on 20 years of the time step chosen. In the next section, the key elements of the modeling approach will be presented.

It would use a random-walk/steepest-decent algorithm to simulate sediment supply from catchment area outlet to the depositional shoreline. The volume of sediment is transported from an input cell (catchment area outlet) and out to open water (a lake or marine basin). When the sediments come to the open water, it will be deposited where there is available accommodation space. In the model, the modification of delta front of the tidal and wave processes is not included.
A nonlinear three-dimensional diffusion equation is used in order to model downslope sediment movement (e.g., debris flow, slumping etc.) when delta foresets exceed a critical slope angle.

In the sequence stratigraphy, development of the incision valleys at sea level fall is an important aspect. There are several important factors that control fluvial incision (e.g. sea-level change, bedrock lithology, etc.) but mainly is slope change the most important factor for channel incision (e.g. Posamentier et al. 1992b; Schumm 1993; Wescott 1993; Leeder and Stewart 1996; Ritchie et al. 2004). Therefore, the channel incision in the models are built on a process that is dependent on local slope and erosion rate constant. The models do not account for the varying discharges along the transport pathways (channels). With this, the shoreline would receive sediments from the initial sediment supply and also from the eroded material collected along the transport path.

In the models, a sediment source located in the center of the proximal side where it provides varying amount of sediment in a basinward-dipping ramp with a slope of 2°. Sediment supply is based on a drainage area of 146 km^2 (see Appendix I), where the amount of sediment supplied to the models are based on Collier et al. (2000) data from the last glacial lowstand and the last interglacial highstand deposits from the Alkyonides Gulf, Greece (Appendix I). Since the drainage area of the reference model (Chapter 4.1) is half the size of drainage area at Alkyonides (280 km^2 for inter glacial and 305 km^2 for the glacial), the volume of sediment has also been halved to get a more realistic sediment supply to the model.

Colliers data state that during the Last Glacial lowstand then the sediment discharge rate of 22,200 m^3/yr, while the last inter glacial highstand was the sediment discharge rate of 12,900 m^3/yr. Divide these values by two, then glacial lowstand sediment supply to the models would be 11,100 m^3/yr, while inter-glacial highstand sediment supply would have a value at 6450 m^3/yr. Mean value of a highstand and lowstand would then be 8775 m^3/yr. As a result, the reference model value of sediment supply is 8775 m^3/yr with amplitude of ± 2325 m^3/yr to achieve maximum- and minimum sediment supply. The calculations have not taken into account for the possibility of different bedrock lithology.

There will be used the same frequency to sediment supply in the reference model, as Ritchie et al. (2004) used for sinusoidal sea-level cycle (50 kyr), but apply the variation over the experiment to investigate the impact frequency variations have on a deltaic depositional sequences. The sea-level curve that was used in Ritchie et.al (2004) paper cover a range of rates and magnitudes of sea-level variation likely to be experienced by natural systems (e.g., Miall 1997).

Cycles of sea-level change are regarded as the main control in sequence stratigraphy and the rate and magnitude of sea level changes have a strong influence on the timing of key stratal surfaces, such as maximum flooding surface, the magnitude of facies shift, and the geometry of incised valleys. Cycles of sea-level change will be absent during the first study (Chapter four), where sea-level is kept constant for the first 25000 years and then there would be a simple constant linear sea level rise of 7.5 m/ kyr. The result of the interplay between the cycles of sea level changes and variations in sediment supply will be presented in Chapter Five.

Chapter Four - Sequence stratigraphic response to sediment supply with a constant linear sea-level rise

4.1 Reference model, description

The deltaic of a reference model is described first to illustrate a response to a 50 kyr amplitude of a sinusoidal cycle of sediment supply change under conditions of constant linear sea level rise of 7.5 m/ kyr. First 25 kyr sea-level and sediment supply is kept constant (8775 m^3/yr). The results are presented in the form of 3D perspective views of surface morphology and cross section at selected time intervals during the development of the model. The reference model will act as a standard to the other models that will be presented in this experiment and therefore compared.

For the first 25 kyr, when sea level and sediment supply is constant, the delta builds basinward from the sediment source by 875 m and the thickness of the delta maximum is 137.4 m. In plan view, develops an arcuate delta front (Fig.11A). Under the conditions of constant sea level and sediment supply (0-25 kyr), all sediments get accumulate in the forsets since it is the only accommodation space available. Every foresets (marked with gray line in the dip section, Fig. 12) represents a time interval of 2500 years, where the thicknesses of the foresets are progressively decreasing basinward. The measurements of the foresets thickness will be an average (see Table 3). The first 12.5 kyr foreset is thus the thickest with its 78.6 m in average and a maximum height of 88.9 m

Thickness and height of foresets for the reference model

	Average foresets thickness (m)	Foresets height (m)	Topsets heigth (m)
12.5 kyr	78,6	88.9	0
25 kyr	36,8	127.8	0
37.5 kyr	22,40	150	15,6
50 kyr	13,2	177.8	21,1
62.5 kyr	6,60	205.6	20
75 kyr	7,90	227.8	18,9
87.5 kyr	2,60	244.4	17,8
100 kyr	N/A	263.3	17,8
112.5 kyr	N/A	277.8	20
125 kyr	2,60	305.6	22,2
137.5 kyr	3,40	322.2	21,1
150 kyr	3,70	350	21,1

N/A, unable to measure

Table. 3: Results from measuring the forsets average thickness, height of the foresets and topsets height in the main dip profile line of the reference model. *Note:* See approach and methodology for details of measurement.

(measured from the middle foresets to the sea-floor). At 25 kyr, the foresets get thinner as they are located further basinward and water depth increased. The average foreset thickness at 25 kyr is 36.8 m and a maximum foreset height from the bottom of the delta at 127.8 m.

From 25 kyr to 50 kyr, sediment supply is increased to its maximum of 11100 m^3/yr, while sea level has risen 18.75 m. Delta begins to develop topsets, and the thickness of foresets decreases. Delta is progradational to aggraditional with a break-point trajectory climbing steeply basinward (Fig. 12B), as the rate of sediment supply reaches its maximum at 50 kyr. The majority of the sediments have been deposited along the delta front (foresets), but significant amounts of sediment have also been deposited on the delta plain (topsets) (Fig. 11B, C). Between 25 -50 kyr, delta built basinward 164.5 m, while the maximum thickness increases by 54.9m (see Table 12).

Between 50 kyr and 100 kyr, sediment supply falls from 11100m^3/yr to its minimum at 6450 m^3/yr (at 100 kyr). During the initial phase of decreasing sediment supply from 50 kyr to 75 kyr, deposition still occurs as a continuous fringe along the delta front (Fig.11D, E). The delta continues its basinward-climbing break-point trajectory (Fig. 12C), as the sediment supply reaches its initial values of sediment supply at 75 kyr. The foresets continue to decrease in thickness, with the average thickness of foresets during this interval almost halved in size (Table.3). At the same period, sea level has a rise of 18.75 m and delta front has expanded basinward with 68.4 m, while the maximum thickness has increased by 44 m (Table. 12).

As the sediment supply continues to decrease from 75 kyr to 87.5 kyr, the break-point trajectory indicates that the delta change from being progradational to aggraditional to aggradational (Fig. 12D). From 87.5 kyr to 100 kyr sediment supply continue to decrease, which is associated with the break-point trajectory changing to a landward-climbing break-point trajectory at 87.5 kyr (backstepping; not representative in left or right dip profile line, see Appendix III), before the break-point trajectory gain an aggraditional pattern (Fig. 12D). At 100 kyr, delta has retreated 18.4 m since 75 kyr, due to the backstepping at 87.5 kyr. The thickness of delta increases to 38.4 m (Table. 12). Hardly any sediment accumulates in the foresets, which become too thin to measure. In contrast, sediment continues to accumulate in topsets (17.8 m per 12.5 kyr). This can also be seen in Figure 11G, showing that sediments are deposited mainly on the delta plain, with minor amounts of sediment deposited at the delta front.

Following sediment minimum at 100 kyr, sediment supply begin to increase, and continues to increase until 150 kyr. During the initial increase of sediment supply between 100 kyr and 125 kyr, the break-point trajectory climbs vertically in an aggraditional trajectory. Delta follows this pattern until 125 kyr (Fig. 12E), as a result, delta have not expanded further basinward, but increase its maximum thickness of 38.5 meters (Table.12). At 125 kyr, foresets acquire enough sediment so that the measurements can be made (Table. 3), but still the sediments have been deposited mainly on the delta plain (topsets), while delta front (foresets) has had minimal deposition between 100 - 125 kyr (Fig. 11H, I).

In the last 25 kyr of the model run (from 125 kyr to 150 kyr), sediment supply reaches its maximum. Delta has continued an aggradation break-point trajectory and deposition of sediment occurs throughout the delta and generates a continuous fringe of sediment accumulation along the delta front (Fig. 11J, K). The maximum thickness of delta has increased 43.95 m between 125 - 150 kyr and has throughout the model run gained a total of maximum thickness of 357.15 meters (Table. 12). The delta has expanded 2.6 m over the last 25 kyr, resulting that the delta has reached a basinward position at 150 kyr by 1092.1 m (Table. 12). The average thickness to foresets have increased slightly (by 1.1 m) over the past 25 kyr (Table. 3).

REFERENCE MODEL

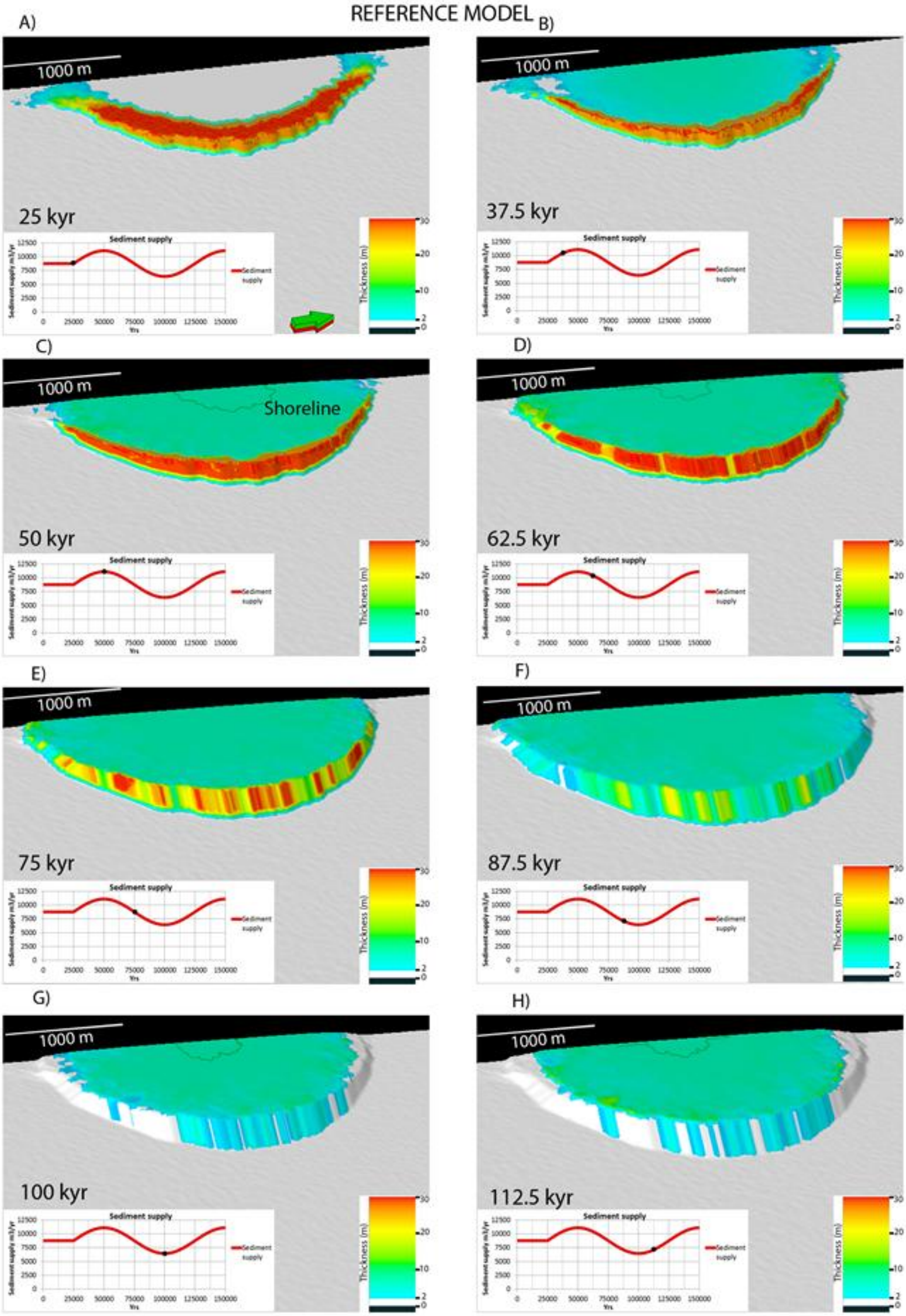

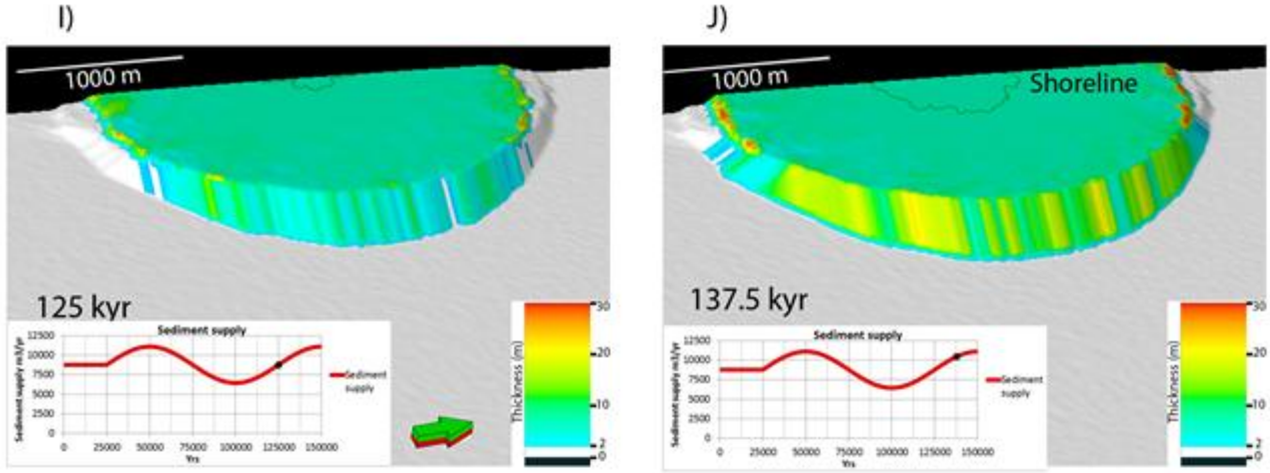

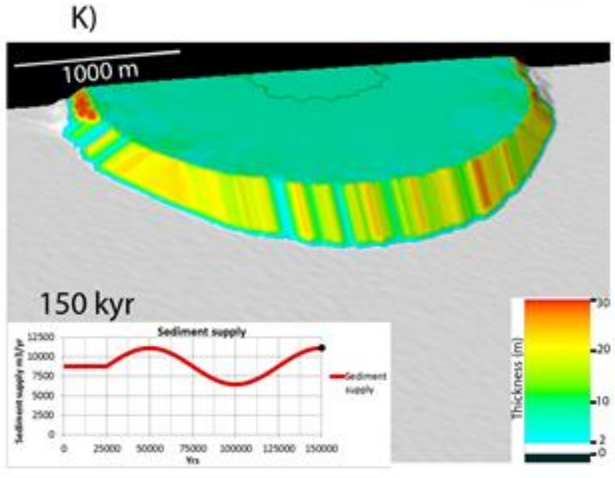

Fig. 11: Sequential evolution of the reference model at intervals of 12.5 kyr. Images show oblique view of the delta morphology and the isopach for previous 12.5 kyr. Note the shoreline (drawn) that shows that the delta is continuously drowned. Vertical exaggeration 2:1.

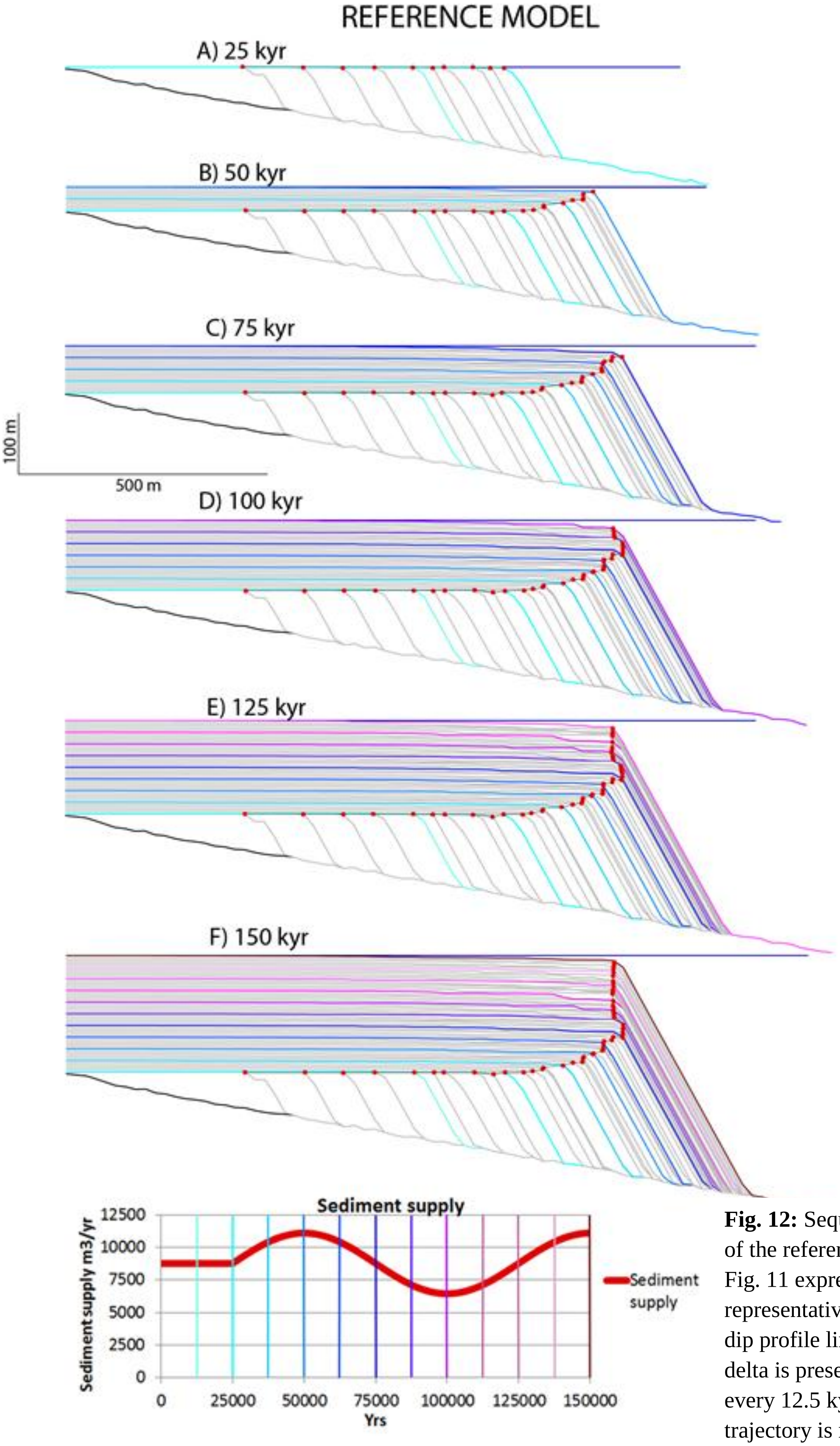

Fig. 12: Sequential development of the reference model shown in Fig. 11 expressed in a representative dip section (Main dip profile line). Evolution of the delta is presented with a color every 12.5 kyr. Break-point trajectory is marked in red.

4.2 Sequence stratigraphic response to different values in sediment supply

The interaction between accommodation development and the rate of sediment supply is recognized as an important control on facies patterns and the timing and magnitude of facies shifts associated with transgression and normal regression (e.g. Mitchum et al. 1977; Jervey 1988; Galloway 1989; Schlager 1993; Wehr 1993; Ritchie et al. 2004). To investigate the impact of different volume of sediment supply change on delta geometry and stratigraphic architecture, the different models runs with sediment supply with half (4388 m^3/yr) and double (17552 m^3/yr) sediment supply of the reference model. In both the high- and low sediment supply models, it would be the same linear sea-level rise, as well as the frequency for sediment supply; also all other parameters are the same as the reference model.

4.2.1 High sediment supply model and low sediment supply model, description

During the initial stage of the model run (0-25 kyr), both low- and high sediment supply models got constant sediment supply and sea-level. The deposition architecture at the delta are likewise as the reference model, with deposition occurs as a continuous fringe of sediment accumulation along delta fronts and no topsets development (Fig. 13A; Fig. 14A). Although the shape and deposition pattern on the delta is similar, the size differs in detail. During the first 25 kyr, the high sediment supply model expanded basinward from the sediment source by 1131.6 m, while low sediment supply model has expanded basinward by 615.8 meters (Table. 12). The high sediment supply model have an average foreset thickness of 50 m, while low sediment supply model has an average foreset thickness at 25 kyr of 23.7 m, which is 26.3 m less than the high sediment supply model (Table. 4; Table. 5). In contrast, average foreset thickness for the reference model at 25 kyr is 36.8 m (Table.3). Also, the maximum thickness of deltas differs where high sediment supply model is 76, 9 meters thicker (175.8 m) than the low sediment supply model (98.9 m) and 38.4 m thicker than the reference model (Table. 12).

From 25 kyr, sediment supply begins to increase and continues to increase until 50 kyr. During the initial increase of sediment supply until maximum sediment supply (at 50 kyr), both low- and high sediment supply deltas contain regressive elements (Fig. 15B; Fig. 16B). At 50 kyr, both high-and low sediment supply models are at a maximum of sediment supply, where low sediment supply model provide an amount of sediment of 5551 m^3/yr to the model, while high sediment supply model is providing four times as much (22,200 m^3/yr) sediment as the low sediment supply model. Both the low- and high- sediment supply models show similar features to the reference model, with development of topsets and foresets with deposition occurs as a continuous fringe along the delta front (Fig. 13C; Fig. 14C). High sediment supply model has a break-point trajectory climbing steep basinward and deltas stacking pattern is progradational to aggradational. As low sediment model approach maximum sediment supply, break-point trajectory changes from climbing approximately 45° basinward to get progressively steeper and the stacking pattern becomes aggraditional to progradiational (Fig. 15B; Fig. 16B) as the water depth increasing. The delta front at low- and high sediment supply deltas are like the reference model, with a smooth and arcuate front in plan view (Fig. 13C; Fig. 14C). Deltas are drowned and due to constantly available accommodation space, sediments accumulate both in topsets and foresets. At 50 kyr, the foresets have been progressively decreasing in average thickness as they are located further basinward and water depth increases. The high sediment supply model have at 50 kyr an average foreset thickness of 21 m (Table. 4), while reference and low sediment supply models have an average foreset thickness of 13.2 m (Table 5, Table 12). Between 25 - 50 kyr, the low sediment supply delta has extended basinward by 114.5 m and increased its maximum thickness of 54.9 m (Table. 12). At the same time, the high sediment supply model extended basinward of 236.8 m (Total 1368.4 m) and its maximum thickness has increased by 60.5 m (Table 12).

Thickness and height of foresets for the high sediment supply model

	Average foresets thickness	Foresets height (m)	Topset height
12.5 kyr	103,6	111,1	0
25 kyr	50	164,4	0
37.5 kyr	28,95	188,9	17,8
50 kyr	21	222,2	22,2
62.5 kyr	7,9	250	20
75 kyr	13,2	272,2	21,1
87.5 kyr	8,7	300	17,8
100 kyr	N/A	316,7	20
112.5 kyr	4,4	335,6	20
125 kyr	N/A	355,6	22,2
137.5 kyr	5,3	383,3	20
150 kyr	8,4	405,6	20

N/A, unable to measure

Table. 4: Results from measuring the forsets average thickness, height of the foresets and topsets height in main dip profile line of the high sediment supply model.

From 50 to 100 kyr sediment supply decreases in both models, but by different magnitude and at different maximum rates. Both deltas are continued to build basinward during the initial part of decreasing sediment supply. In the low sediment supply model, break-point trajectory have a aggraditional to progradiational climbing trajectory until 87.5 kyr, where the break-point trajectory changing to landward climbing break-point trajectory (backstepping), before the break-point trajectory climbs vertically in an aggraditional trajectory (Fig. 15D). The low sediment supply delta have at 75 kyr expanded basinward by 60.2 meters (Total of 790.5 m) over the last 25 kyr and increased its maximum thickness of 44 m (Table. 12). The average foresets thickness has been decreased from 13.2 at 50 kyr to 3.95 m at 75 kyr (Table. 5). Deposition of sediments occurs throughout the low sediment supply delta at 75 kyr (Fig. 13E). In the same period, high sediment supply model has expanded basinward of 79 m (1447.4 m total) and has increase maximum thickness of 49.4m. The high sediment supply model deposits the majority of the sediment along the delta plain (topsets), but also significant amount of sediment at the delta front (Fig. 14D, E). As the delta is located further basinward and the water depth increases the average foresets thickness has decreased from 50 kyr to 75 kyr by 7.8 m (Table. 4).

Thickness and height of foresets for the low sediment supply model			
	Average foresets thickness (m)	Foresets height (m)	Topsets height (m)
12.5 kyr	64,1	72.2	0
25 kyr	23,7	91,1	0
37.5 kyr	15,3	111,1	17,8
50 kyr	13,2	138.9	20
62.5 kyr	10,5	161,1	21,1
75 kyr	3,95	183,3	20
87.5 kyr	2,63	205.6	21,1
100 kyr	N/A	227.8	21,1
112.5 kyr	N/A	244.4	17,8
125 kyr	2,9	261.1	17,8
137.5 kyr	2,9	283.4	18,9
150 kyr	3,95	300	21,1

N/A, unable to measure

Table. 5: Results from measuring the forsets average thickness, height of the foresets and topsets height in the main dip profile line of the low sediment supply model.

At 75 kyr, the rate of decreasing sediment supply is at maximum. The high-sediment supply models break-point trajectory continues to climb basinward with an angle of 45 ° as the model approaches towards minimum sediment supply at 100 kyr. The break-point trajectory gets progressively steeper and at 87.5 kyr, high sediment supply delta changes from having a progradational to aggraditional stacking pattern of parasequence sets to gain an aggraditional stacking pattern (Fig. 14D). At 100 kyr, the high sediment supply models have expanded basinward of 39.4 m and have increase maximum thickness of 39.6 meters (Table. 12). The foresets deposition along the delta front has diminished, and at 100 kyr, have the model similar deposition pattern as low sediment supply model at 75 kyr, with the majority of sediment are accumulate on delta plain and minor amounts on the delta front (Fig. 14G; Fig. 13E). The average foresets thickness for high sediment supply model has a decrease between 75 - 100 kyr by 10.6 m (Table. 4).

At the same time, the low sediment supply model have aggraditional stacking pattern by 87.5 kyr. At 87.5 kyr, the break-point trajectory makes an abrupt change by climbing landward (backstepping; representative in both left and right dip profile line, see appendix) for a short space of time (Fig. 15D). After backstepping, the low sediment supply model is from 87.5 kyr, to 100 kyr, aggraditional (trajectory climbing vertically). Between 75 – 100 kyr the low sediment supply delta has retreated landward of 20.8 meters, while the maximum thickness increased by 38.5 m (Table. 12).

Deposition for the low- and high sediment supply deltas between 75-100 kyr differs from reference delta. While low-and high sediment supply delta accumulate the majority of sediments along the delta front (foresets) forming an arcuate shape (Fig. 13F,G; Fig 14F, G) as the sediment supply reaches minimum, so have reference model the majority of the sediment deposited along the delta plain, with hardly any sediments accumulates in the foresets (Fig. 11F, G). Although accumulation of sediment in the foresets occur in low sediment supply model, the amount of sediment deposited (as the reference model) too thin to measure. The topsets accumulation in low sediment supply model is 21.1 m per 12.5 kyr between 75-100 kyr (Table. 5).

At 100 kyr sediment supply starts to increase, low sediment supply model continue to be aggraditional (Fig.15E). In high sediment supply model, stratal geometry changes from aggraditional to progradational stacking pattern to aggraditional stacking pattern (Fig. 16E). Deposition on deltas between 100 kyr and 125 kyr, however, has resemblances between the different models. Both models have deposition on delta plain and along the front part of the delta front (Fig. 13G, H, I; Fig. 14G, H, I). Only the foresets for the low sediment supply model are measurable at 125 kyr (Table. 5). Low sediment supply model delta has between 100-125 kyr extended 6.6 meter basinward while it has increased its maximum thickness by 38,4 m. High sediment supply model during the same period have not expanded any meters basinward, while over the last 25 kyr, its maximum thickness have had an increase of 42.8 m (Table. 12).

From 125 kyr until the end of the model run at 150 kyr, low-and high sediment supply models have the same vertically climbing break-point trajectory until 137.5 kyr. At 137.5 kyr, both models break-point trajectories gained a pulse of progradation (forestepping) before high sediment supply model get an aggraditional to progradational direction and low sediment supply an aggraditional stratal geometry throughout the model run (Fig. 15F; Fig. 16F). At 150 kyr, the models reach maximum sediment supply, and as a result, sediments accumulate in the foreset and an increase in average thickness of the foresets of both low-and high sediment supply model (Table. 4; Table. 5).

Over the models run at 150 kyr, high sediment supply model have expanded basinward from the sediment source in a total of 1506.6 m and gained a maximum thickness of 412.1 m. Low sediment supply model have reached a basinward position from the sediment source in a total of 790.5 m, with a total of maximum thickness of 307.7 m. At 150 kyr have the low sediment model have gained the same basinward extension as at 75 kyr in its model run. High sediment model, however, has increased its horizontal extension from 75 kyr to 150 kyr with 59.2 meters, which represents approximately 4% increase in length (Table. 12). In contrast, the reference model has throughout the model run expanded basinward of 1092.1 m and gained a maximum thickness of 357.15 m (Table. 12).

LOW SEDIMENT SUPPLY WITH INITIAL FREQUENCY

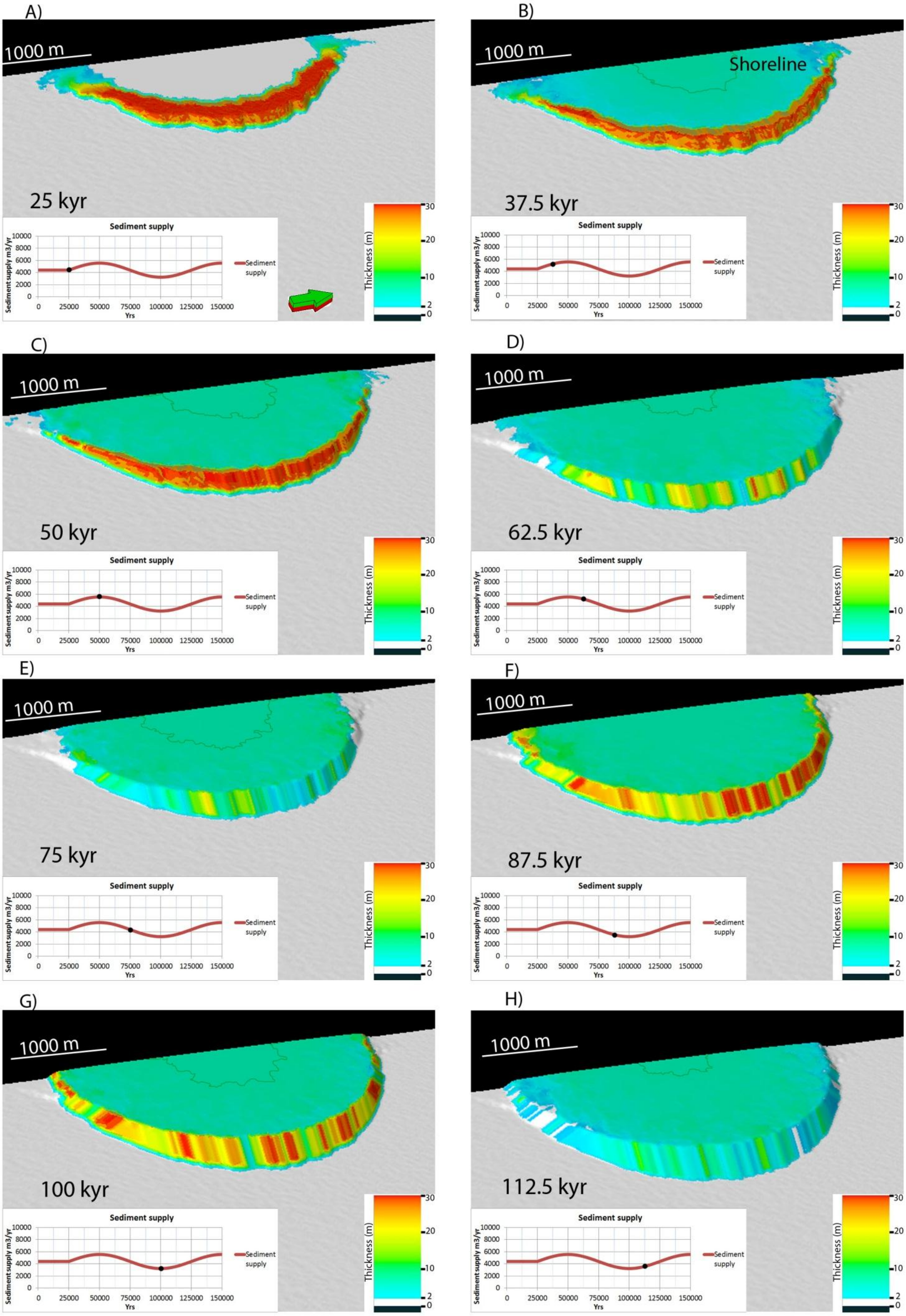

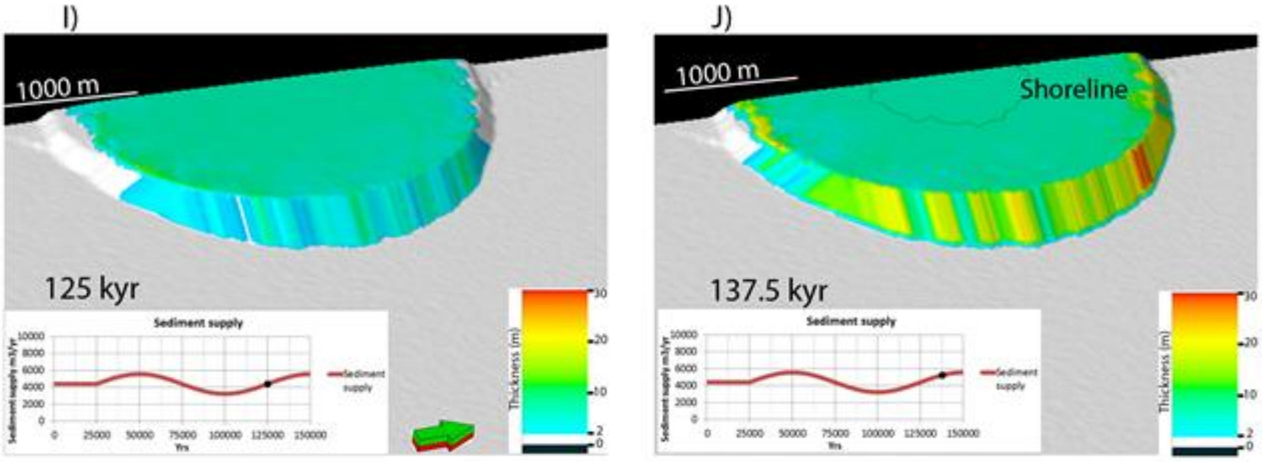

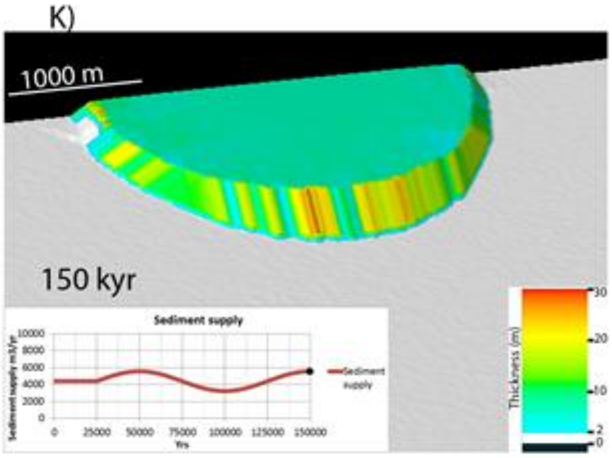

Fig. 13: Sequential evolution of the low sediment supply model at intervals of 12.5 kyr. Images show oblique view of the delta morphology and the isopach for previous 12.5 kyr. Vertical exaggeration 2:1.

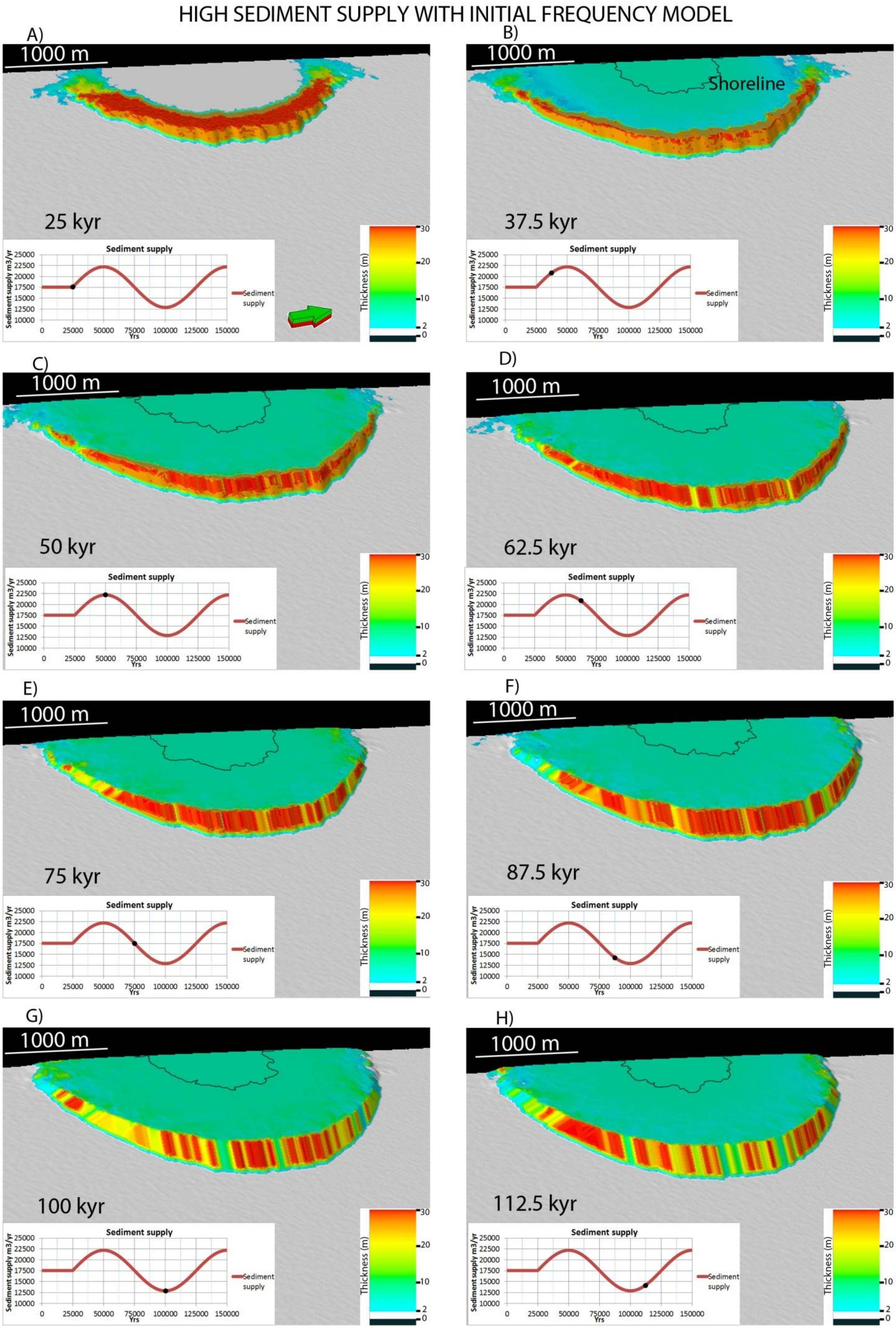
HIGH SEDIMENT SUPPLY WITH INITIAL FREQUENCY MODEL
A)
1000 m
25 kyr
B)
1000 m
Shoreline
37.5 kyr
C)
1000 m
50 kyr
D)
1000 m
62.5 kyr
E)
1000 m
75 kyr
F)
1000 m
87.5 kyr
G)
1000 m
100 kyr
H)
1000 m
112.5 kyr
Sediment supply
Sediment supply m3/yr
25000
22500
20000
17500
15000
12500
10000
0
25000
50000
75000
100000
125000
150000
Yrs
Sediment supply
Thickness (m)
30
20
10
2
0

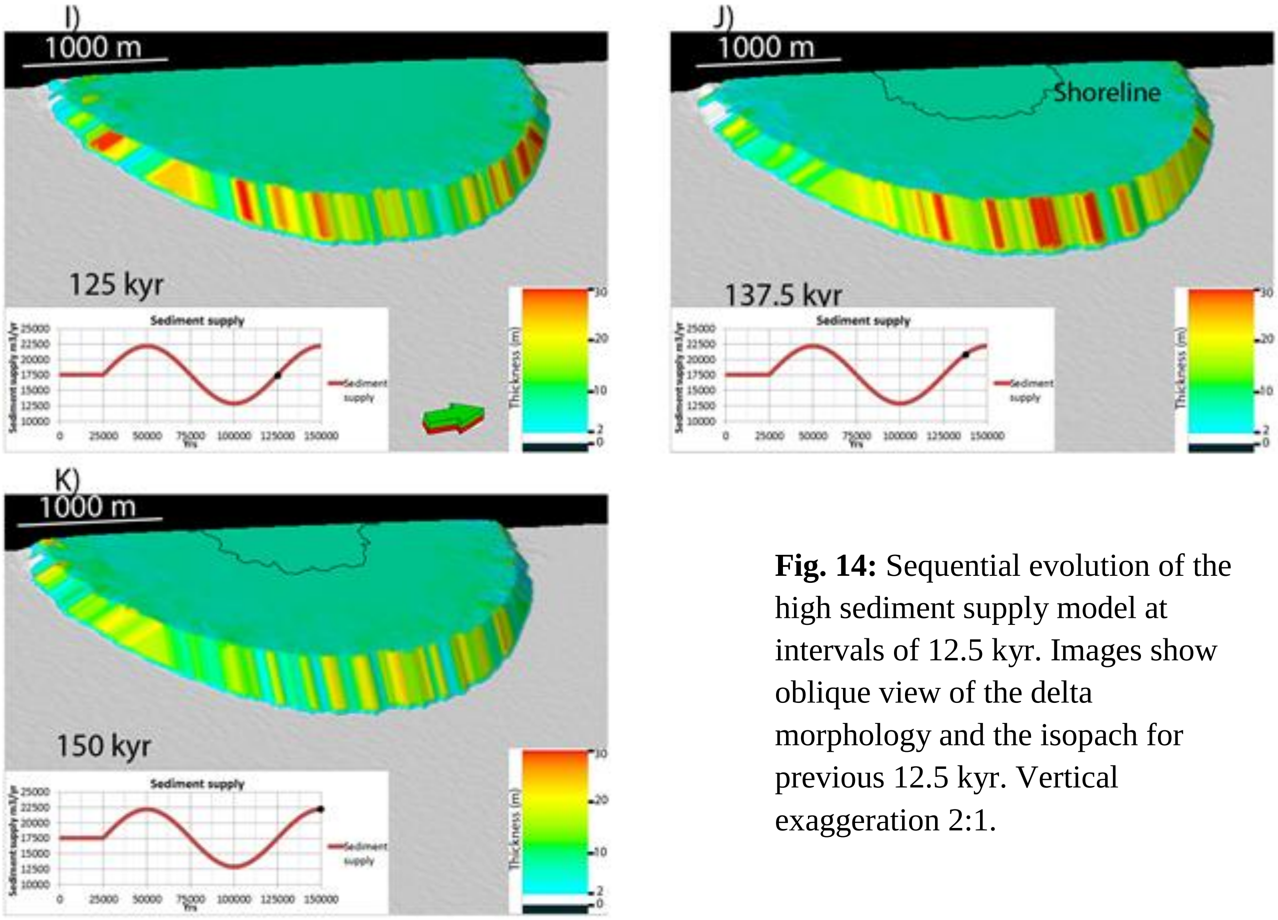

Fig. 14: Sequential evolution of the high sediment supply model at intervals of 12.5 kyr. Images show oblique view of the delta morphology and the isopach for previous 12.5 kyr. Vertical exaggeration 2:1.

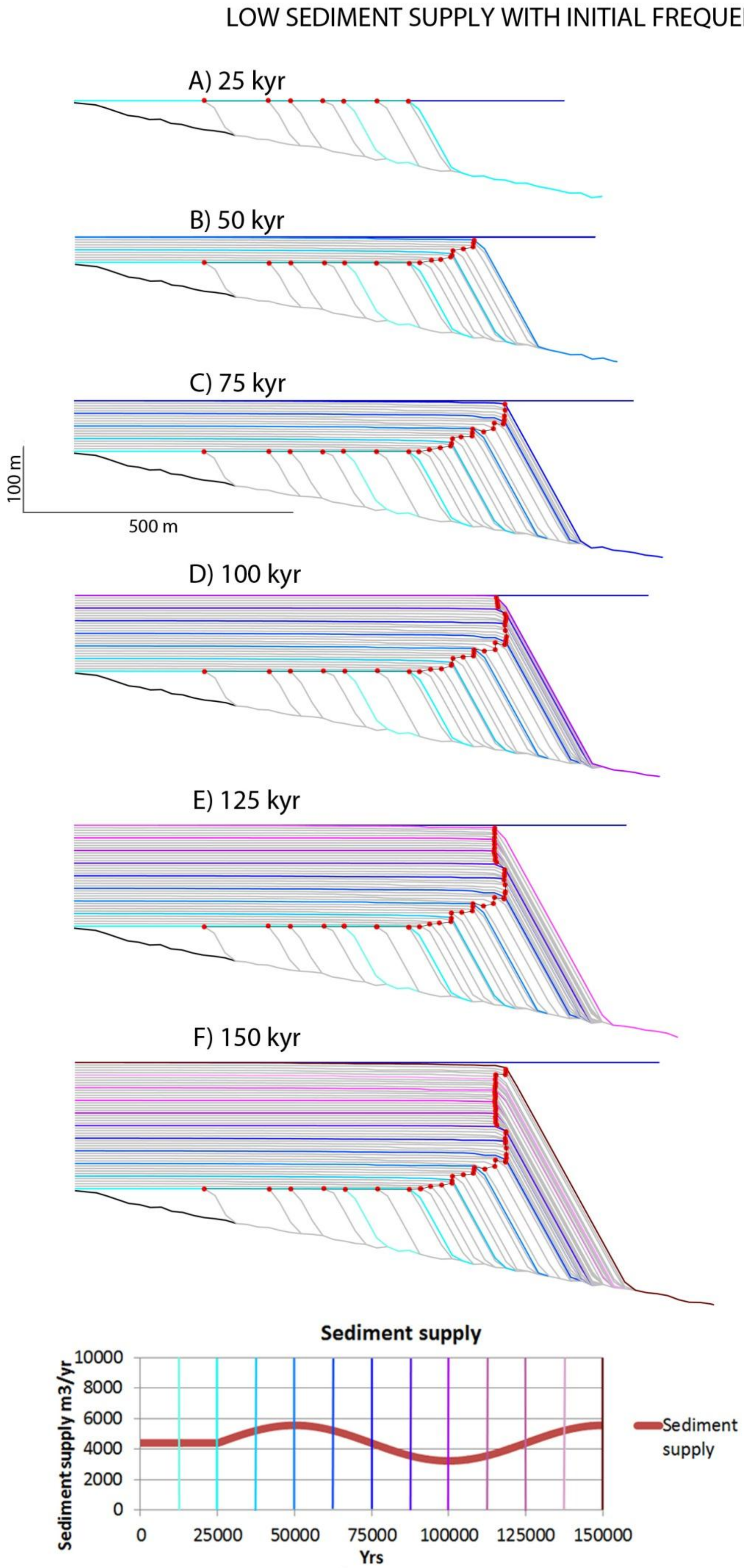

Fig. 15: Sequential development of the low sediment supply model shown in Fig. 13 expressed in a representative dip section (main dip profile line). Evolution of the delta is presented with a color every 12.5 kyr. Break-point trajectory is marked in red.

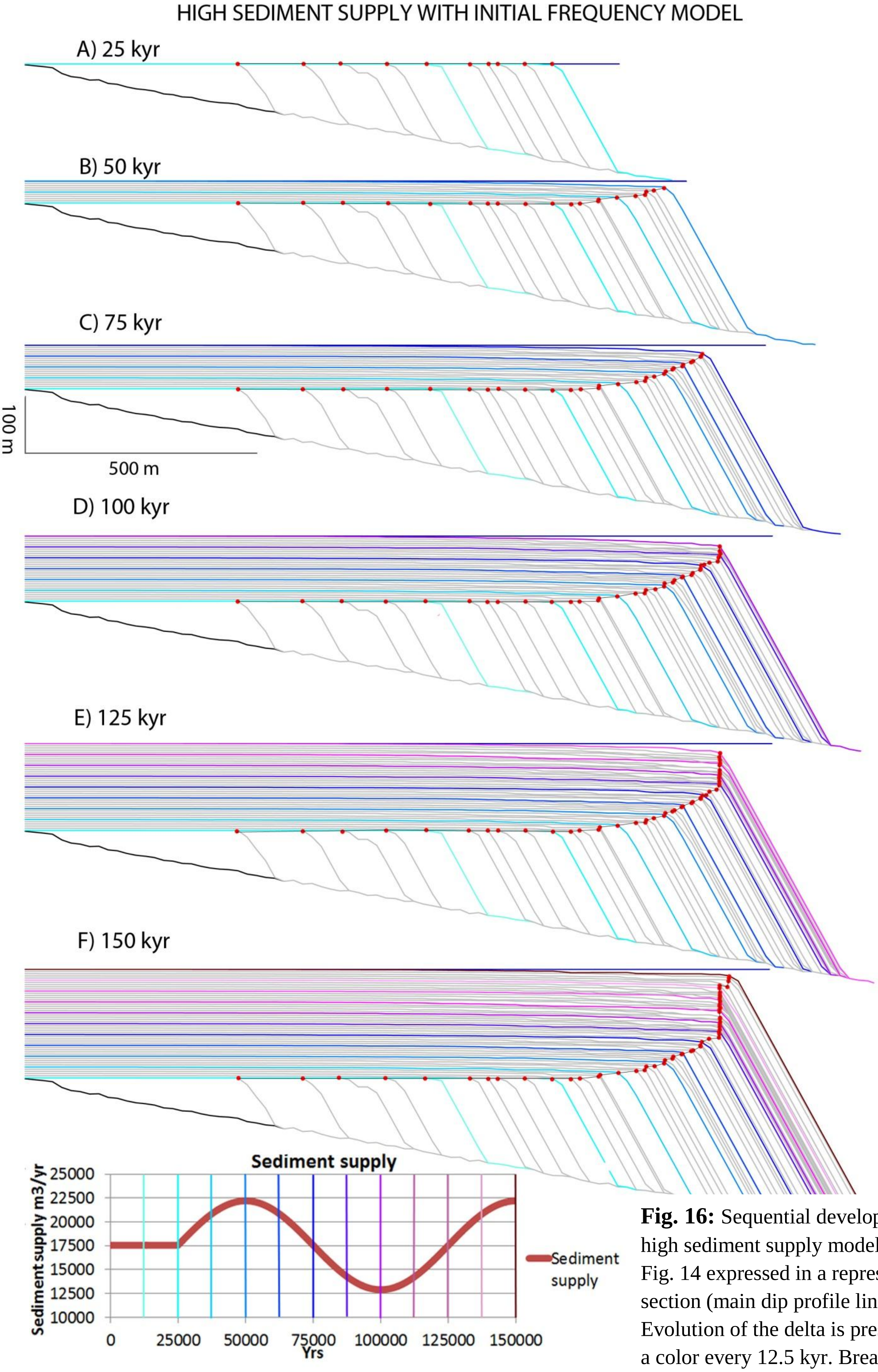

Fig. 16: Sequential development of the high sediment supply model shown in Fig. 14 expressed in a representative dip section (main dip profile line). Evolution of the delta is presented with a color every 12.5 kyr. Break-point trajectory is marked in red.

4.3 Sequence stratigraphic response to different sediment supply frequency

In addition to variations in values of sediment supply, there have been investigated the influence of sediment supply with different frequency. The reference model had a frequency of 50 kyr; in this investigation, there have been used a double frequency of ½ of frequency of the reference model (25 kyr) and four times higher frequency (12.5 kyr), called highest frequency model. These frequency have been used to make the sediment supply more extreme and thus investigate the influence the frequency has. As for the sediment supply value are the same as for the reference model (8775 m^3), but for the highest frequency model, there been needed to start the frequency after the constant sediment supply at 18740 yrs in order to get the maximum and minimum output image at the same time as the other models. All other model parameters are the same as for the reference model.

4.3.1 Double frequency model and highest frequency model description

For the first 25 kyr, both the double and the highest frequency models the delta are deposited likewise as the reference model at 25 kyr, with no topsets development and deposition occurs as a continuous fringe of sediment accumulation along the delta front (Fig. 17A; Fig. 18A). The highest frequency model have the same depositional architecture as the as reference and double frequency models, although sediment supply starts 6260 years earlier and is at maximum sediment supply at 25 kyr. By 25 kyr, the highest frequency delta has a maximum thickness of 142,85 m, while reference and double frequency model have a maximum thickness of 137,85 (Table. 12). The foresets average thickness for the double frequency model at 25 kyr is 42.1 m (Table. 6), while the highest frequency delta have 4.2 m larger average thickness of the foresets delta than double frequency delta (Table. 7). The highest frequency delta has at 25 kyr expanded 36 m further basinward from the sediment source than half wavelength (Table. 12).

Between 25 kyr to 75 kyr, sediment supply in both models would reach the maximum (11080 m^3/yr) and minimum (6430 m^3/yr) sediment supply. The highest frequency model have already been at its minimum sediment supply twice and are currently at its third maximum sediment supply at 75 kyr (Fig. 18E), while the double frequency model was at maximum sediment supply at 37.5 kyr and reached minimum sediment supply at 62.5 kyr and at 75 kyr sediment supply increases towards maximum sediment supply (Fig. 17E). The delta in highest frequency model has a break-point trajectory climbing 45° basinward up to 62.5 kyr, before it gain an aggraditional-progradational direction (Fig. 20C). In contrast, in the double frequency model, break-point trajectory switches from climbing basinward (progradational to aggraditional) to climbs vertically in an aggraditional break-point trajectory, just after maximum sediment supply at 37.5 kyr (Fig. 19B). The aggraditional pattern at double frequency model continues up to 75 kyr. In depositional architecture for double and highest frequency models, the sediments in double frequency delta still accumulate at delta plain (topsets) and along the delta front (foresets) (Fig. 17D; Fig 18D), with an average thickness of foresets decreasing (Table. 6; Table. 7). The highest frequency model that is at maximum sediment supply at 75 kyr still deposited significant amount of sediments to the foresets, but to a lesser extent than previously (Fig.18E). The average foresets thickness at 75 kyr is 4.7 m for the highest frequency model and 3.7m for double frequency model (Table. 6; Table. 7). As the double frequency model has been aggradational between 50-75 kyr, the highest frequency model have expanded 23.6 meters further basinward than double frequency model during the last 25 kyr (Table. 12).

Thickness and height of foresets for the double frequency model

	Average foresets thickness (m)	Foresets height (m)	Topset height (m)
12.5 kyr	72,4	88.9	0
25 kyr	42,1	127.8	0
37.5 kyr	26,3	150	18,9
50 kyr	8,2	177.8	20
62.5 kyr	N/A	194.4	17,8
75 kyr	3,7	211.1	21,1
87.5 kyr	7,4	238.9	22,2
100 kyr	9,2	266.7	21,1
112.5 kyr	N/A	283.3	20
125 kyr	2,9	302.2	18,9
137.5 kyr	2,9	322.2	22,2
150 kyr	5,3	350	20

N/A; Unable to measure

Table. 6: Results from measuring the forsets average thickness, height of the foresets and topsets height in the main dip profile line of the double frequency model.

From 75 kyr to 100 kyr, the deposition pattern for the highest frequency which is by its fourth maximum sediment supply, still accumulate sediment to the topsets and foresets, only with slightly smaller amounts of sediment that were previously deposited along the foresets (Fig. 18F, G). In double frequency model, sediment supply decreases, although it have increase its average thickness of the foresets from 75 kyr to 100 kyr by 5.5 m (Table. 6), and the majority of sediments accumulate as a continuous fringe of sediments along the delta front with large amounts of sediment on the delta plain (topsets) (Fig. 17G). From 75 kyr, the double frequency models break-point trajectory changes from climbing vertically to climb basinward (forestep) at 75 kyr, before the trajectory start climbing upward 45° basinward and the delta become progradational to aggradational after 75 kyr and up to 100 kyr, (Fig. 19D). Highest frequency break-point trajectory does also climb basinward (forestep) just after 75 kyr, before it gain an aggradational pattern (Fig. 20D). The highest frequency model has between 75 kyr and 100 kyr expanded basinward by 19.8 m, while double frequency model has had a basinward expansion of 56.5 m (Table. 12).

Thickness and height of foresets for the highest frequency model

	Average foresets thickness (m)	Foresets height (m)	Topset height (m)
12.5 kyr	72,4	88.9	0
25 kyr	46,3	127.8	0
37.5 kyr	13,7	156	20
50 kyr	11,3	172.2	21,1
62.5 kyr	8,2	194,4	21,1
75 kyr	4,7	216,7	22,2
87.5 kyr	5,5	233,3	18,9
100 kyr	2,6	261,1	21,1
112.5 kyr	3,95	277,8	18,9
125 kyr	3,95	300	18,9
137.5 kyr	N/A	316,7	20
150 kyr	5	344,4	20

N/A; unable to measure

Table. 7: Results from measuring the forsets average thickness, height of the foresets and topsets height in the main dip profile line of highest frequency model.

Following 100 kyr, break-point trajectory changes in both models. In double frequency model, the break-point trajectory is changing from climbing 45° basinward to climbs vertically and thus the stacking pattern is changed from progradational to aggradational to be aggradational (Fig. 19E). For highest frequency model the break-point trajectory changes from vertically climbing basinward to climb basinward (forestep) at 100 kyr for a period of 2500yr (Fig. 17E), before it continue to climb vertically in an aggradational trajectory. At 125 kyr have the highest frequency model expanded 36.8 m basinward since 100 kyr (Table. 12), while double frequency model has expanded basinward during the same time by 4 m. Beside a forestepping event at 150 kyr for double frequency model (Fig. 19F), both double and highest frequency models will have the same aggraditional break-point trajectory patterns from about 100 kyr and throughout the model run (at 150 kyr) (Fig. 19E, F; Fig. 20E, F).

During the time from 100 kyr to 150 kyr, the double frequency model deposits sediment along the delta front, but also significant amounts of sediment accumulate on the delta plain (Fig. 18H, I, J, K). At the time double frequency model have been through minimum sediment supply (at 112.5 kyr), the deposition pattern at 125 kyr, show that the deposit has the majority of the sediments accumulate throughout the delta (Fig. 17I). From 125 kyr to 150 kyr, the double frequency model has the deposition pattern with deposition of sediment on both topsets and foresets at the delta, where the majority of sediments accumulate as a continuous fringe along the delta front (Fig. 17J, K). At 150 kyr, the average foreset thickness at the double frequency model is approximately 0.3 meter thicker than the highest frequency model (Table. 6; Table. 7). The total basinward expansion during the model run for double frequency model is 1105.3 m with a maximum thickness of 355 m. The highest frequency model has not expanded any meters during the last 25 kyr, as a result, the total basinward expansion is 1109.2 m (Table. 12). In contrast, reference model has a total basinward expansion of 1092.1 m. The highest frequency deltas maximum thickness has increased from 313.2m at 125 kyr to 357.15 m at 150 kyr (Table. 12).

INITIAL SEDIMENT SUPPLY WITH DOUBLE FREQUENCY MODEL

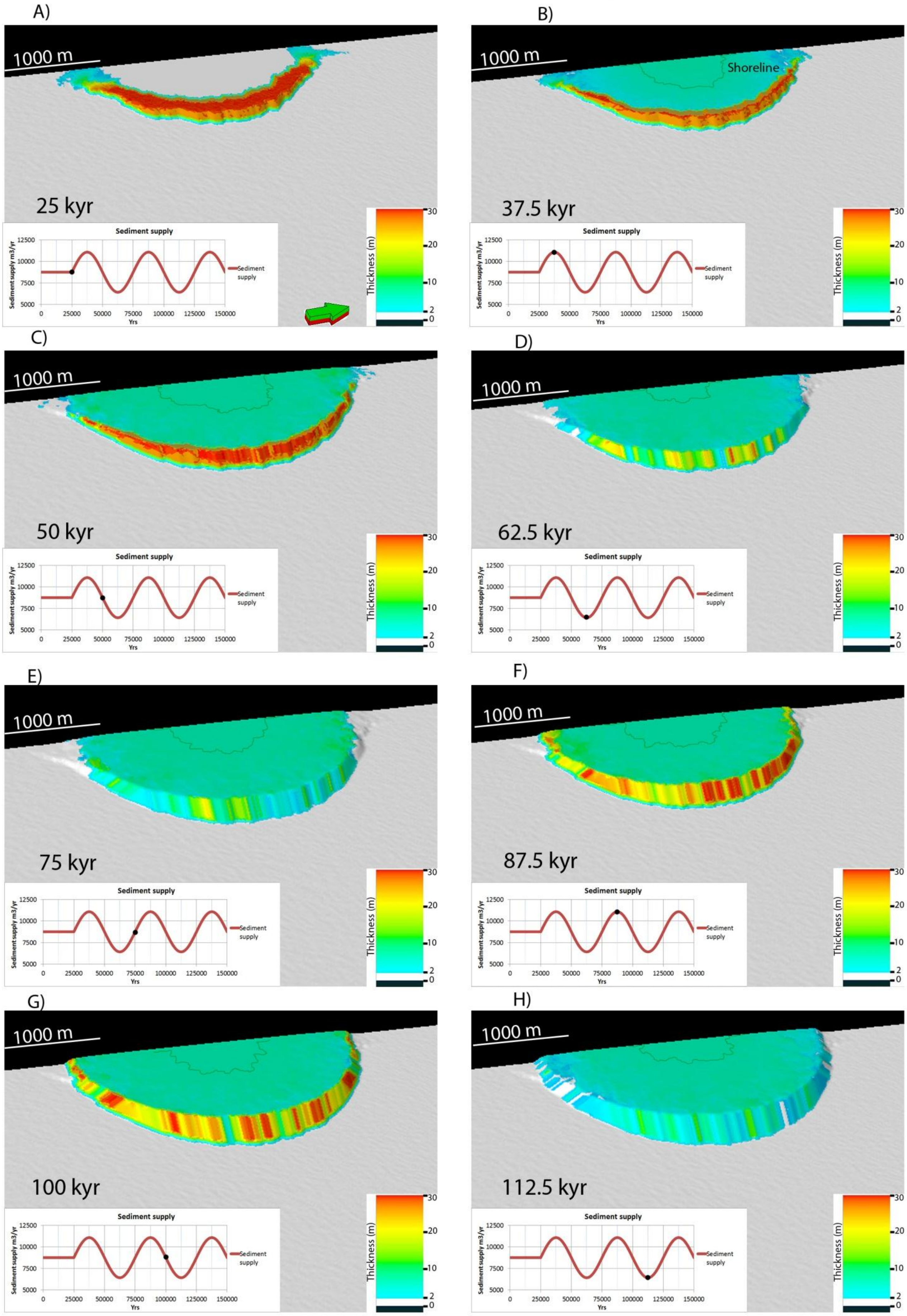

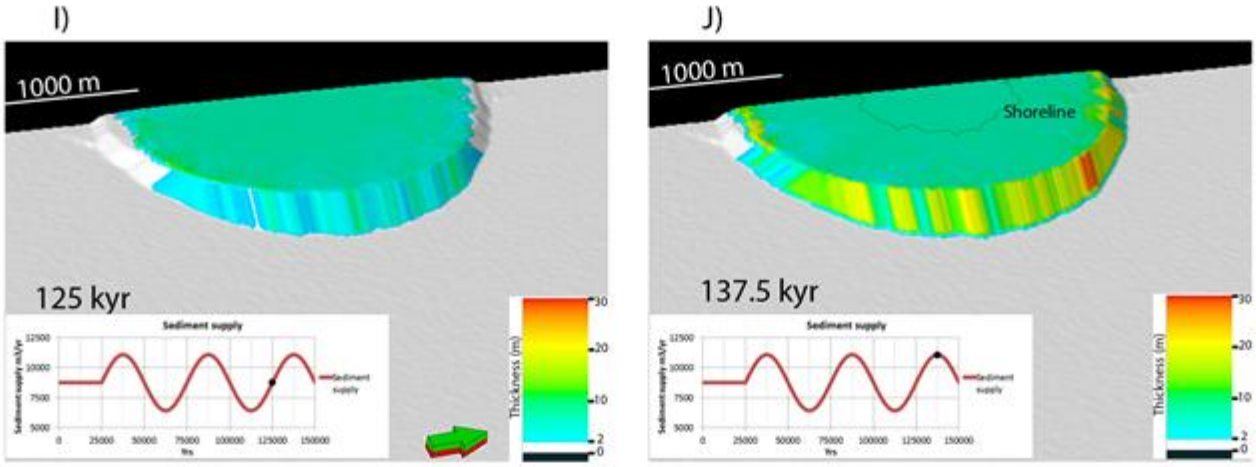

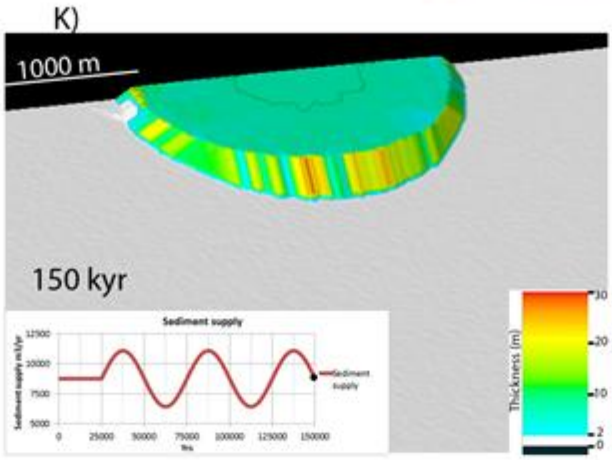

Fig. 17: Sequential evolution of the double frequency model at intervals of 12.5 kyr. Images show oblique view of the delta morphology and the isopach for previous 12.5 kyr. Vertical exaggeration 2:1.

INITIAL SEDIMENT SUPPLY WITH HIGHEST FREQUENCY MODEL

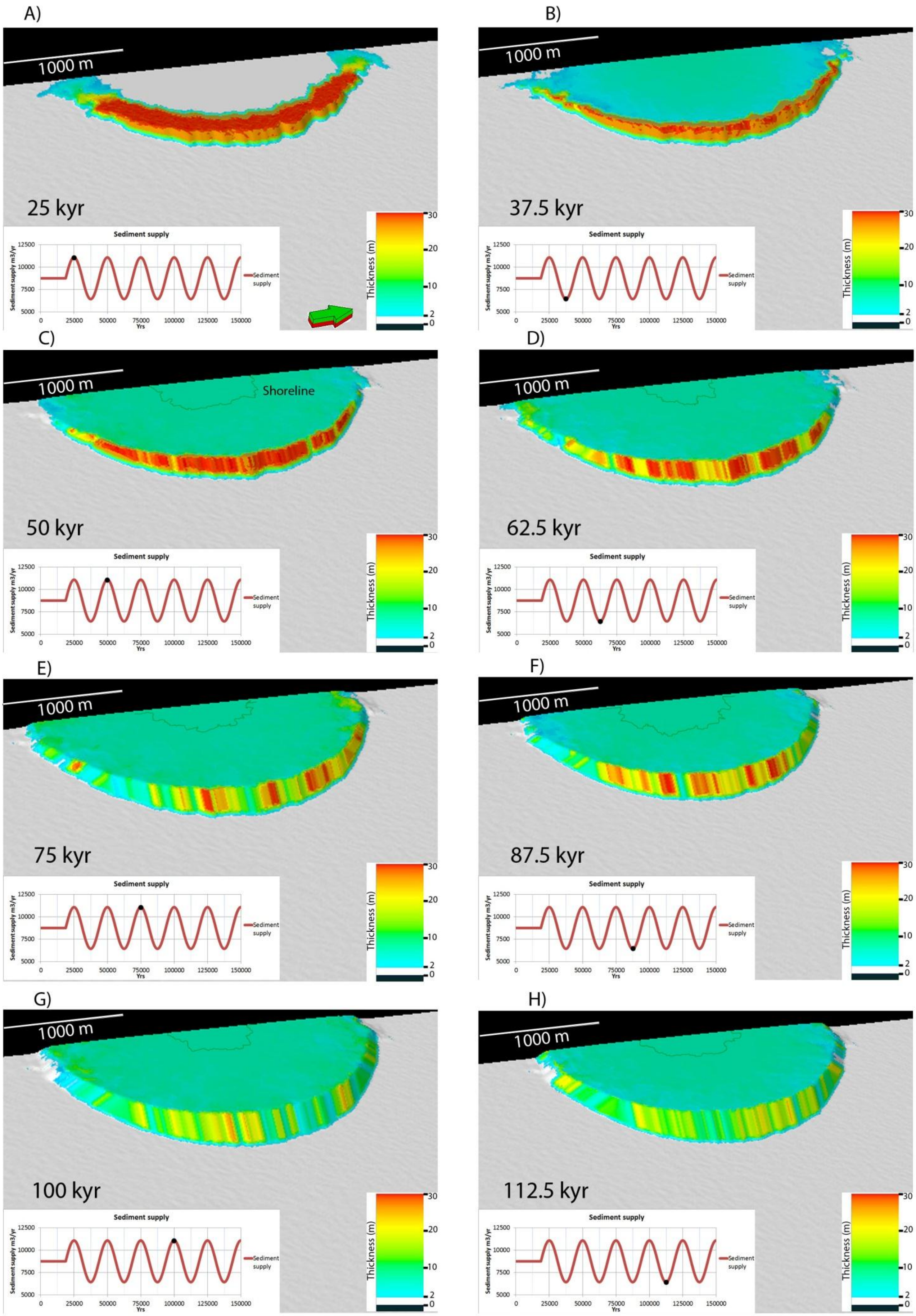

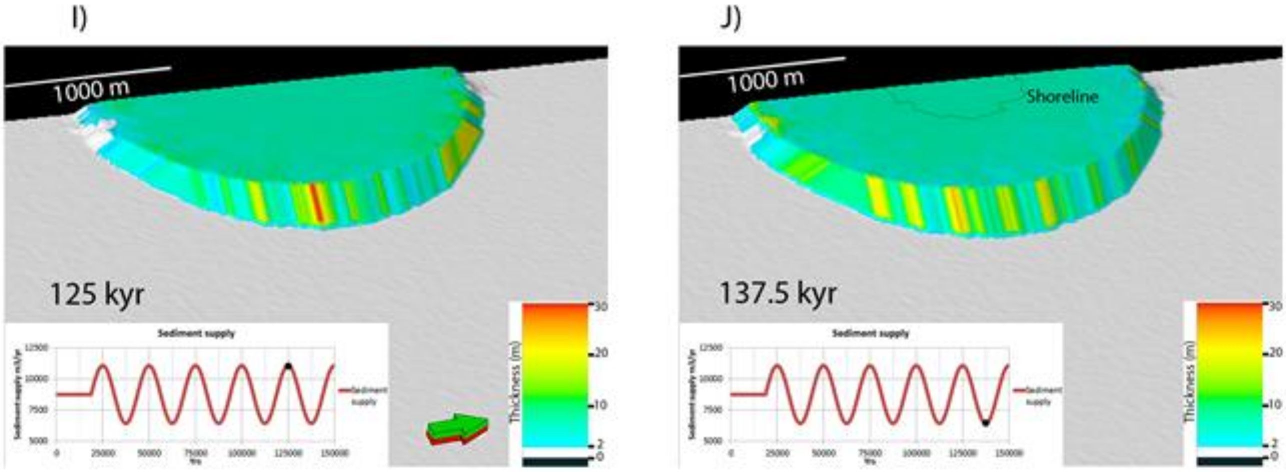

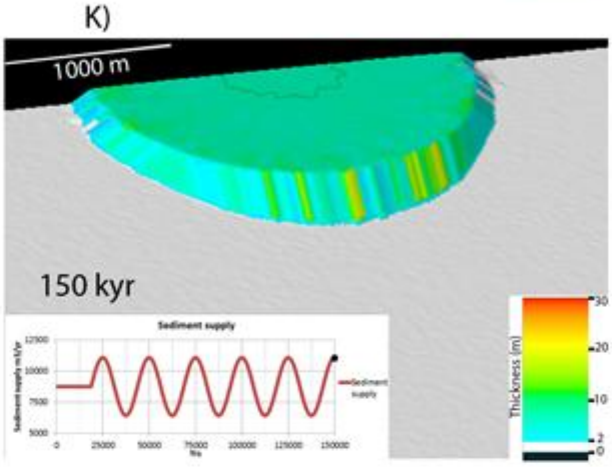

Fig. 18: Sequential evolution of the highest frequency model at intervals of 12.5 kyr. Images show oblique view of the delta morphology and the isopach for previous 12.5 kyr. Vertical exaggeration 2:1.

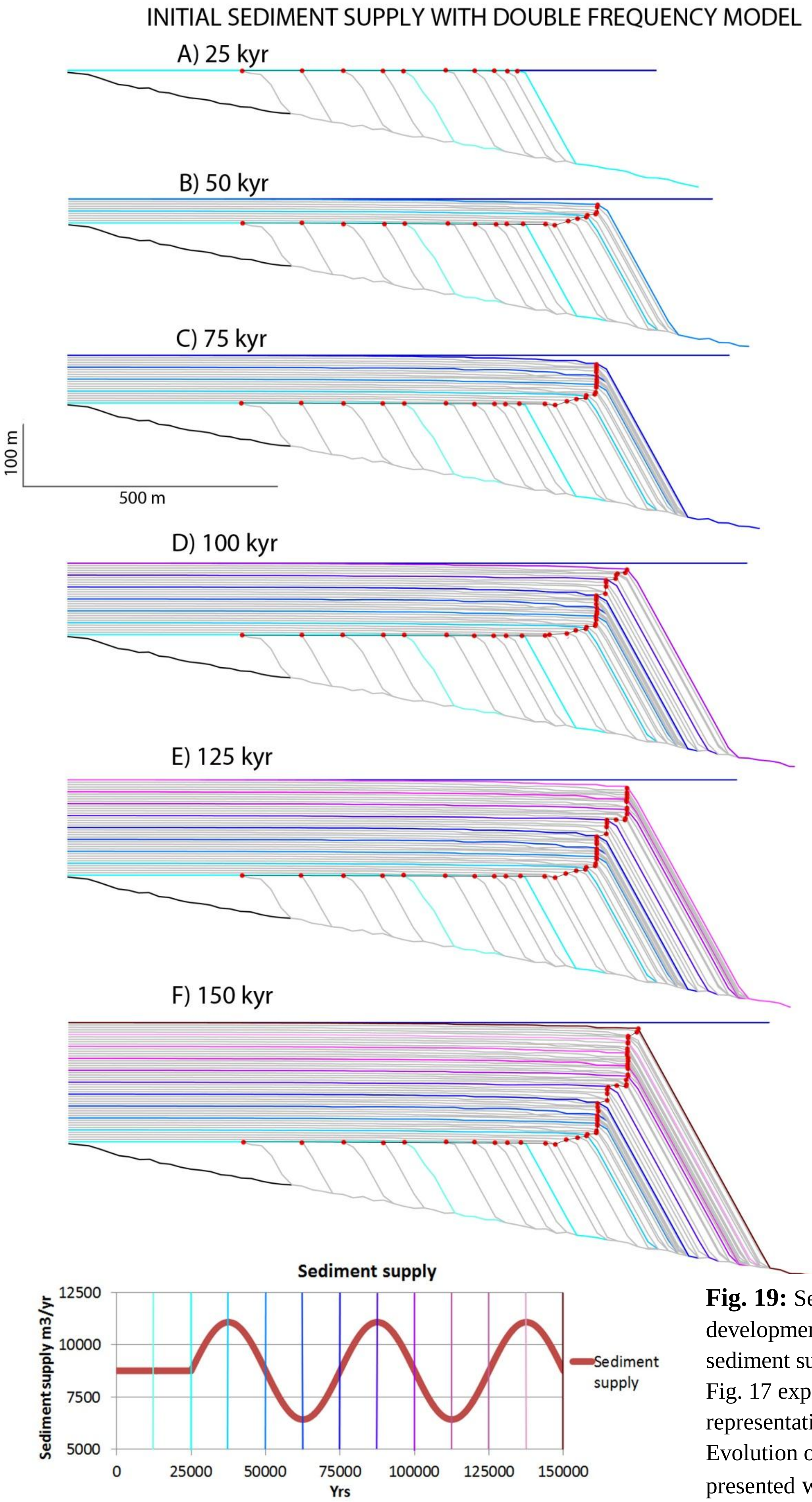

Fig. 19: Sequential development of the low sediment supply model shown in Fig. 17 expressed in a representative dip section. Evolution of the delta is presented with a color every 12.5 kyr.

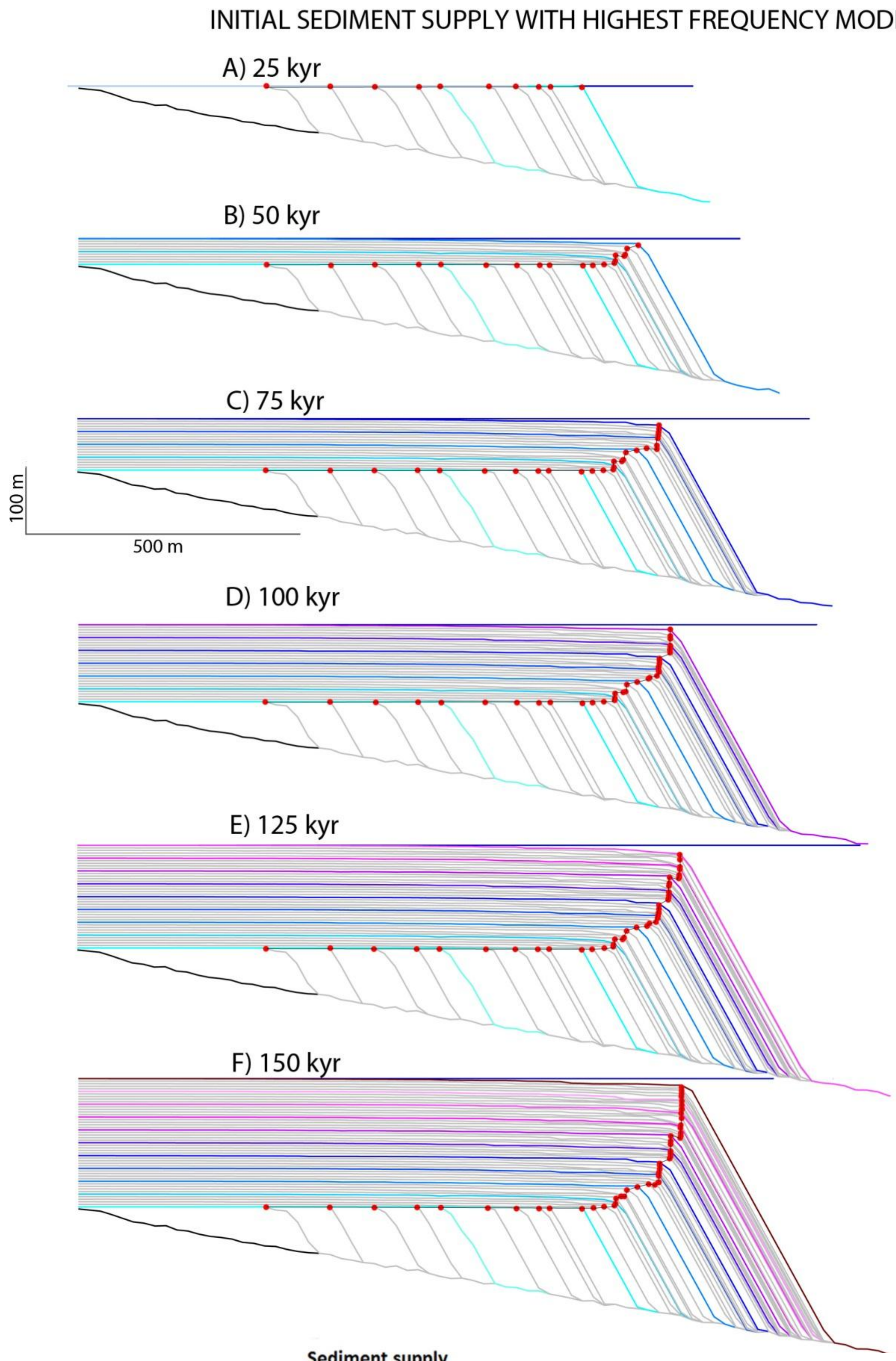

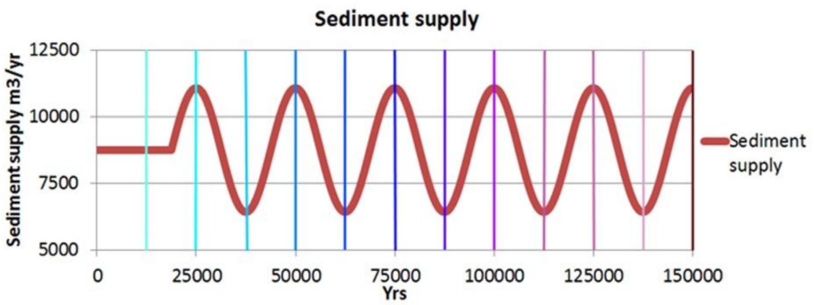

Fig. 20: Sequential development of the low sediment supply model shown in Fig. 18 expressed in a representative dip section. Evolution of the delta is presented with a color every 12.5 kyr.

4.4 Stratigraphic response to different values and frequency of sediment supply

To obtain a more extreme models, it has been investigated the impact of different volumes of sediment with different frequency. A total of four different models have been run, where two of the models have low sediment supply (4388 m^3/yr) and the two remaining models have a high sediment supply (17,552 m^3/yr). The models with low sediment supply will again be divided into a model with double frequency (25 kyr) and one with highest frequency (12.5 kyr). This division also applies to high sediment supply models. All four models have the same linear sea level rise as for the reference model (7.5m/10kyr), including the period in which sediment and sea level is kept constant. This period of constant sea level and sediment supply will be for the high sediment supply with highest frequency model and low sediment with highest frequency model from 0 to 18,740 yrs, this allows that one can take the maximum and minimum output images for the sediment supply. For the high sediment supply with double frequency and low sediment supply with double frequency models, the period of constant sediment supply and sea-level is the same as the reference model (0-25 kyr). All other parameters for the four models are the same as the reference model.

4.4.1 High sediment supply with double frequency model, Low sediment supply with double frequency model, High sediment supply with highest frequency model and Low sediment supply with highest frequency model, description

For the first 25 kyr, the four different models have the same deposition pattern as the previous models at constant sediment supply and sea level, with no topsets development and sediment are deposited in the foresets that form a continuous fringe along the delta front. This also applies the high sediment supply with highest frequency model and low sediment with highest frequency model, although they start the sinusoidal sediment supply 6260 years earlier and are by their maximum sediment supply at 25 kyr. For the first 25 kyr, high sediment supply model and the high sediment supply with double frequency, have the same basinward extension and the average thickness of the foresets (Table. 12; Table. 4 and Table. 8). This also applies to low sediment supply model and low sediment supply with double frequency model (Table. 12; Table. 5 and Table. 9). The highest frequency models (high sediment supply with highest frequency and low sediment supply with highest frequency) has a slightly longer basinward expansion than the models with the same sediment supply, but with a different frequency as they began with an increase in sediment supply earlier than the models with the same sediment volume (Table. 12). This applies also for the average foresets thickness, where high sediment supply with highest frequency model is on average 2.4 m thicker than the average foresets at high sediment supply with double frequency model (Table. 8; Table. 10). For low sediment supply with highest frequency model has the model equal average foresets thickness as the low sediment supply with double frequency model.

From 25 kyr, the double frequency models start to increase sediment supply, and at 50 kyr, the highest frequency models are at its second maximum sediment supply. The double frequency models were on maximum sediment supply at 37.5 kyr and have at 50 kyr a decreasing sediment supply. Common to all four models at 50 kyr are that they all have a break-point trajectory that dips approximately 45 degrees basinward (Fig. 25B; Fig. 26B; Fig. 27B and Fig. 28B). The only model that differs slightly is the high sediment supply with highest frequency model, which has by 37.5 kyr a more weakly climbing break-point trajectory (aggraditional to progradiational) just after 37.5 kyr (at minimum sediment supply), before it acquires an approximately 45 degree climbing break-point trajectory (progradiational to aggraditional) again at 45 kyr (Fig. 27B). Depositional architecture for the four different models at 50 kyr are similar to the reference model, with deposition occurs as a continuous fringe of sediment accumulation along the delta front (Fig. 25C; Fig. 26C; Fig. 27C and Fig. 28C), with decreasing average foresets thickness as the deltas are located further basinward. Most decrease in the average foreset thickness is high sediment supply with highest frequency

Thickness and height of foresets for the high sediment supply and double frequency model

	Average foresets thickness (m)	Foresets height (m)	Topset height (m)
12.5 kyr	103,6	116.7	0
25 kyr	50	161.1	0
37.5 kyr	27,6	191.1	16,7
50 kyr	19,7	222.2	20
62.5 kyr	7,6	244.4	18,9
75 kyr	6,6	272.2	22,2
87.5 kyr	14,5	294.4	20
100 kyr	9,2	322.2	20
112.5 kyr	2,6	338.9	21,1
125 kyr	2,6	355.6	21,1
137.5 kyr	3,9	377.8	21,1
150 kyr	7,9	400	22,2

N/A; unable to measure

Table. 8: Results from measuring the forsets average thickness, height of the foresets and topsets height in the main dip profile line of the high sediment supply with double frequency model.

model that has decreased its average foresets thickness between 25 - 50 kyr by 32.1 m, equivalent to 53.3 percent reduction (Fig. 28B; Table 10). Between 25-50 kyr, high sediment supply with double frequency delta have expanded furthest basinward by 57.2 m, which corresponds to 19.5% expansion, while the low sediment supply with double frequency and low sediment supply with highest frequency models (49,5 m, equivalent to 66.7 % increase) had the largest increase in maximum thickness (Table. 12).

From 50 kyr to 75 kyr, the break-point trajectory get more gently climbing basinward direction (aggraditional to prograditional) among both the high sediment supply models and low sediment with double frequency (Fig. 25C; Fig. 26C; Fig. 27C).

Thickness and height of foresets for the low sediment supply with double frequency model

	Average foresets thickness (m)	Foresets height (m)	Topset height (m)
12.5 kyr	64,1	66	0
25 kyr	23,7	92,2	0
37.5 kyr	15,8	111,1	17,8
50 kyr	10,5	138.9	20
62.5 kyr	5,3	157,8	22,2
75 kyr	2,6	178.9	18,9
87.5 kyr	8,4	205.6	16,7
100 kyr	4	222,2	20
112.5 kyr	N/A	244.4	22,2
125 kyr	2,6	266.7	16,7
137.5 kyr	4,9	283.3	17,8
150 kyr	3,3	305.6	20

N/A; unable to measure

Table. 9: Results from measuring the forsets average thickness, height of the foresets and topsets height in the main dip profile line of the low sediment supply with double frequency model.

The low sediment supply with highest frequency model have just after 62.5 kyr (minimum sediment supply) a landward climbing trajectory (Fig. 28C), before it starts climbing steep basinward up to 75 kyr (maximum sediment supply). The highest frequency models who are at its third maximum sediment supply at 75 kyr, continues to have the same depositional architecture with sediment deposits along the delta front and delta plain (Fig. 23D, E; Fig. 24D, E). This also applies for high sediment supply with a double frequency, although at 62.5 kyr, had a minimum of sediment supply (Fig. 21D, E). During the same time period(50 -75 kyr), the low sediment supply with double frequency model accumulate the majority of sediment along the delta plain, while minor amount of sediment accumulates at delta front (foresets) (Fig. 22D, E). As a result, the low sediment supply with double frequency model has the thinnest average thickness of foresets with only 2.6 m at 75 kyr (Table. 9). Although the low sediment supply with highest frequency model had for a short period of landward climbing shoreline trajectory, expanded the model's second furthest with 43,4 m, which corresponded to 5.9% increase and also had the highest percentage increase in maximum thickness (from 148.4, 8 m to 194.5 m) (Table. 12).

Just after 75 kyr, all models except low sediment supply with highest frequency model have a break-point trajectory that changing from climbing aggradational to progradational to progradational to aggradational climbing break-point trajectory. This progradational to aggradational climbing trajectory continues until 87.5 kyr (Fig. 25D; Fig. 26D; Fig. 27D). The low sediment supply with highest frequency model has after 75 kyr, a vertically climbing trajectory with a landward climbing event at 87.5 kyr, before straight after returning to an aggradational trajectory and continues its vertically climbing throughout the model run (Fig. 28D, E, F). The double frequency models are at their second maximum sediment supply at 87.5 kyr, and the sediments are accumulated along the topsets and foresets and deposition architecture form a continuous fringe along the delta front (Fig. 21F; Fig. 22F). This depositional architecture is also in highest frequency models (Fig. 23F; Fig. 24F).

Thickness and height of foresets for the high sediment suppy and highest frequency model

	Average foresets thickness (m)	Foresets height (m)	Topsets height (m)
12.5 kyr	103,6	116.6	0
25 kyr	49,2	161.1	0
37.5 kyr	24,5	188.9	15,6
50 kyr	17,1	216.7	21,1
62.5 kyr	17,1	238.9	20
75 kyr	7,9	266.7	21,1
87.5 kyr	11,8	288.9	20
100 kyr	3,9	316.7	22,2
112.5 kyr	3,4	338.9	20
125 kyr	5,3	355.6	21,1
137.5 kyr	5	377.8	14,4
150 kyr	5,3	402	22,2

N/A; unable to measure

Table. 10: Results from measuring the forsets average thickness, height of the foresets and topsets height in the main dip profile line of the high sediment supply with highest frequency model.

For the next 12.5 kyr (to 100 kyr), the break-point trajectory deviates among models that had a progradational to aggradational climbing basinward trajectory up to 87.5 kyr. While high sediment supply with double frequency model (Fig. 25D) continues its progradational to aggradational climbing trajectory (dipping 45° basinward), so changes the break-point trajectory from the climbing progradational to aggradational to an aggradational to progradational direction among high sediment supply with highest frequency and low sediment supply with double frequency models (Fig. 26D; Fig. 27D). From 75 to 100 kyr, so have the low sediment supply with double frequency model increased its average foresets thickness by 53,8% (from 2,6m to 4m), but at its maximum sediment supply at 87.5 kyr, the increase was as much as 123% (had average foresets thickness at 87,5 by 8.4 m) (Table. 9). The low sediment supply with double frequency model had also the largest increase in maximum thickness (increasing 44m), with an increase of 22.9% (Table. 12). In this period was it high sediment supply with double frequency model that migrate furthest basinward with 98.7 m expansion (Table. 12).

From 100 kyr, sediment supply the models with double frequency decreases towards the minimum sediment supply (at 112.5 kyr) and as a result, break-point trajectory changes. Low sediment supply with double frequency models trajectory take a step landward just after 100 kyr, before the trajectory climbs vertically until125 kyr and the stacking pattern have changed from being aggradational to progradational to become aggradational (Fig. 26E). The high sediment with double frequency models break-point trajectory changes at 100 kyr, from progradational to aggradational to an aggradational climbing (Fig. 25E) during the period of decreasing sediment supply (from 100- 112.5 kyr). By the time the model has reached minimum sediment supply (at 112.5 kyr), the break-point trajectory has a pulse of progradation (forestep) when the sediment supply starts to increase before it continue to climb vertically towards 125 kyr. These changes in breakpoint trajectory just after 100 kyr (maximum

Thickness and height of foresets for the low sediment supply with highest frequency model

	Average foresets thickness (m)	Foresets height (m)	Topset height(m)
12.5 kyr	64,14	66.7	0
25 kyr	23,76	94.4	0
37.5 kyr	15,5	114.4	20
50 kyr	11,8	138.9	16,7
62.5 kyr	3,95	161.1	23,3
75 kyr	9,2	183.3	16,7
87.5 kyr	N/A	187.8	22,2
100 kyr	4,74	222.2	15,5
112.5 kyr	2,63	238.9	23,3
125 kyr	3,16	261.1	15,5
137.5 kyr	N/A	277.8	22,2
150 kyr	3,95	300	14,4

N/A; unable to measure

Table. 11: Results from measuring the forsets average thickness, height of the foresets and topsets height in the main dip profile line of the low sediment supply with highest frequency model.

sediment supply) are not the case at high sediment supply with highest frequency model. The aggradation to progradation direction continue to climb until 125 kyr (maximum sediment supply), where it takes a step basinward (Fig. 27E).

The minimum sediment supply at 112.5 kyr also affects the depositional architecture for the double frequency models. The high sediment supply with double frequency model deposit most of the sediments along delta plain, while the delta front accumulate smaller amounts of sediments than previously (Fig. 21H, I). The low sediment supply with double frequency model deposit sediment only at the delta plain at 112.5 (minimum sediment supply) and the delta front has sediment starvation (Fig. 22H). As the sediment supply increases, small amounts of sediment are supplied to the delta front (Fig. 21I).

The highest frequency deltas do not get sediment starved, as the sediments are deposited on both foresets and topsets. By those, the high sediment supply with highest frequency model has the most sediment accumulated in the foresets and is the only model that have increased (increased by 1,4 m) its average foresets thickness from 100 kyr to 125 kyr (Table. 10). The high sediment supply with highest frequency model has also extended furthest basinward with 19.7 m during this period. In the same period, have low sediment supply with double frequency delta retreated 20.8 m (Table. 12). The low sediment supply with highest frequency model which has throughout this period been aggradational has had an increase in the maximum thickness of 16.4%, which corresponds to 38.4 m (Table. 12).

From 125 kyr to the end of the models run (150 kyr), the deposition architecture shows that more amounts of sediment accumulated in the foresets in double frequency models as they reach the maximum sediment supply at 112.5 kyr (Fig. 21I, J; Fig. 22I, J). At high sediment supply with double frequency model, deposition of sediments forms an arcuate delta front again, while low sediment supply with double frequency filling up sediments on the delta front that were previously sediment starved (Fig. 21I, J; Fig. 22I, J). As for highest frequency models, they continues to deposits sediments along the delta front and on the delta plain (Fig. 23I, J; Fig. 24I, J).

At the low sediment supply with double frequency model, the break-point trajectory take a step basinward just after 125 kyr and vertically climbing trajectory up to 150 kyr where it take a step in landward direction (Fig. 26F). The high sediment supply with double frequency model has an aggraditional to progradational climbing break-point trajectory from 125 kyr and up to 150 kyr, where it takes a step in basinward direction (Fig. 25F). The high sediment supply with highest frequency climbs vertically and has also a basinward step at 150 kyr (Fig. 27F).

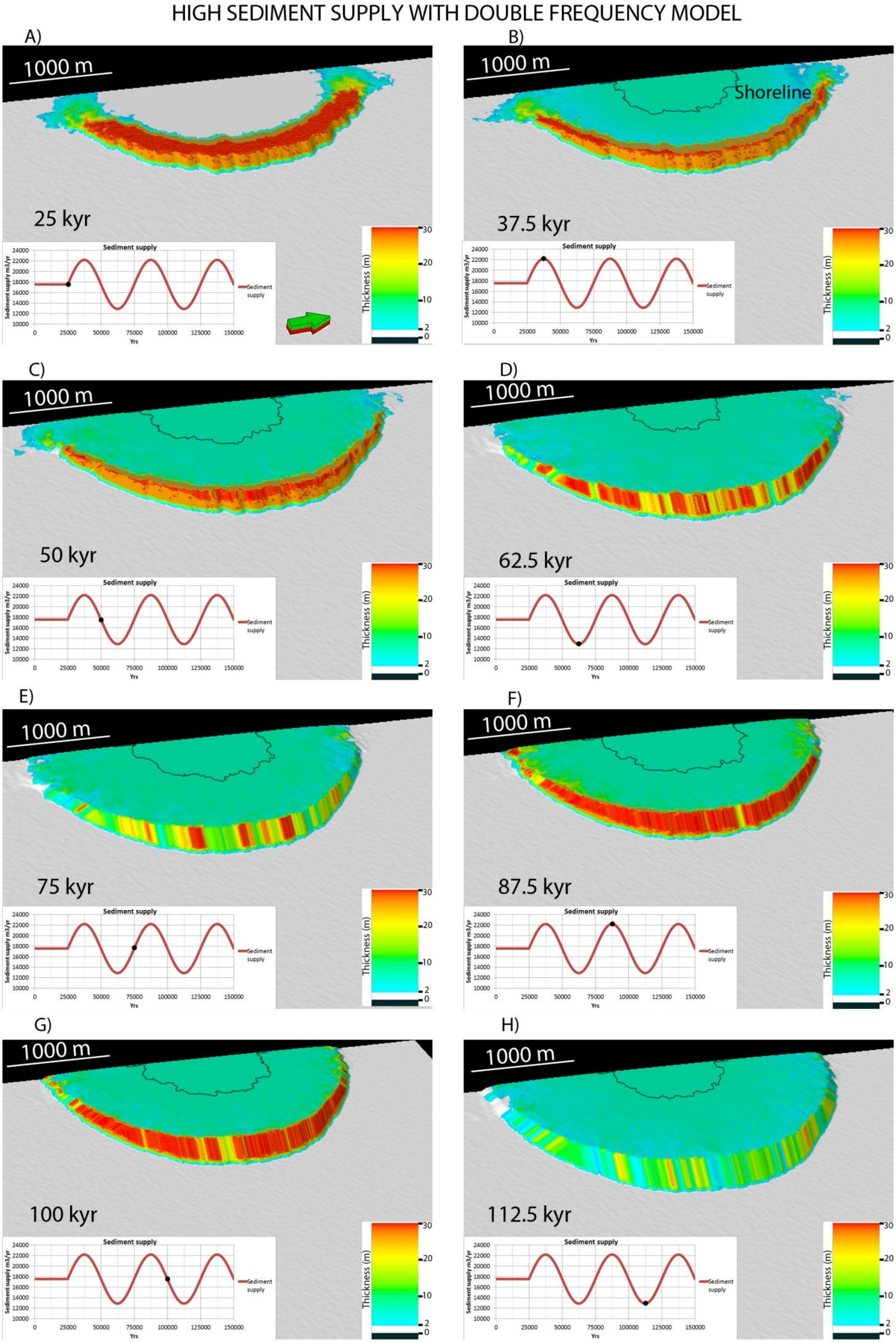
HIGH SEDIMENT SUPPLY WITH DOUBLE FREQUENCY MODEL
A)
1000 m
25 kyr
B)
1000 m
Shoreline
37.5 kyr
C)
1000 m
50 kyr
D)
1000 m
62.5 kyr
E)
1000 m
75 kyr
F)
1000 m
87.5 kyr
G)
1000 m
100 kyr
H)
1000 m
112.5 kyr
Sediment supply
Sediment supply m3/yr
Yrs
Thickness (m)

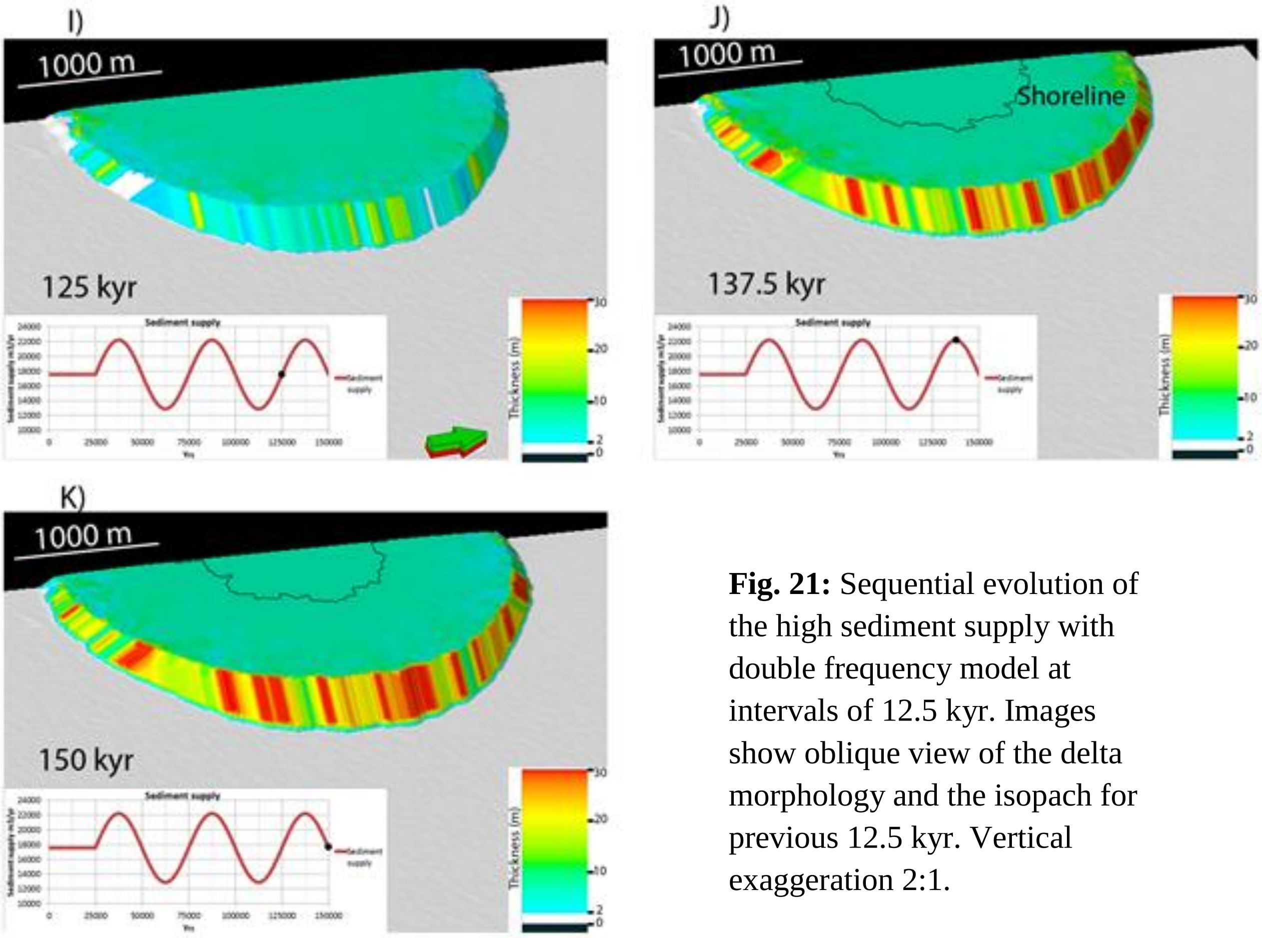

Fig. 21: Sequential evolution of the high sediment supply with double frequency model at intervals of 12.5 kyr. Images show oblique view of the delta morphology and the isopach for previous 12.5 kyr. Vertical exaggeration 2:1.

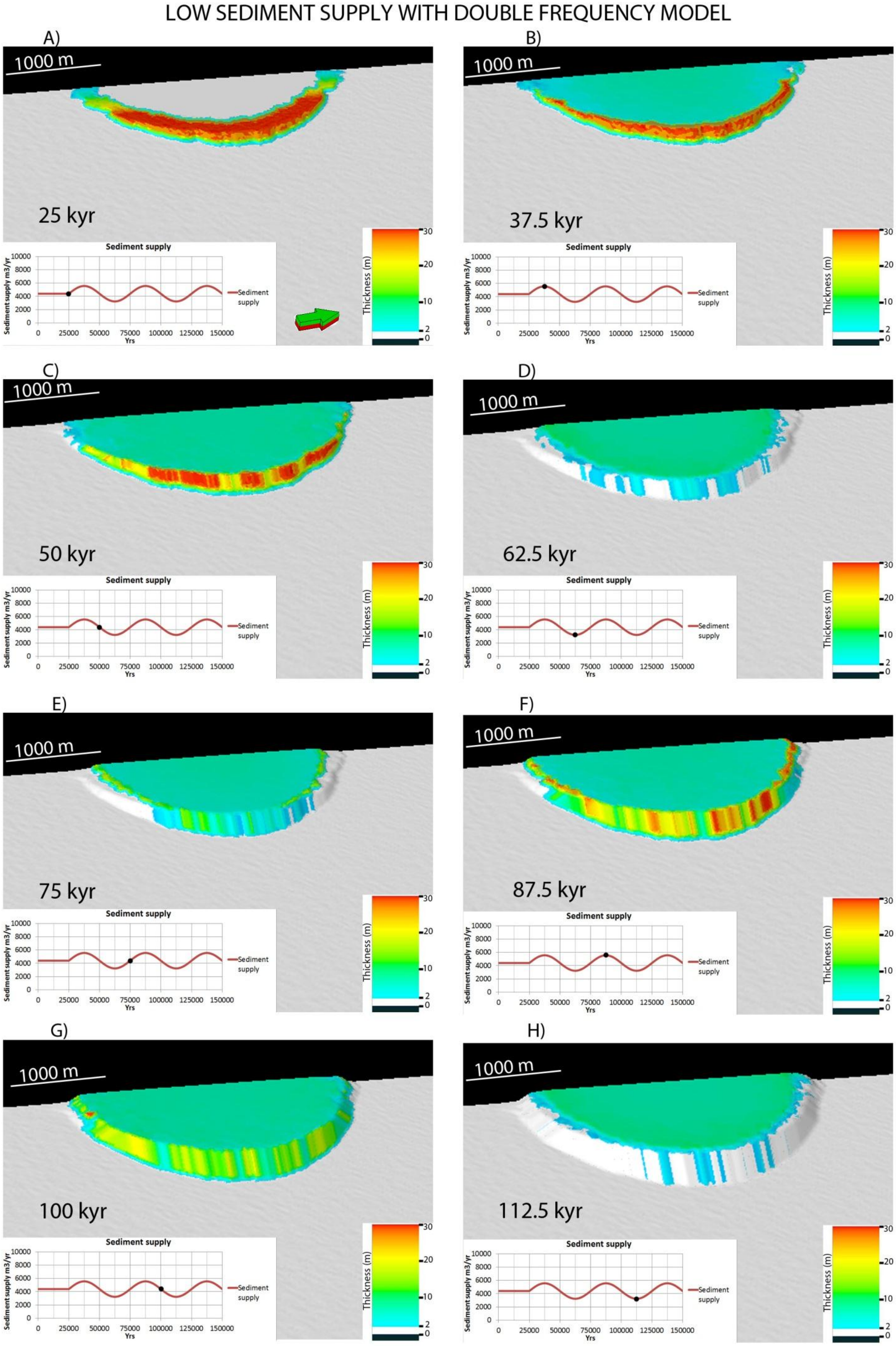
LOW SEDIMENT SUPPLY WITH DOUBLE FREQUENCY MODEL
A)
1000 m
25 kyr
B)
1000 m
37.5 kyr
C)
1000 m
50 kyr
D)
1000 m
62.5 kyr
E)
1000 m
75 kyr
F)
1000 m
87.5 kyr
G)
1000 m
100 kyr
H)
1000 m
112.5 kyr
Sediment supply
Sediment supply m3/yr
Yrs
Thickness (m)

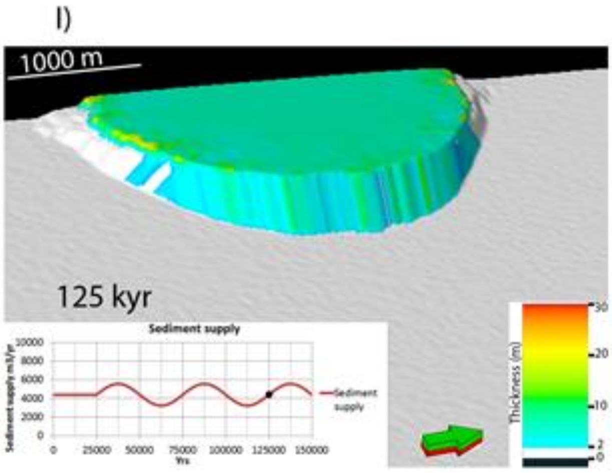

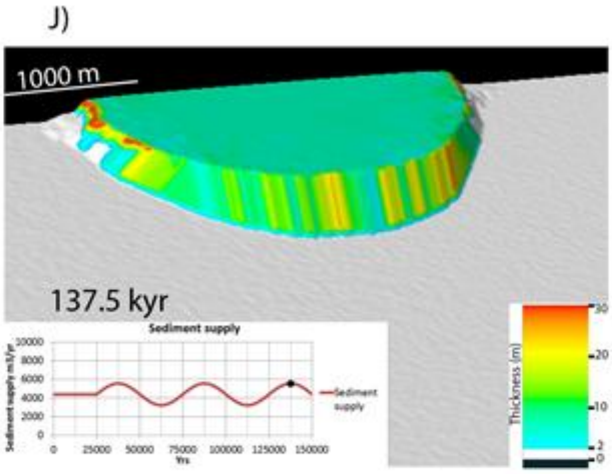

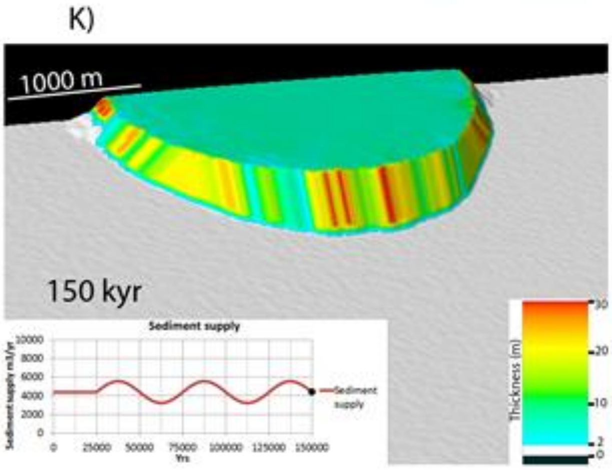

Fig. 22: Sequential evolution of the low sediment supply with double frequency model at intervals of 12.5 kyr. Images show oblique view of the delta morphology and the isopach for previous 12.5 kyr. Vertical exaggeration 2:1.

HIGH SEDIMENT SUPPLY WITH HIGHEST FREQUENCY MODEL

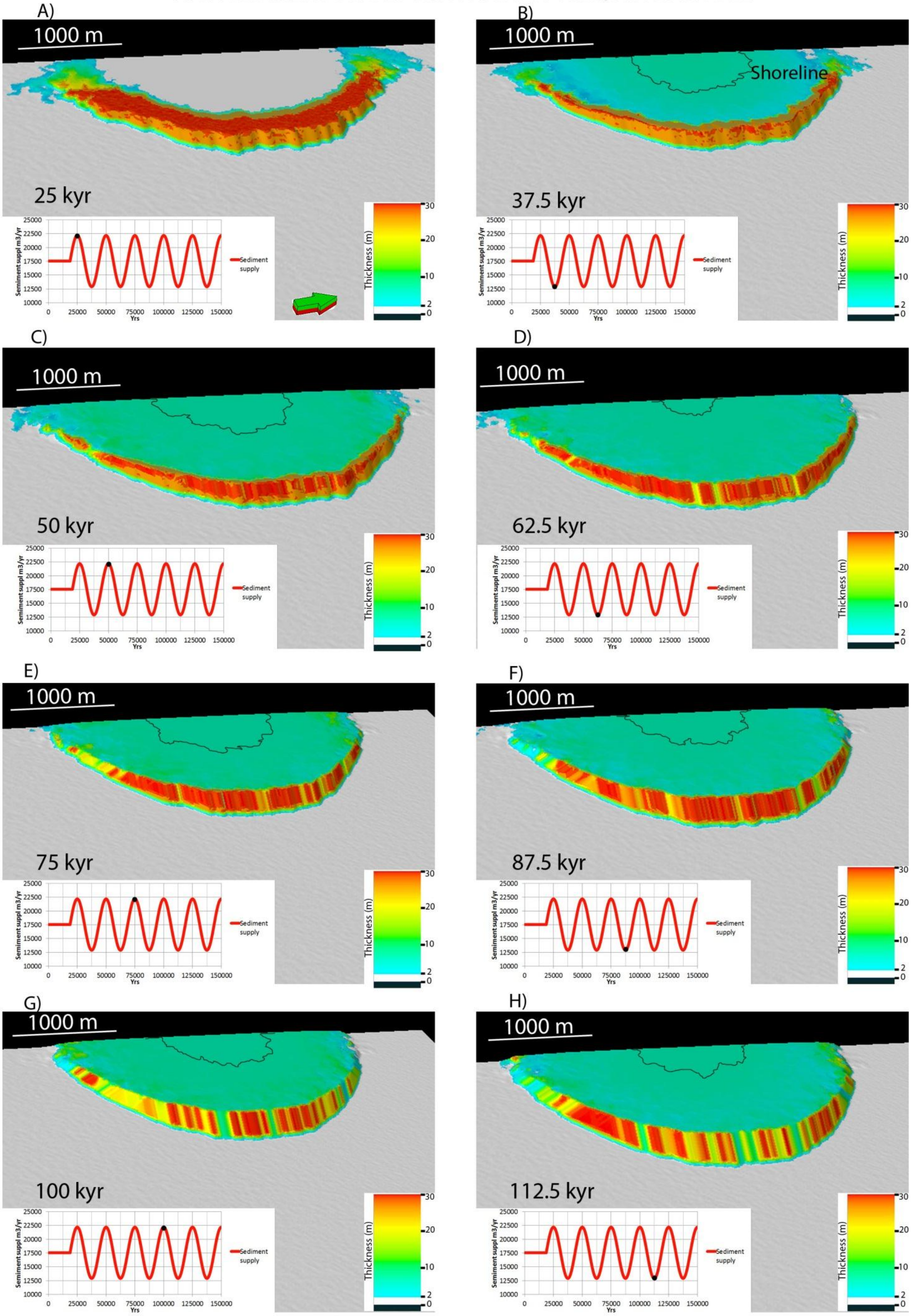

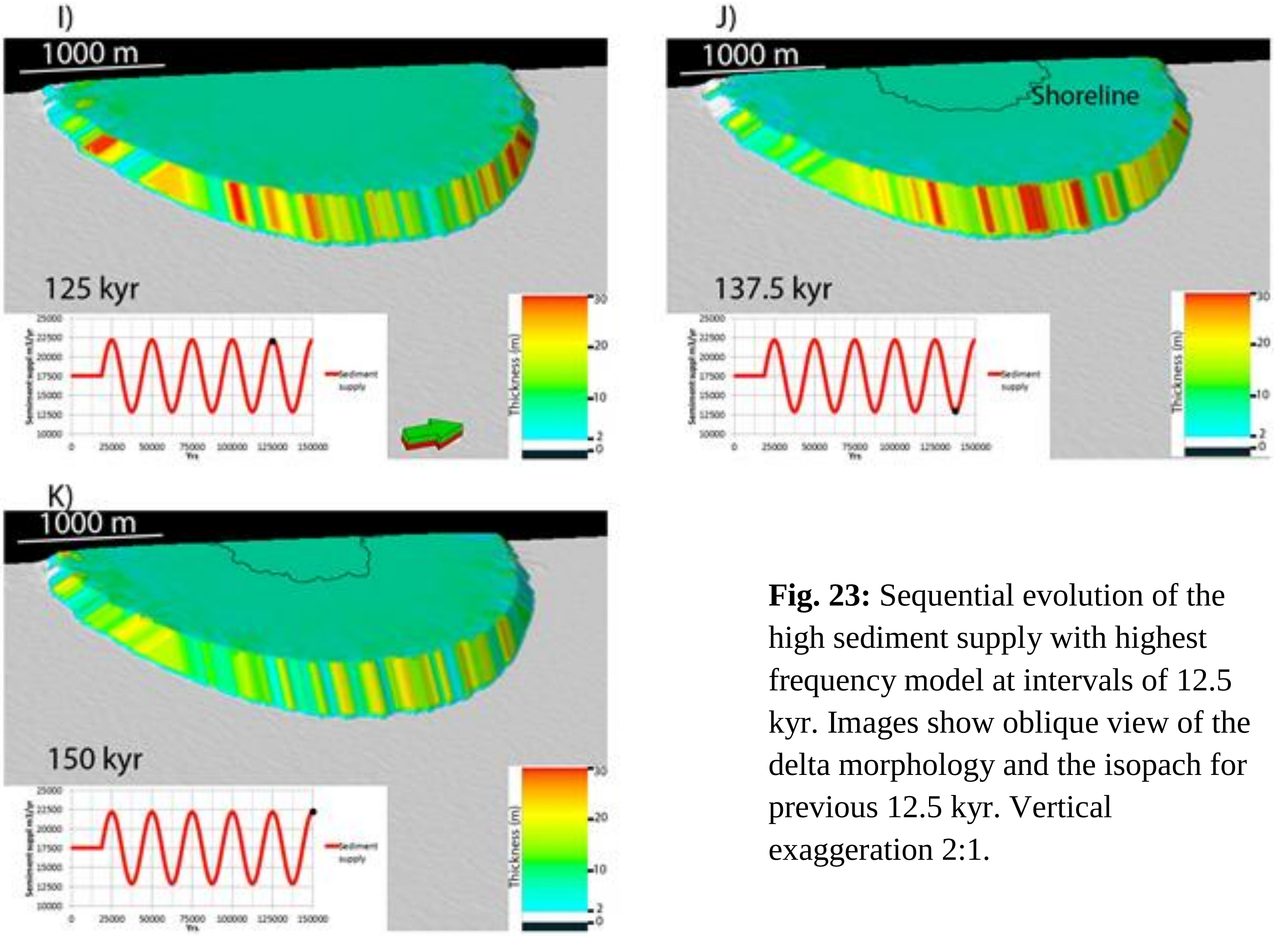

Fig. 23: Sequential evolution of the high sediment supply with highest frequency model at intervals of 12.5 kyr. Images show oblique view of the delta morphology and the isopach for previous 12.5 kyr. Vertical exaggeration 2:1.

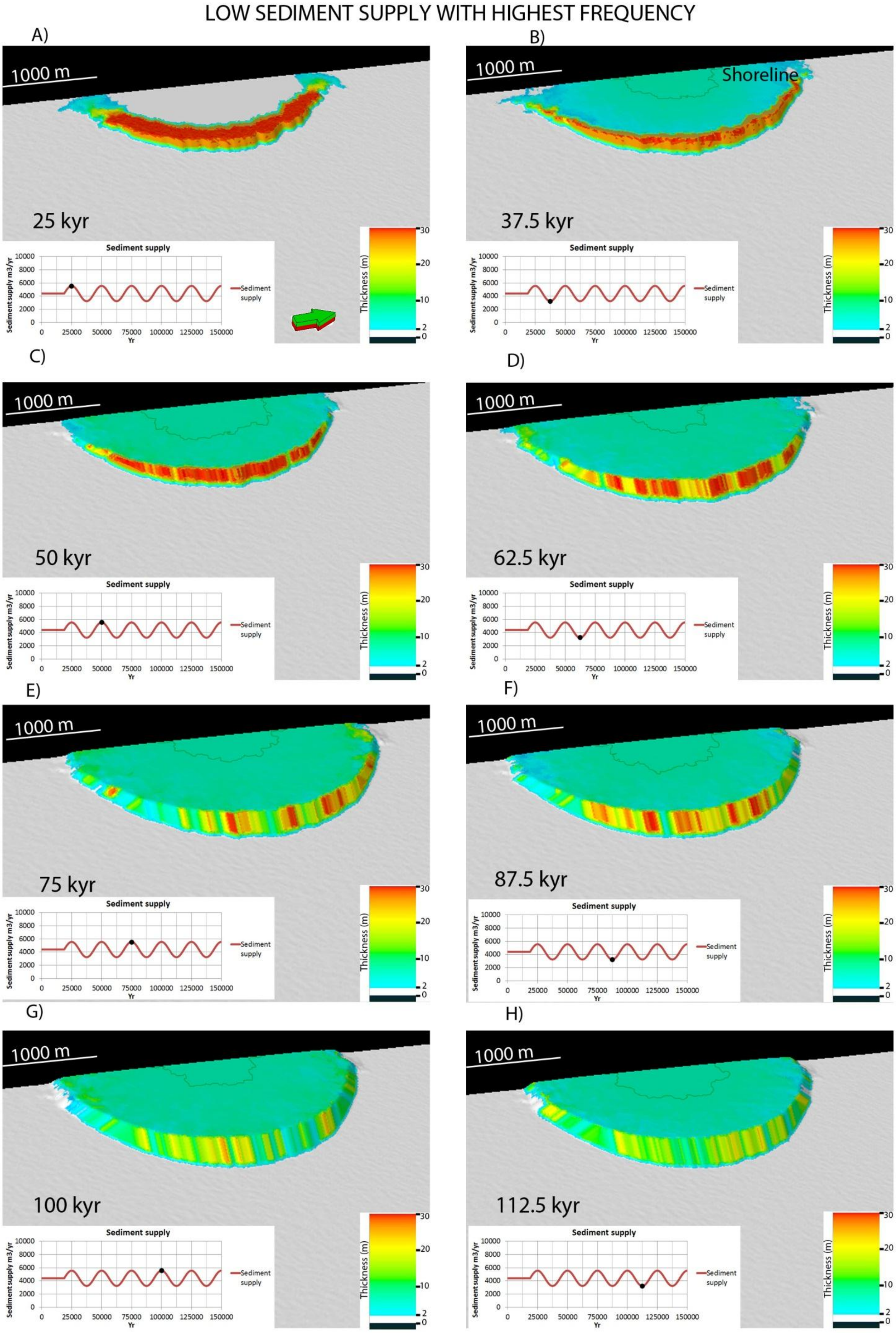
LOW SEDIMENT SUPPLY WITH HIGHEST FREQUENCY
A)
1000 m
25 kyr
Sediment supply
Sediment supply m3/yr
Yr
Sediment supply
Thickness (m)
B)
1000 m
Shoreline
37.5 kyr
C)
1000 m
50 kyr
D)
1000 m
62.5 kyr
E)
1000 m
75 kyr
F)
1000 m
87.5 kyr
G)
1000 m
100 kyr
H)
1000 m
112.5 kyr

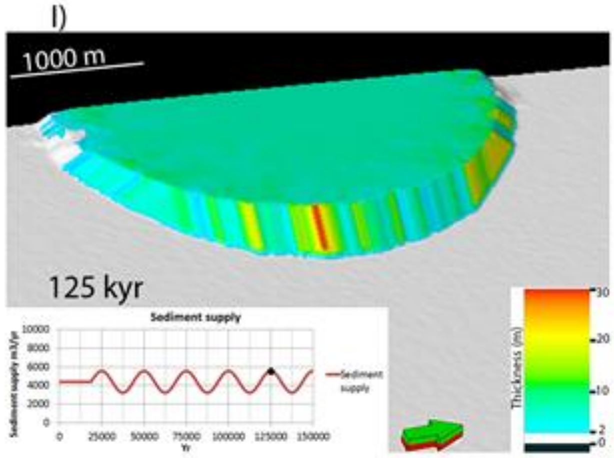

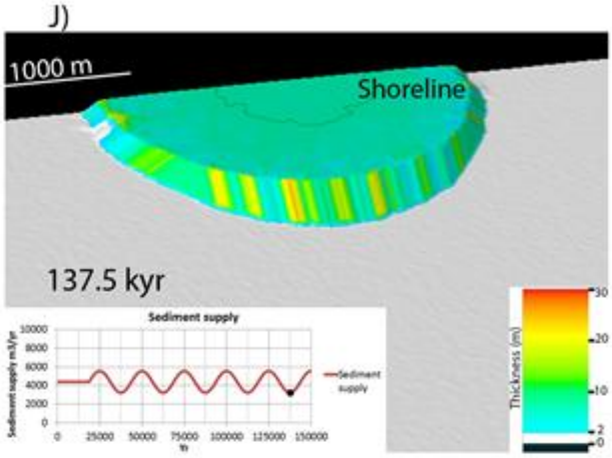

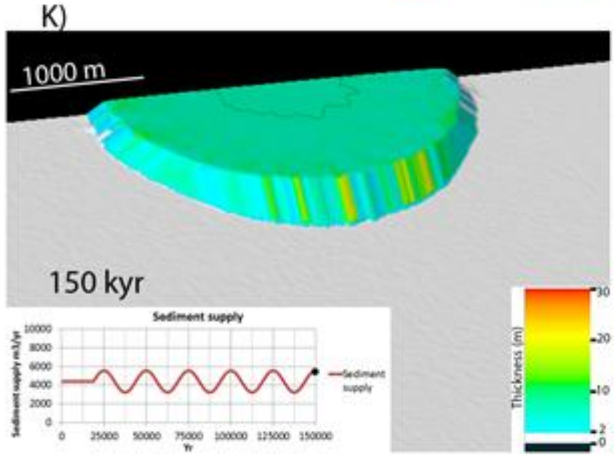

Fig. 24: Sequential evolution of the low sediment supply with highest frequency model at intervals of 12.5 kyr. Images show oblique view of the delta morphology and the isopach for previous 12.5 kyr. Vertical exaggeration 2:1.

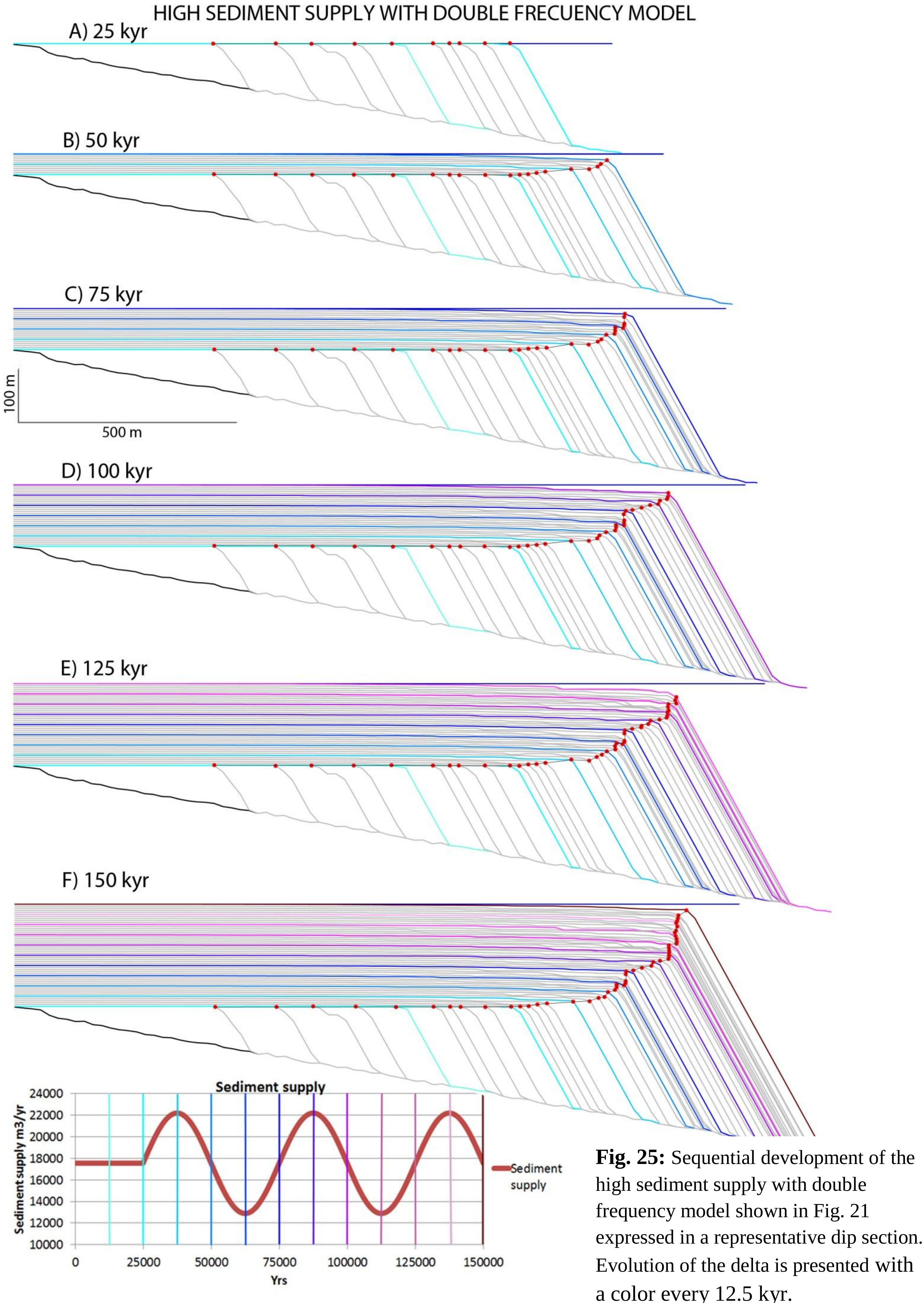

Fig. 25: Sequential development of the high sediment supply with double frequency model shown in Fig. 21 expressed in a representative dip section. Evolution of the delta is presented with a color every 12.5 kyr.

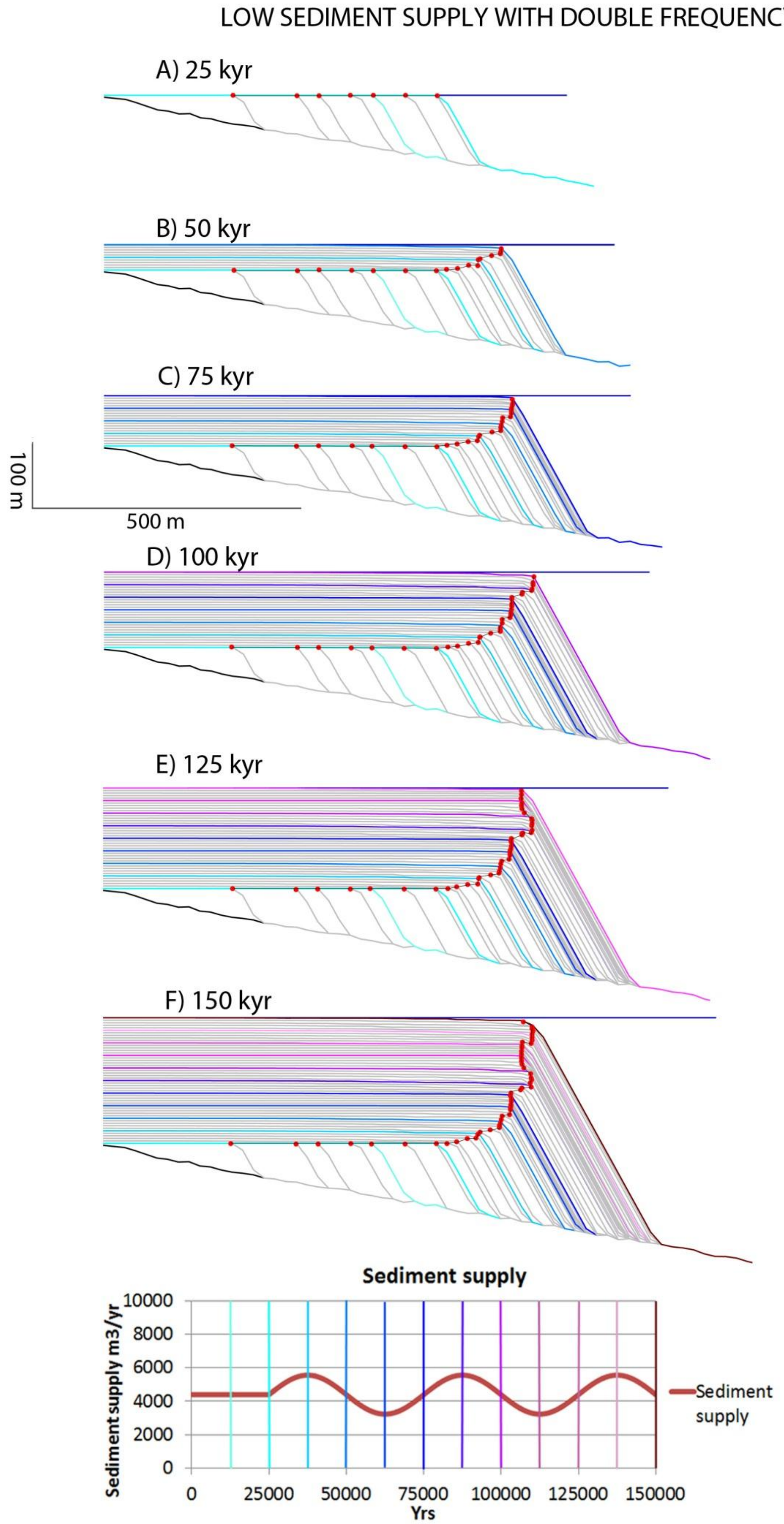

Fig. 26: Sequential development of the low sediment supply with double frequency model shown in Fig. 22 expressed in a representative dip section. Evolution of the delta is presented with a color every 12.5 kyr.

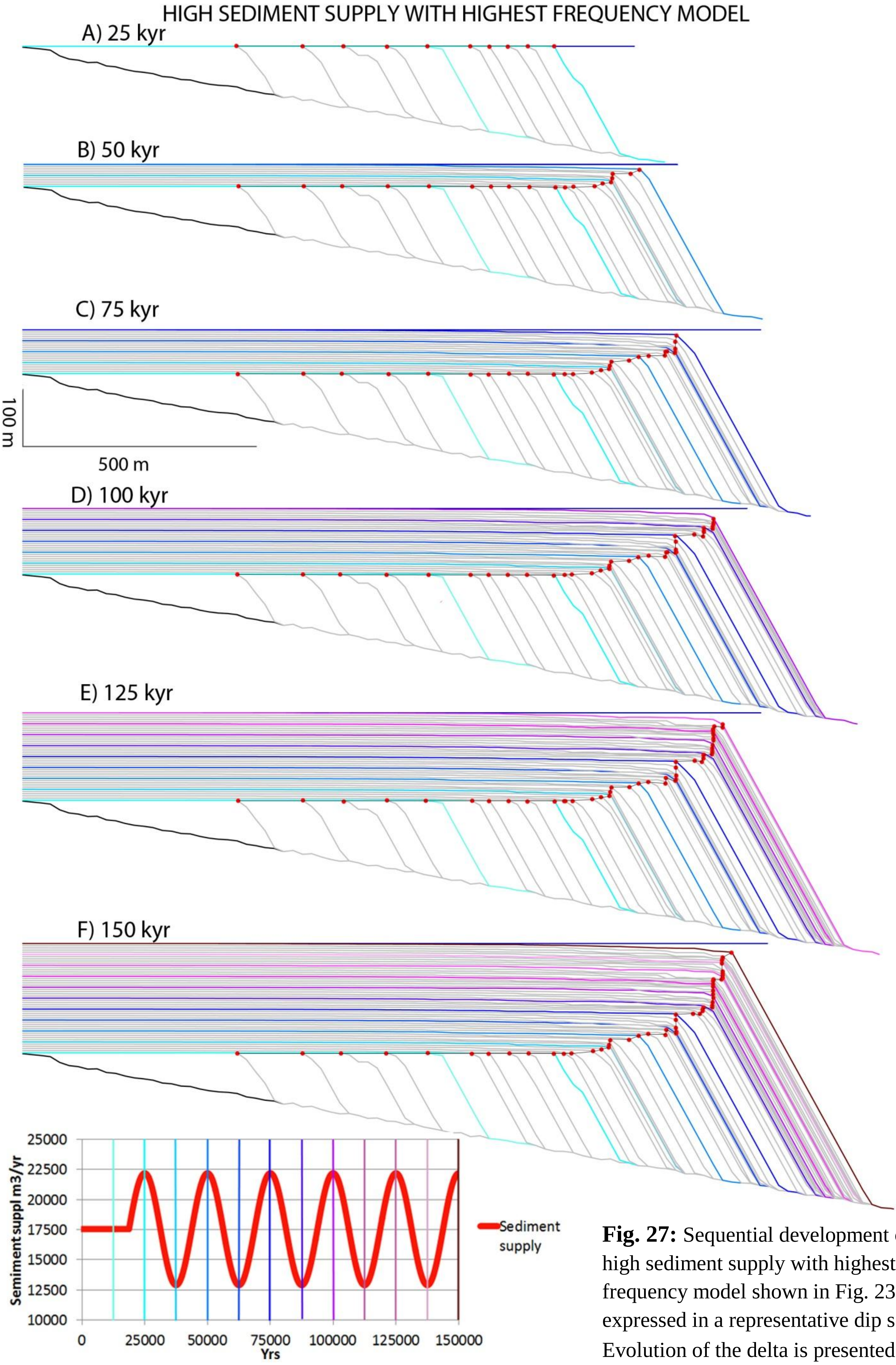

Fig. 27: Sequential development of the high sediment supply with highest frequency model shown in Fig. 23 expressed in a representative dip section. Evolution of the delta is presented with a color every 12.5 kyr.

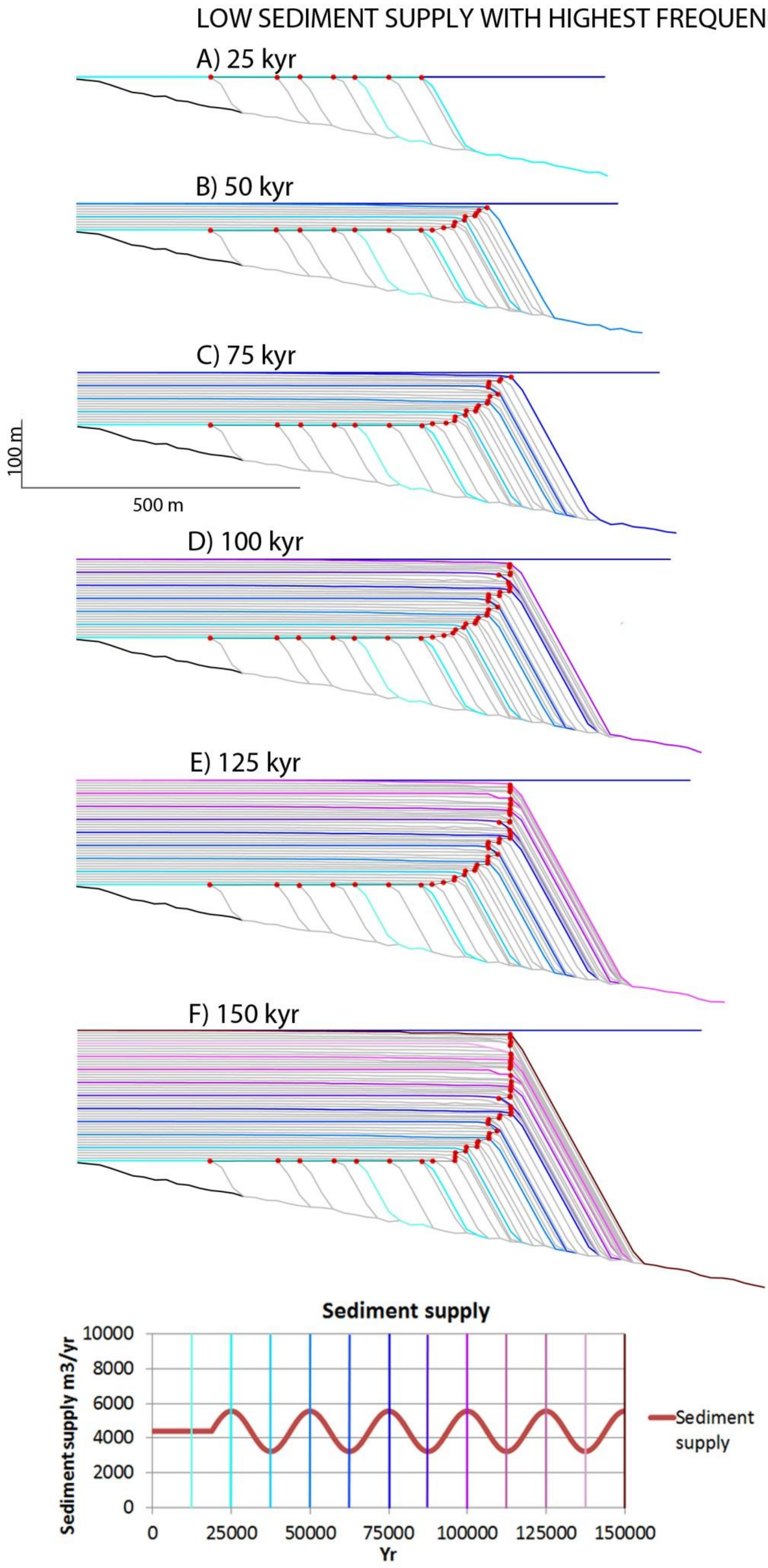

Fig. 28: Sequential development of the low sediment supply with highest frequency model shown in Fig. 24 expressed in a representative dip section. Evolution of the delta is presented with a color every 12.5 kyr.

Model:	25 kyr	50 kyr	75 kyr	100 kyr	125 kyr	150 kyr	Total amount sediment added
Reference model: Basinward expansion (m)	875	1039,5	1107,9	1089,5	1089,5	1092,1	67 672 876 m3
Reference model: Maximum Thickness (m)	137,4	192,3	236,3	274,7	313,2	357,15	
High sediment supply model: BE (m)	1131,6	1368,4	1447,4	1486,8	1486,8	1506,6	135 345 467 m3
High sediment supply model: MT (m)	175,8	236,3	285,7	325,3	368,1	412,1	
Low sediment supply model: BE (m)	615,8	730,3	790,5	769,7	776,3	790,5	33 840 638 m3
Low sediment supply model: MT (m)	98,9	153,8	197,8	236,3	274,7	307,7	
Double frequency model: BE (m)	875	1029	1029	1085,5	1089,5	1105,3	67 521 652 m3
Double frequency model: MT (m)	137,4	186,8	219,8	276,9	313,2	355	
Highest frequency model: BE (m)	911,8	1013,15	1052,6	1072,4	1109,2	1109,2	66 136 364 m3
Highest frequency model: MT (m)	142,85	186,8	230,75	269,23	313,2	357,15	
High sed. Supply with double frequency: BE (m)	1131,6	1352,6	1394,7	1493,4	1506,6	1526,3	135 343 139 m3
High sed. Supply with double frequency: MT (m)	175,8	233	280,2	329,7	362,6	412,1	
High sed. Supply with highest frequency: BE (m)	1138,2	1302,6	1388,2	1464,5	1484,2	1500	132 572 572 m3
High sed. Supply with highest frequency: MT (m)	173,6	230,8	280,2	324,2	364,8	406,6	
Low sed. Supply with double frequency: BE (m)	615,8	730,3	756,6	790,5	769,7	776,3	33 840 056 m3
Low sed. Supply with double frequency: MT (m)	98,9	148,4	192,3	236,3	274,7	307,7	
Low sed. Supply with highest frequency: BE (m)	618,4	730,3	773,7	773,7	773,7	773,7	33 147 106 m3
Low sed. Supply with highest frequency: MT (m)	99	148,4	194,5	230,8	269,2	313,2	

Table. 12: Overview of the nine different models basinward expansion and their maximum thickness. In addition, an overview of how much sediment is supplied to the model during run time. *Note:* See section; 1.3 Approach and methodology for the description of measurements.

Chapter Five - Sequence stratigraphic response to different sediment supply with sinusoidal sea-level

To illustrate the influence of sediment supply, three different models will be presented. All three subject with a sea-level cycle with 25 m amplitude. It will be used the same amount of sediment supply as the reference model (8775 m^3/yrs), where the models have a constant sediment supply, in-phase sediment supply (relative to sea level cycle) and an out-phase sediment supply. The total run times for the models are 200 kyr. All other model parameters are the same as for the reference model. In each model run, the sediment supply and sea-level was kept constant for the first 25 kyr.

5.1 Description for constant sediment supply model

During the initial stage of the model run (0-25 kyr), the deposition architecture at the constant sediment supply delta are likewise as the reference model, with deposition occurs as a continuous fringe along the delta front and with no topsets development (Fig. 29A). The delta builds out basinward by 875 m and has a maximum thickness at 137.4 m (Table. 16).

From 25 kyr, the constant sediment supply model start with a sea-level rise of 25 m over the next 25 kyr. The delta starts developing topsets, due to available accommodation space. Detailed analysis of the model results indicates that the delta is aggraditional to progradational, with a progressively steeper basinward-climbing break-point trajectory (Fig. 30D), as the rate of sea-level rise slows towards zero at 50 kyr (sea-level highstand). The majority of the sediment has been deposited on the right side of the delta front (from up-dip view), but significant amounts of sediments have also been deposited on the delta plain. The left side of the delta front got no sediment deposited. At the time the delta reaches the sea level highstand (at 50 kyr), the delta has prograde basinward by 89.3 m and have increased its maximum thickness by 55.4 m (Table 16).

Between 50 kyr and 100 kyr, sea level falls by 50 m. During the initial period of sea-level fall from 50 to 62.5 kyr, two delta lobes (labeled 1 and 2; Fig. 29D) begin to form, supplied by channels. These lobes are spaced approximately 1400 m apart, attached to the delta front, and lack topset development, and have a basinward-falling break-point trajectory (Fig. 30C, E). Deposition occurs as a continuous fringe along the delta front, deposition focused on the channel mouths as the delta plain is exposed (Fig. 29D).

As sea level continues to fall from 62.5 to 75 kyr, the main channel changes direction from flowing towards lobe 1, to create lobe 3 at the left side of the delta. Lobe 1 still gets sediment and continues to build basinward, while lobe 2 receives no sediment and becomes inactive (Fig. 29E). Lobe 3 which is spaced approximately 1900 m apart from Lobe 1, receive most of the sediments as the channels incise into the exposed delta front and feeding lobe 3 and 1 (Fig. 29E). Between 50 and 75 kyr the delta have progressively steeper basinward-climbing break-point trajectory (prograditional to aggraditional) (Fig. 30C), with an average foreset thickness from 50 to 62.5 kyr at 10.7 m (Table. 13). Between 62.5 and 75 kyr, there have been no deposition along the delta front. The deposition between 50 to 62.5 kyr results that the delta has expanded basinward by 62.5 m and increased its maximum thickness by 7.2 m (Table. 16).

As sea-level fall continues towards lowstand at 100 kyr, the main channel continue to grow as it cut back towards the sediment source and capture more flow. As a result, lobe 1 become inactive, and the main channel distribute all the sediments to lobe 3 which is expanding between 75 and 100 kyr (Fig. 29F, G). In this period, the channels have been eroding the exposed delta front and delta plain, which makes the delta retreat 5.4 m (Table 16).

Thickness and height of foresets at constant sediment supply model			
	Average foresets thickness (m)	Foresets heigth (m)	Topsets height (m)
12.5 kyr	**67**	**88.9**	0
25 kyr	**38.5**	**127.8**	0
37.5 kyr	**13,6**	**142.8**	28,6
50 kyr	**13,6**	**178.6**	21
62.5 kyr	**10,7**	**192.9**	0
75 kyr	N/A	N/A	0
87.5 kyr	N/A	N/A	0
100 kyr	N/A	**200**	0
112.5 kyr	N/A	N/A	0
125 kyr	N/A	**192.8**	0
137.5 kyr	N/A	N/A	0
150 kyr	N/A	**214.3**	0
162.5 kyr	N/A	N/A	0
175 kyr	N/A	**207.1**	0
187.5 kyr	N/A	N/A	0
200 kyr	N/A	N/A	0

N/A; unable to measure

Table. 13: Results from measuring the forsets average thickness, height of the foresets and topsets height of the constant sediment supply model. In contrast to chapter four where the sinusoidal cycle of sea level change not occurred, there are minimal measurements that could be done along the main dip profile line of the constant sediment supply model.

Following sea-level lowstand at 100 kyr, sea-level rises until 150 kyr, with a rate of maximum rise of 1.4 m/kyr occurring between 112.5 and 137.5 kyr. Initially lobe 3 that developed during the preceding sea-level fall continue to grow , and the isopach show that the lobe expand laterally and infilling relict topography around the lobe that were starved of sediment during the sea-level fall (Figs. 29H, I, Fig. 31E).The stratal geometries within the lobe are aggraditional to progradational to aggraditional, with a basinward-climbing break-point trajectory, during the early part of sea-level rise (Fig. 32E; Fig. 33E). The main channel incised increasingly deeper as the delta plain is still exposed (Fig. 29H, I). At the time 125 kyr where sea-level are at zero, the delta have retreated 39.3 meters from sea-level lowstand (at 100 kyr) and decreased its maximum thickness by 7.2 m (Table. 16).

As sea-level rise continues from 125 to 150 kyr, the lobe 3 retrogrades and the sediment keep filling the relict topography around the lobe and expanding laterally (Fig. 29J, K). As a result, the deposition is moving landward (retrogradation) and the incised channels become filled (Fig. 29J). At sea-level highstand (at 150 kyr), the relict topography around lobe 3 area are filled and attach to become a huge southeast (green arrow pointing north) going apron. At this time, the delta front that was starved of sediment during the sea-level fall, starts to get sediment deposited (Fig. 29K). As a result, the delta has expanding basinward by 71.5 m and has increased its maximum thickness by 21.5 m (Table. 16).

Following sea-level highstand, where the delta was drowned, sea-level falls until the end of the model run at 200 kyr. As a result of the delta drowning, the channels shift avulsion from right side to the left side of the delta and bringing the locus of deposition along (Fig. 29L, M; Fig. 33G; Fig. 34E). The isopach for 150-162.5 kyr (Fig. 29L) shows that deposition builds up around and on lobe 1, before the deposition branches out from lobe 1, leaving lobe 1 area inactive and creating lobe 4a by 175 kyr (Fig. 29M). Lobe 4a has a basinward direction, is spaced approximately 1200 m apart from the apron, attached to the delta front, lack topset development, and have a basinward-falling break-point trajectory (Fig. 30C, E). Deposition of sediments is focused on the lobe, so the rest of the delta is starved for sediment and the delta plain which is exposed, undergoes erosion by the channels. As a result, the delta has retreated 26.8 m and the delta top has been eroded 7 m (Table. 16).

From 175 kyr and throughout the model run (200 kyr), the sea-level fall from 0 to -25 m and reaching sea-level lowstand. Channels have during this period incised the exposed delta, and supplied lobe 4 (Fig. 29N, O). Lobe 4 have at 200 kyr branched out three times (Labeled 4a, b and c), and leave the abandoned lobes (4a, b) inactive, where the sediment just by-passed the lobes and deposited sediment at lobe 4c (Fig. 29O). The lobes all have an east direction (green arrow), fingerlike shape and are expanded approximately 900 m basinward from the delta front (Fig. 32H). Lobe 4c lies ahead of main dip line profile, which not allows precise measurements of the basinward expansion and maximum thickness (Table. 16).

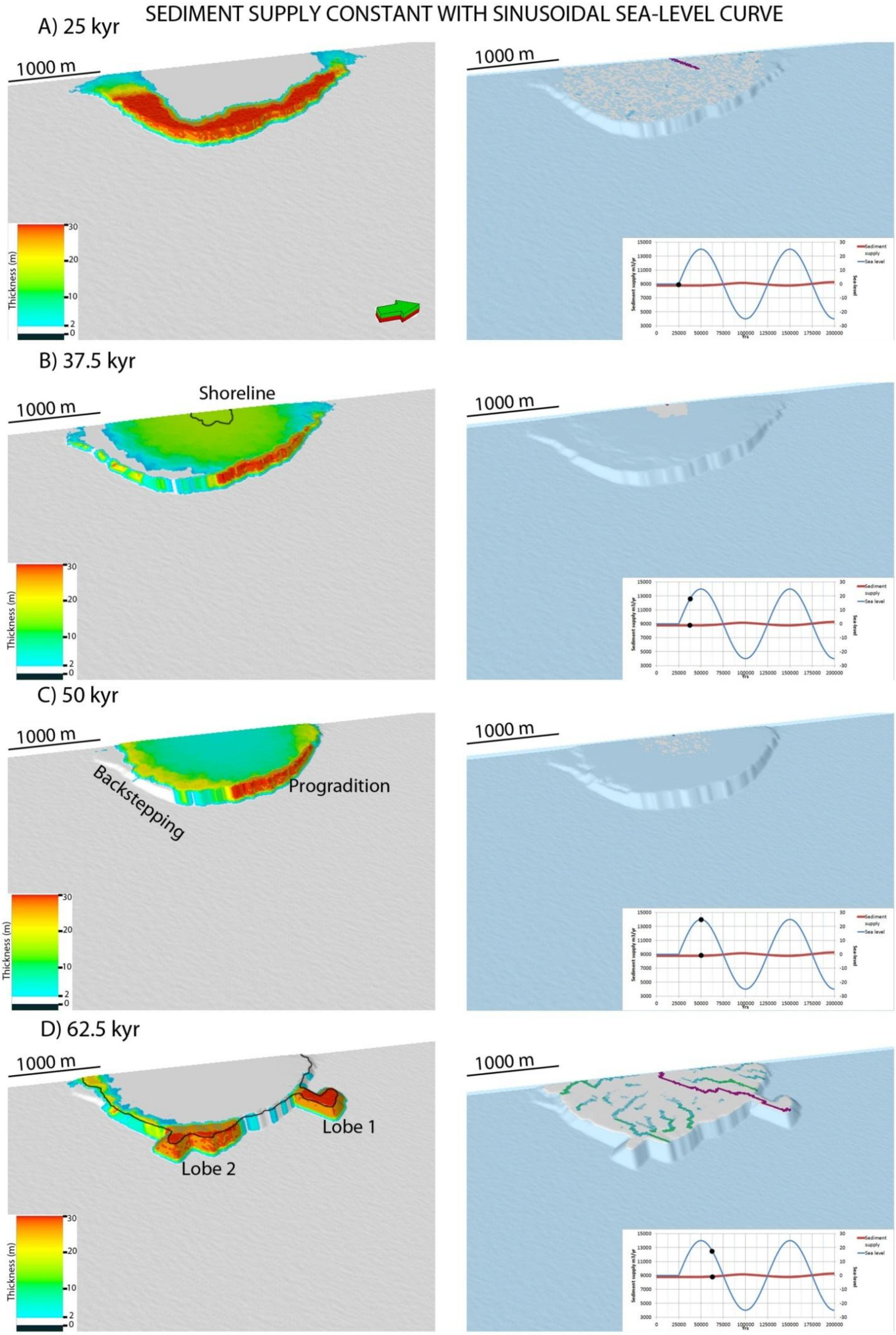
SEDIMENT SUPPLY CONSTANT WITH SINUSOIDAL SEA-LEVEL CURVE
A) 25 kyr
B) 37.5 kyr
C) 50 kyr
D) 62.5 kyr
1000 m
Thickness (m)
Shoreline
Backstepping
Progradition
Lobe 1
Lobe 2
Sediment supply
Sea level

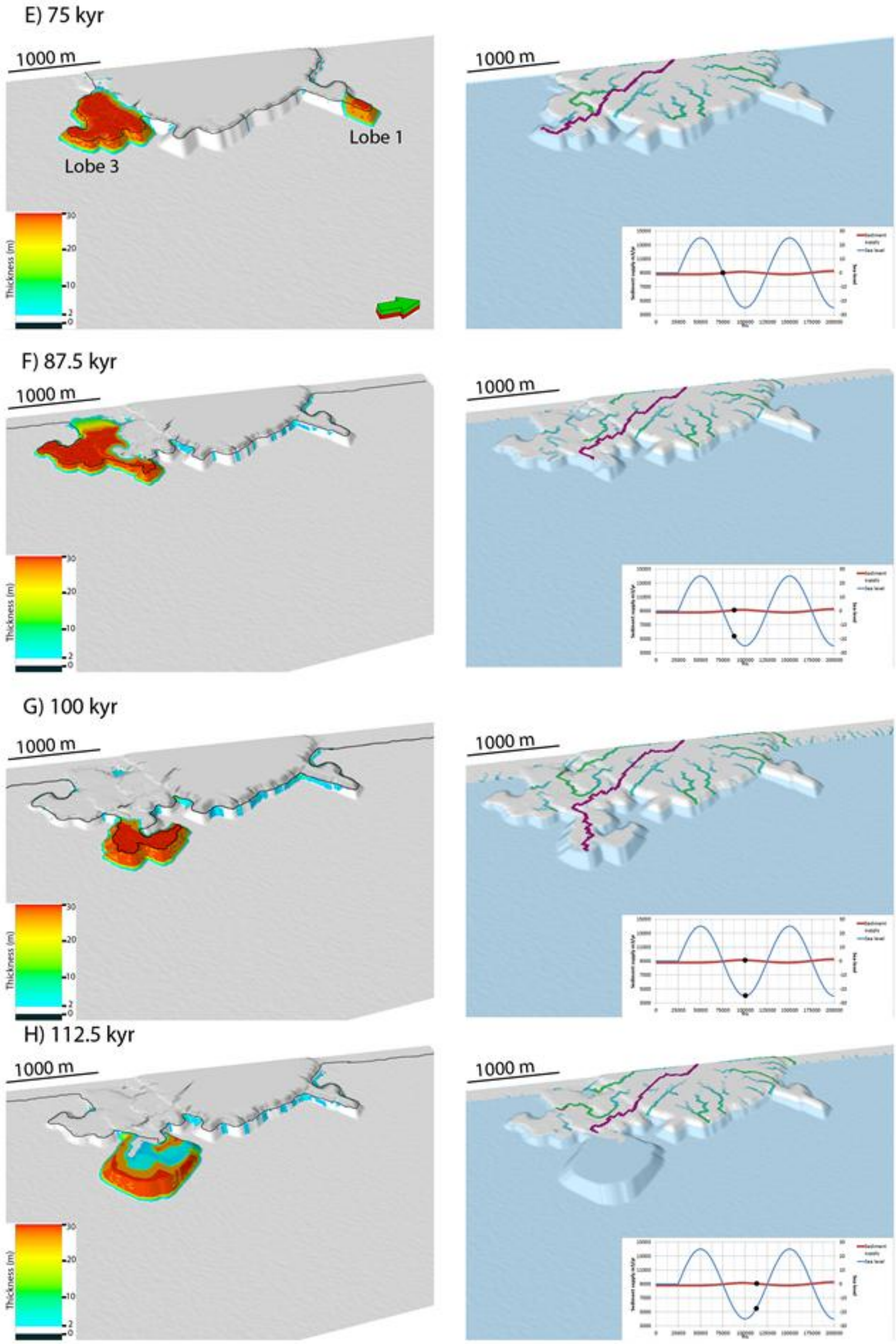
E) 75 kyr
1000 m
Lobe 3
Lobe 1
Thickness (m)
F) 87.5 kyr
1000 m
G) 100 kyr
1000 m
H) 112.5 kyr
1000 m

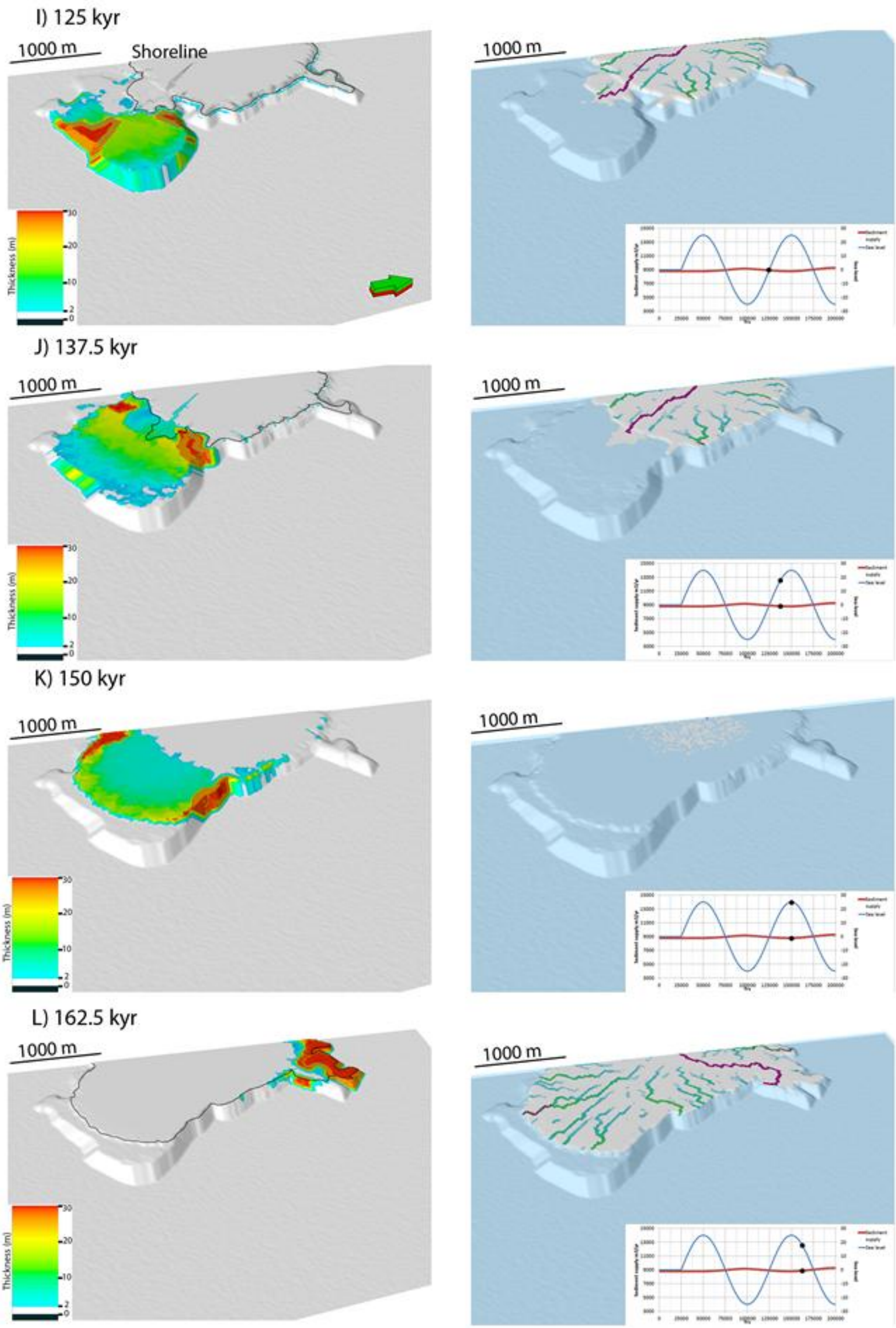
I) 125 kyr
1000 m
Shoreline
Thickness (m)
30
20
10
2
0
J) 137.5 kyr
K) 150 kyr
L) 162.5 kyr

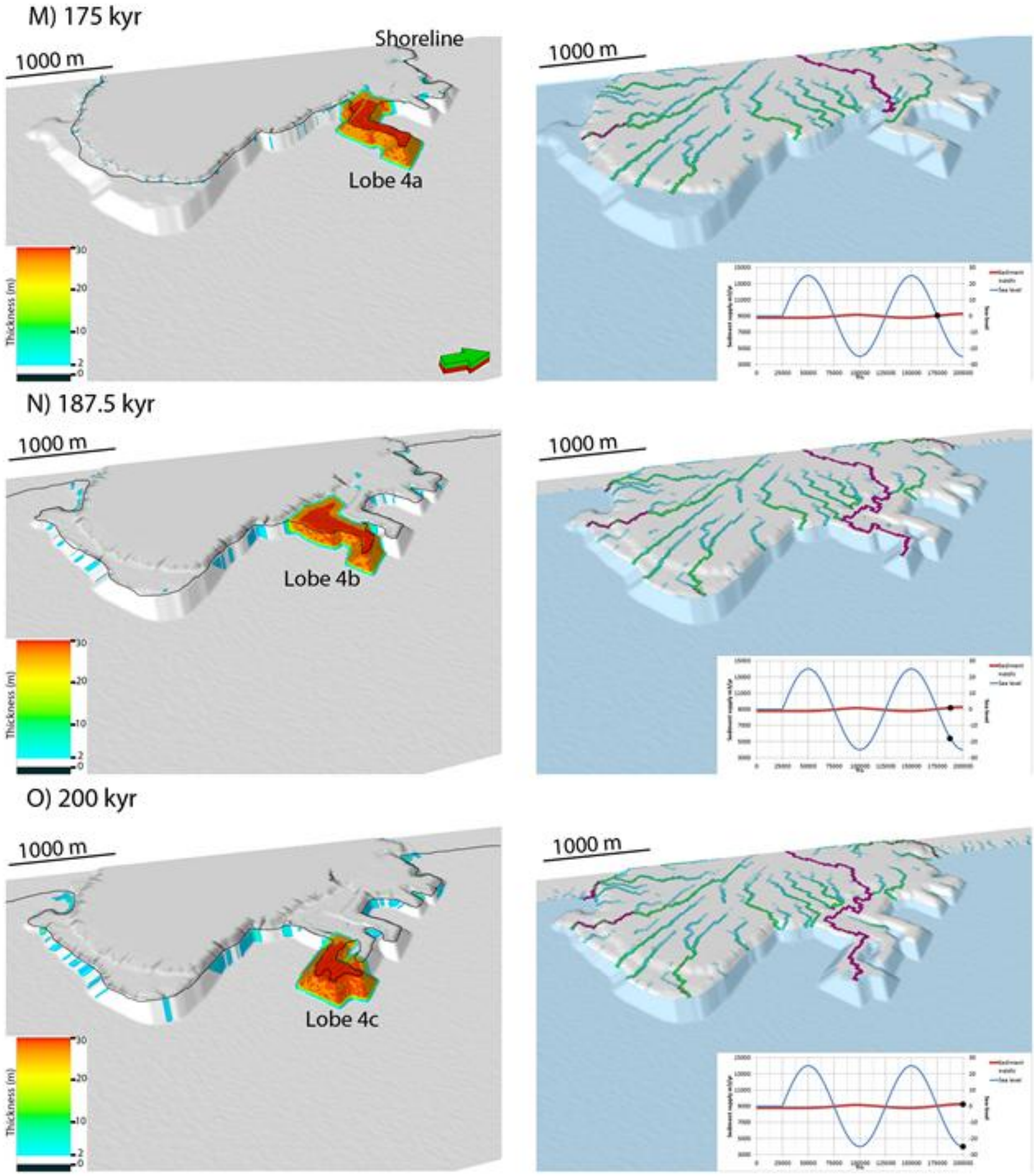

Fig. 29: Sequential evolution of the constant sediment supply model at intervals of 12.5 kyr. Left-hand side shows oblique view of the delta morphology an isopach for previous 12.5 kyr. Shoreline is marked by a black line. Right-hand side shows channel evolution and sea-level (same view as isopach). Vertical exaggeration 2:1.

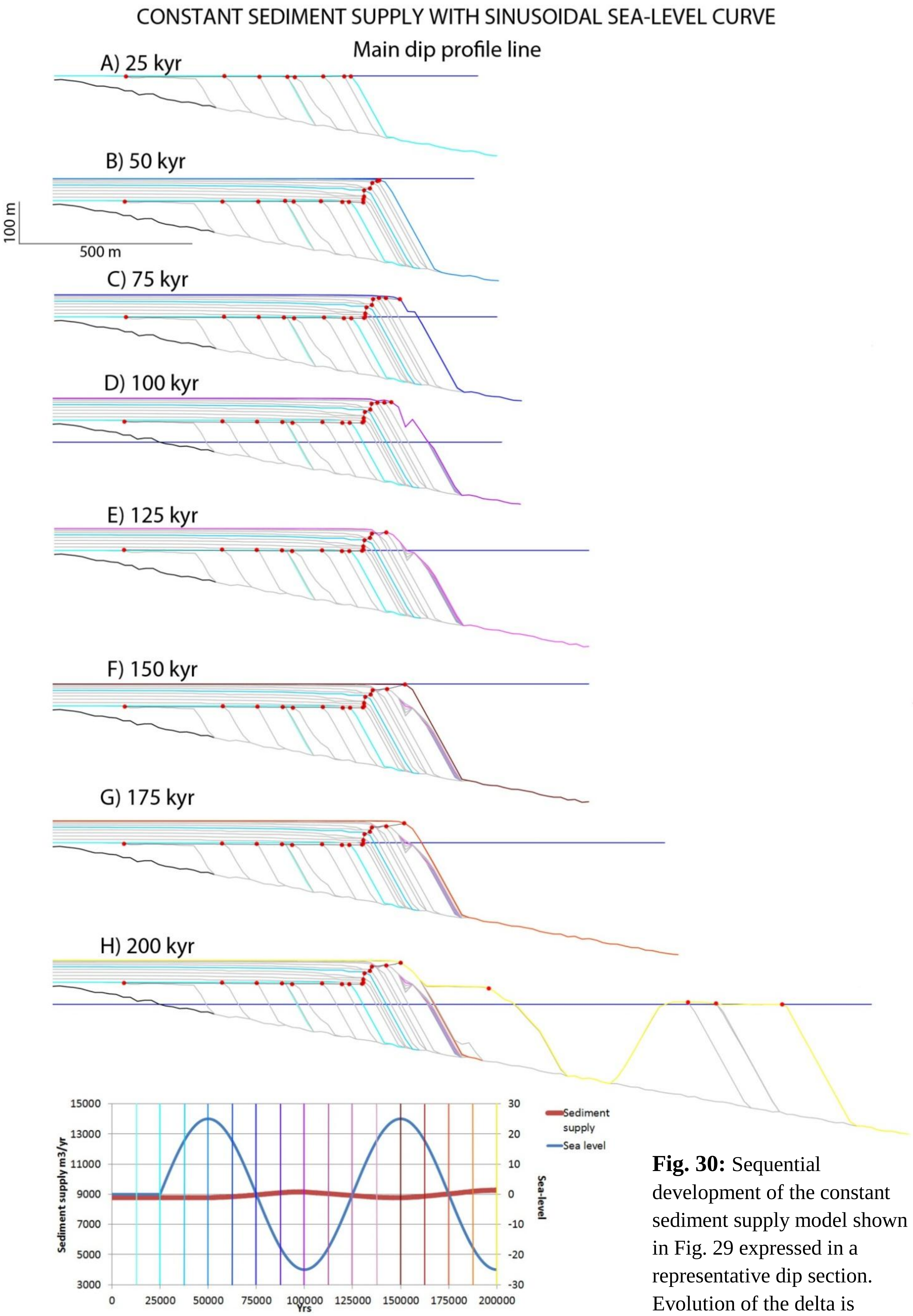

Fig. 30: Sequential development of the constant sediment supply model shown in Fig. 29 expressed in a representative dip section. Evolution of the delta is presented every 25 kyr, with surfaces recorded with a color every 12.5 kyr.

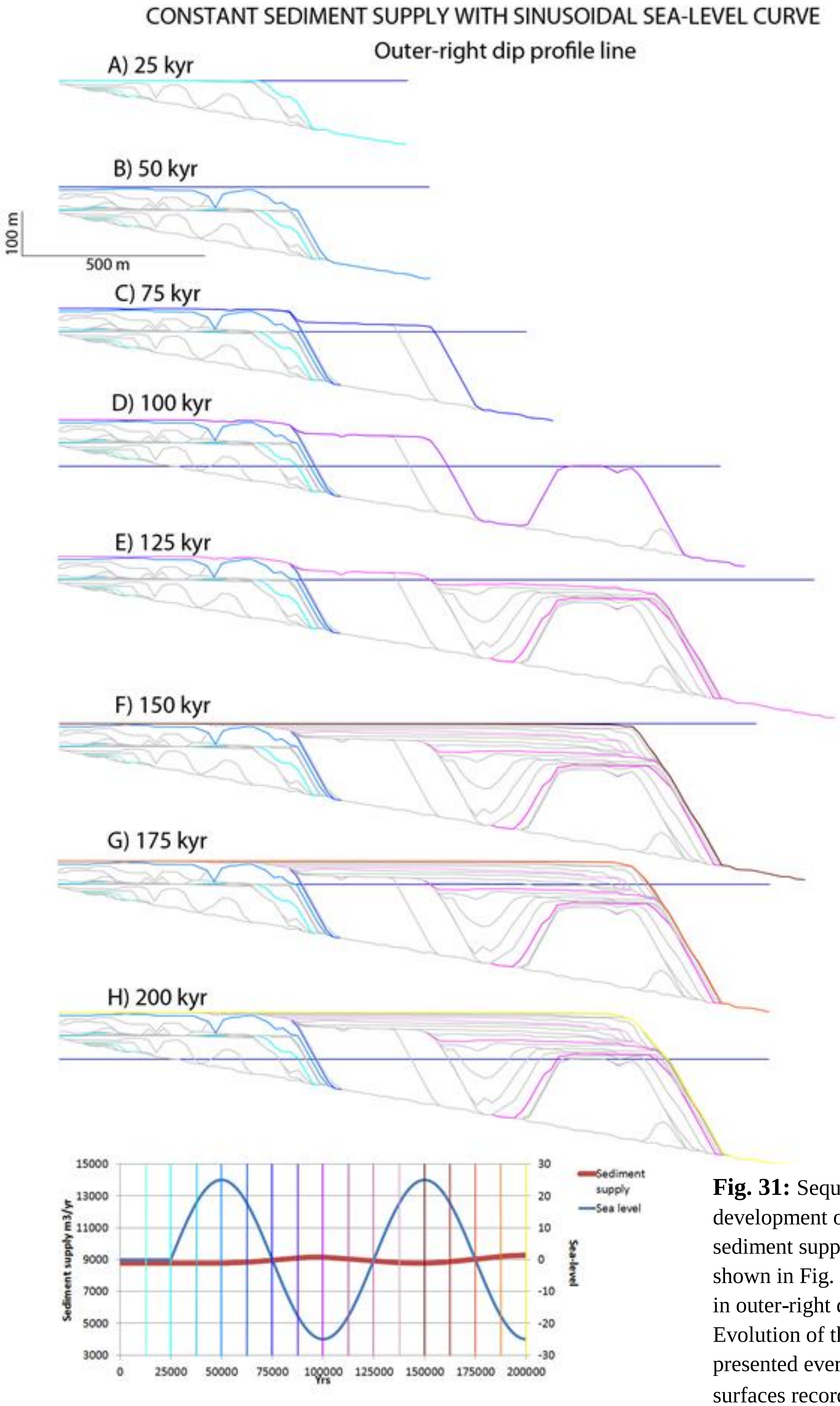

Fig. 31: Sequential development of the constant sediment supply model shown in Fig. 29 expressed in outer-right dip section. Evolution of the delta is presented every 25 kyr, with surfaces recorded with a color every 12.5 kyr.

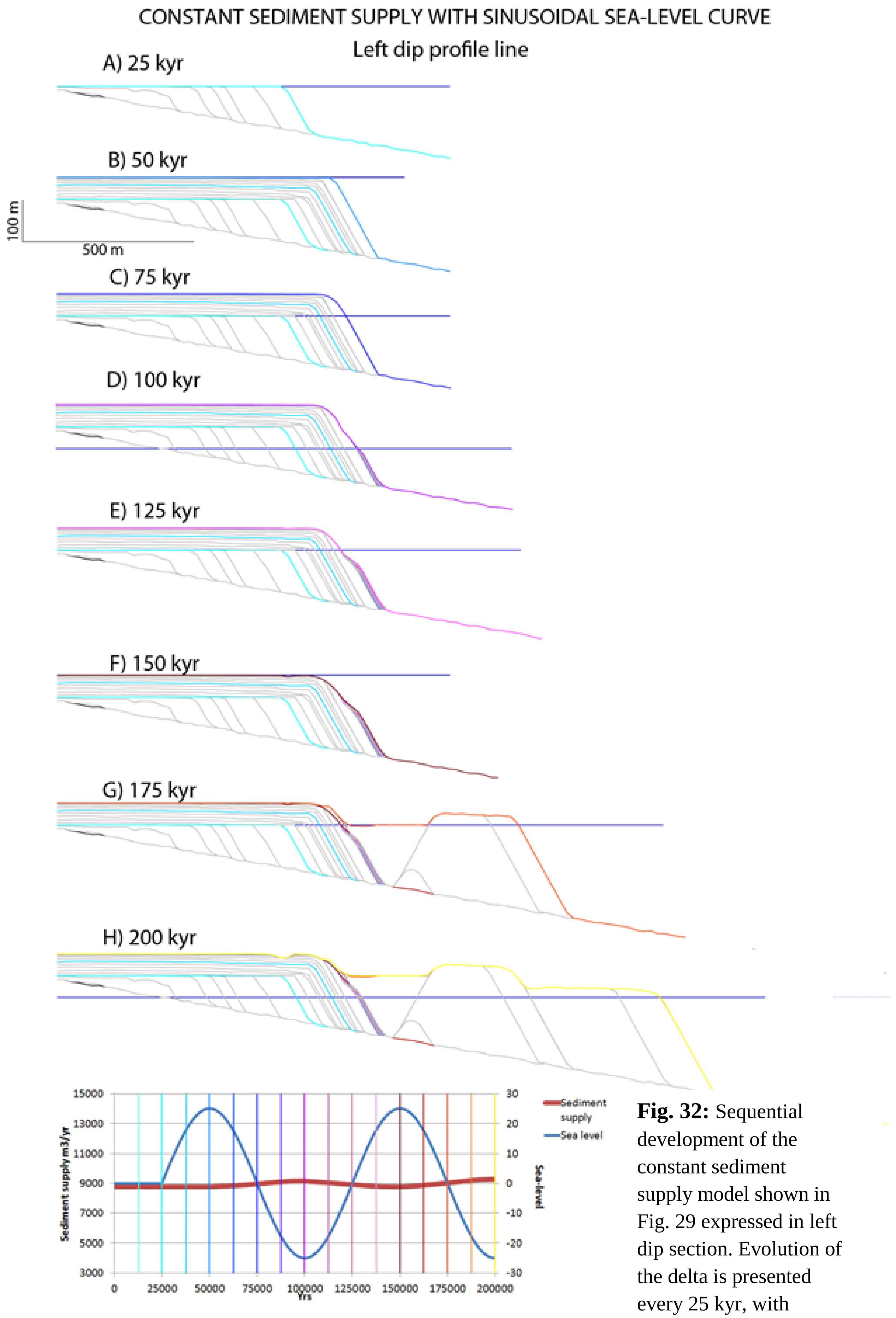

Fig. 32: Sequential development of the constant sediment supply model shown in Fig. 29 expressed in left dip section. Evolution of the delta is presented every 25 kyr, with surfaces recorded with a color every 12.5 kyr.

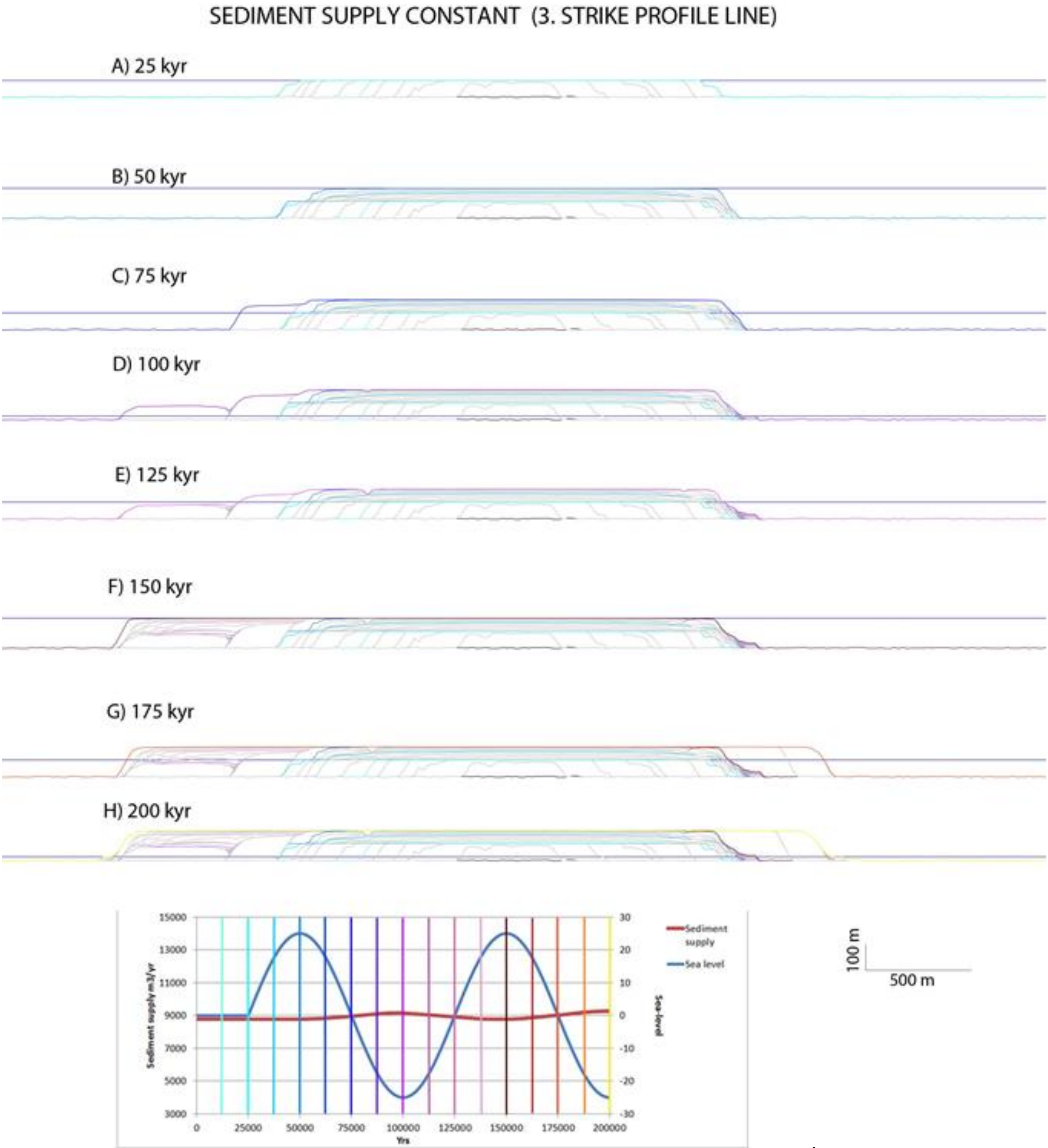

Fig. 33: Sequential development of the constant sediment supply model shown in Fig. 29 expressed in proximal strike section. Evolution of the delta is presented every 25 kyr, with surfaces recorded with a color every 12.5 kyr.

SEDIMENT SUPPLY CONSTANT (6. STRIKE PROFILE LINE)

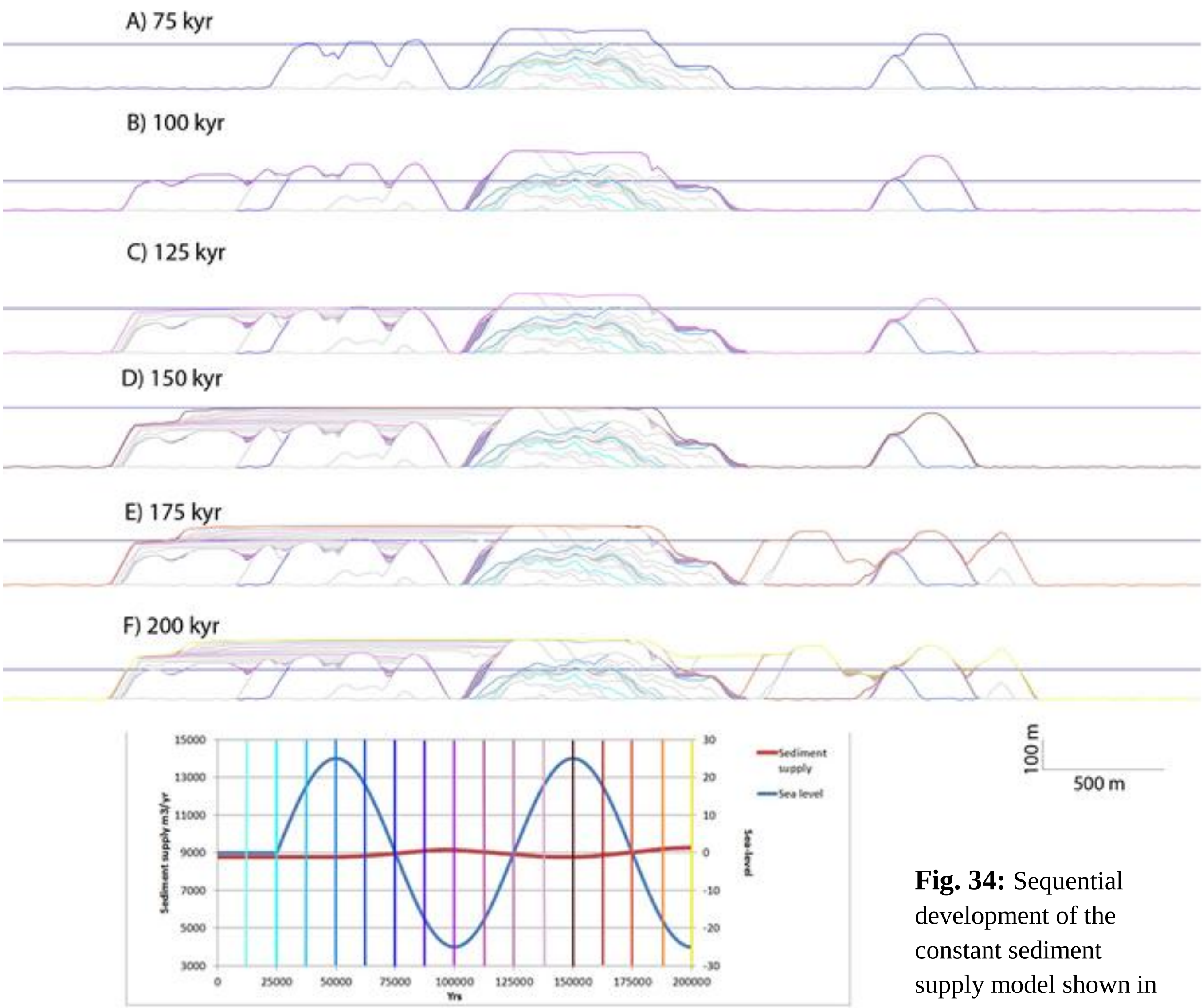

Fig. 34: Sequential development of the constant sediment supply model shown in Fig. 29 expressed distal strike section. Evolution of the delta is presented every 25 kyr, with surfaces recorded with a color every 12.5 kyr.

5.2 Description for in-phase sediment supply model

During the initial stage of the model run (0-25 kyr), the deposition architecture at the in-phase sediment supply delta are likewise the constant sediment supply model, with deposition occurs as a continuous fringe along the delta front and with no topsets development (Fig. 35A). The basinward expansion and maximum thickness are also the same as constant sediment supply model (Table. 16).

From the start of sea level rise and sediment supply at 25 kyr, sea-level will rise by 25 m and the sediment supply would increase to its maximum at 11100 m^3/yr over the next 25 kyr. During the increase in sediment supply and sea-level rise between 25 and 50 kyr, in-phase model show similar features to the constant sediment supply model with progradational to aggradational delta with a progressively steeper basinward-climbing break-point trajectory and transgression (Fig. 35B, C; Fig 36B). However, the sizes differ in detail. The in-phase sediment supply which increases the sediment supply along with sea level rise has expanded 17.8 meters further basinward than the constant sediment supply model at 50 kyr. The maximum thickness of in-phase sediment supply model is 7.2 m thicker than the constant sediment supply model (Table 16). As the sea-level reaches highstand and the sediment supply are at its maximum at 50 kyr, the delta is drowned with sediment deposited mainly as a continued fringe along the delta front, but significant amounts of sediment accumulate along the delta plain (Fig. 35C).

From 50 kyr to 100 kyr sea level falls by 50 m. During the initial period of sea-level fall, channels begin to form and as in constant sediment supply model, two lobes (labeled 1 and 2; Fig. 35D) have developed between 50 and 62.5 kyr. The lobes at the in-phase sediment supply model are thou more oriented more towards the right side (from up-dip view) of the delta than the constant sediment supply model lobes (Fig. 39C; Fig. 33C). The lobes at the in-phase sediment supply delta are attached to the delta, lack topset development and have a basinward-falling break-point trajectory. Deposition of sediments is focused on the two lobes, while the rest of the delta is starved for sediment (Fig. 35D).

By the time sea-level fall at 75 kyr reaches zero, the delta becomes exposed and the channels have started to incise the delta front. The main channel flows towards lobe 2, supplying all the sediments to the lobe, leaving Lobe 1 to become inactive (Fig. 35E). Lobe 2 have extended basinward by approximately 600 m from the delta front (Fig. 38C), while the delta front, which have most of the time been starved have extended basinward by 17.9 m (Table. 16).

During the late stage of sea level fall, the main channel changes its direction between 75 and 87.5 kyr from flowing towards Lobe 2, to create lobe 4 at the left side of the delta front. At 87.5 kyr four different fingerlike lobes are active, as lobe 1 has been reactivated and lobe 3 and 4 have been created during the last 12.5 kyr (Fig. 35F). Lobe 2 that were previously dominant has only been supplied sediment along the tip of the lobe. Lobe 3, which has been formed just to the left of lobe 2, acquire together with lobe 4, most of the sediments being deposited by 87.5 kyr (Fig. 35F).

At 100 kyr, sea level reaches lowstand by -25 m and sediment supply has decreased to its minimum at 6450 m^3/yr. The main channel has continued to flow towards lobe 4, on its way it has captured more flows and incise deeper into the exposed delta. As a result, lobe 4 is the only active lobe, while lobe 1, 2 and 3 becomes inactive (Fig. 35G). From the time lobe 4 was formed, it has expanded approximately 700 m basinward from the delta front (Fig. 37D).

Thickness and height of foresets at the in-phase model

	Average foresets thickness (m)	Foresets height (m)	Topset height (m)
12.5 kyr	**67**	88.9	0
25 kyr	**38.5**	127.8	0
37.5 kyr	**7,14**	**142.8**	28,6
50 kyr	**17,85**	**178.6**	21
62.5 kyr	N/A	N/A	0
75 kyr	N/A	**188.6**	0
87.5 kyr	N/A	N/A	0
100 kyr	N/A	**188.6**	0
112.5 kyr	N/A	N/A	0
125 kyr	N/A	**121.4**	0
137.5 kyr	**14.29**	N/A	0
150 kyr	**17,85**	**225.7**	0
162.5 kyr	**23,21**	**245.7**	0
175 kyr	**20,36**	**264.3**	0
187.5 kyr	**10,71**	N/A	0
200 kyr	N/A	**278.6**	0

N/A; unable to measure

Table. 14: Results from measuring the forsets average thickness, height of the foresets and topsets height in the main dip profile line of the in-phase sediment supply model.

Following sea-level lowstand, sea-level start to rise again by 50 m over the next 50 kyr. During the initial period of sea-level rise, lobe 4 does like lobe 3 at constant sediment supply model (Fig. 29H), it continue to grow, and the isopach show that the lobe expand laterally and infilling the relict topography around the lobe, which were starved of sediment during the sea-level fall (Fig. 35H, I; Fig. 40C). Lobe 4 has started to developing topsets and has shifted from having a basinward downward climbing break-point trajectory to gain a basinward upward-climbing break-point trajectory (Fig. 37E). The main channel has incised increasingly deeper as the delta plain is exposed (Fig. 35H), but by 125 kyr, the deepest incised valley have been started to get filled (Fig. 35I). At this time, sea level is at zero, and the delta front has still the same basinward expansion at 1000 m, while the maximum thickness has decreased by 5.7 m (Table. 16).

As sea-level continued to rise towards sea-level highstand at 150 kyr, the sediment supply increases along with the sea-level rise. As a result, the relict topography around lobe 4 area getting more and more sediment and the area expands laterally as the deposition move further landward (retrogradation) and accumulate sediments at the incised delta front (Fig. 35J, K; Fig. 37F; Fig. 40D). Compared with the constant sediment supply model (Fig. 29K), the in-phase sediment supply model have similar morphology with an attached, huge southeast (green arrow pointing north) going drowned apron at sea-level highstand at 150 kyr (Fig. 35K). Because sediments has accumulate at the delta front again, the delta have a straight basinward break-point trajectory (Fig. 36F) and the delta front have expanded 250 m and increased its maximum thickness by 41.4 m (Table. 16). Due to the delta front expansion, the delta front and the inactive lobe 2 located in front of the delta front, together form a narrow canyon-like valley (Fig. 35K).

From 150 kyr, sea-level starting to fall again, towards the end of the model run at 200 kyr. During the first 25 kyr of sea-level fall, there is no prominent channel and thus no lobe development. The sediment accumulates as a continuous fringe around the delta, with the main deposition occurs in the filling of the canyon-like valley and around apron (Fig. 35L, M). Filling of the canyon-like valley have attach the delta front with the former lobe 2 area, which has led to the delta (main dip profile line) has expanded 285.7 m and increased its maximum thickness by 42.9 m (Table. 16). The break-point trajectory pattern is climbing basinward, with an average foreset thickness at 20.36 m (Table 14) and no topset development (Fig. 36G).

From 175 kyr and throughout the model run (200 kyr), the sea-level fall to sea-level lowstand at -25 m. A prominent channel have formed during this period and started to incise the exposed delta. The main channel flowing towards Lobe 3, and reactivate the lobe. The isopach show that between 175 and 187.5 kyr the main sediment supply is deposited at lobe 3, but significant amounts of sediment still get deposited as a continuous fringe around the delta (Fig. 35N). By the time 200 kyr, deposition of sediment is focused on lobe 3, and the rest of the submarine delta front only get minor amounts of sediment (Fig. 35O). Lobe 3 has a northeast direction, lack topset development and have a basinward break-point trajectory. At 200 kyr, the delta front has expanded basinward by 1575 m and has a maximum thickness at 285.7 m (Table. 16).

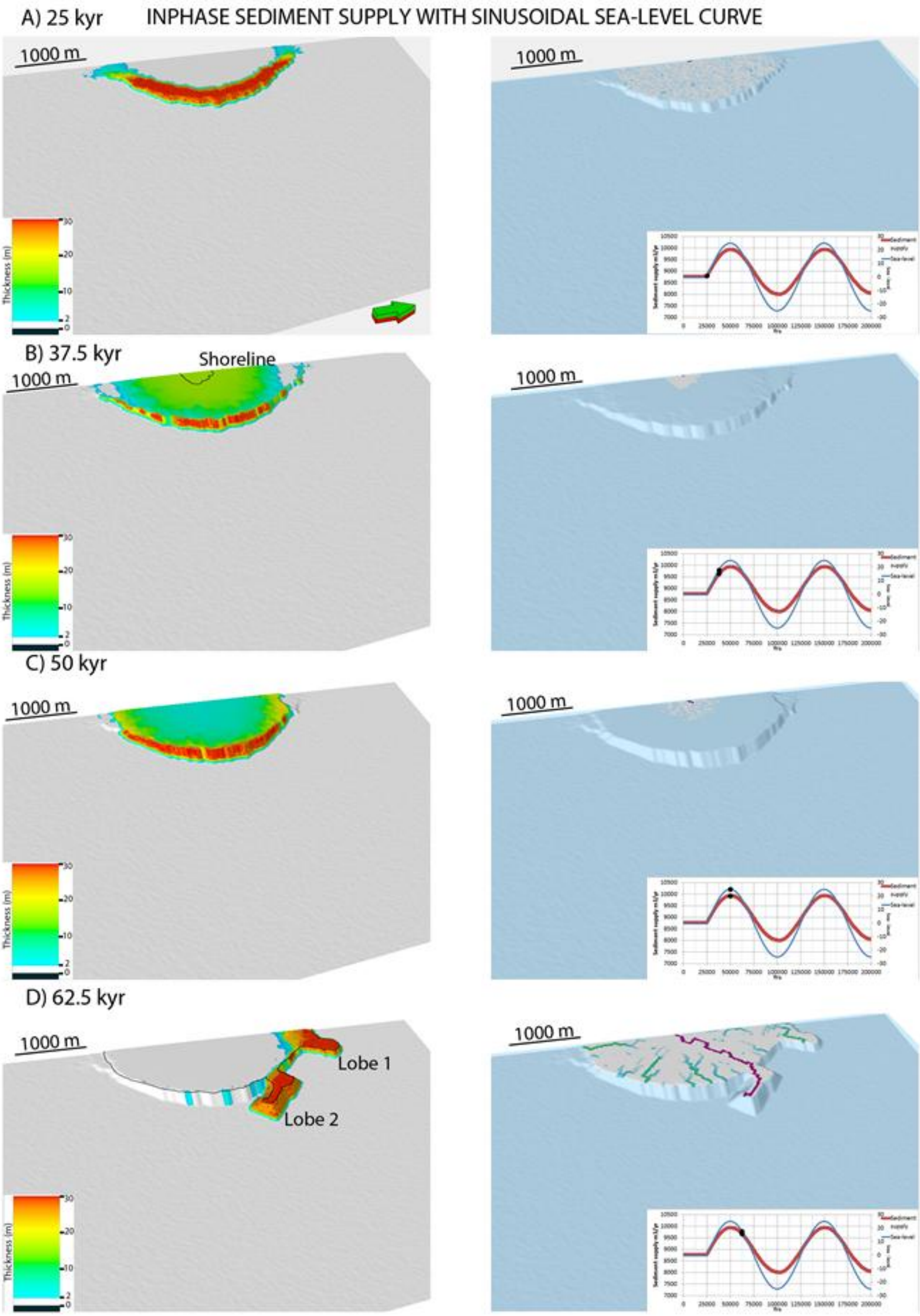
A) 25 kyr
INPHASE SEDIMENT SUPPLY WITH SINUSOIDAL SEA-LEVEL CURVE
1000 m
B) 37.5 kyr
Shoreline
1000 m
C) 50 kyr
1000 m
D) 62.5 kyr
1000 m
Lobe 1
Lobe 2
Thickness (m)
30
20
10
2
0

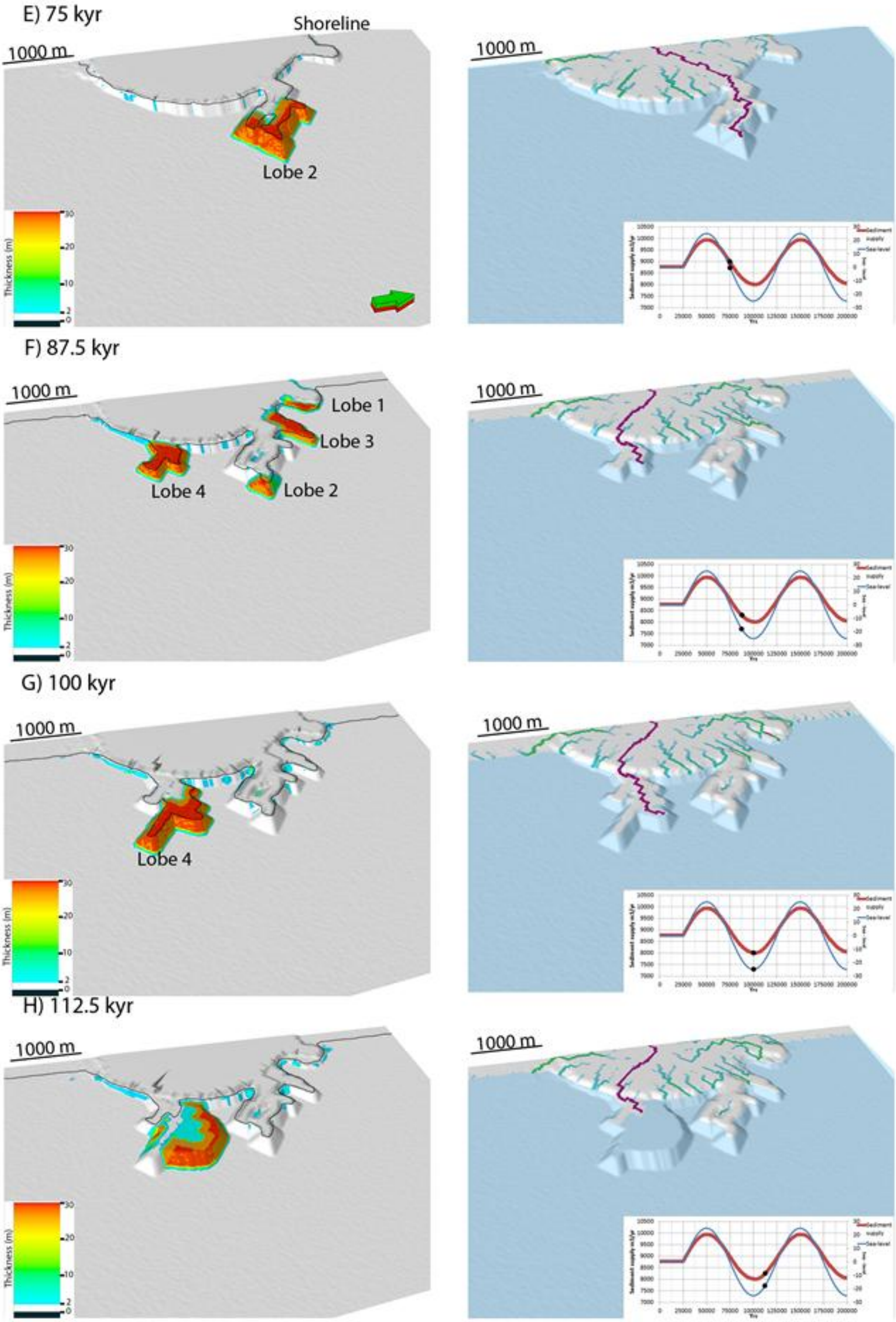
E) 75 kyr
Shoreline
1000 m
1000 m
Lobe 2
Thickness (m)
30
20
10
2
0
F) 87.5 kyr
1000 m
1000 m
Lobe 1
Lobe 3
Lobe 4
Lobe 2
G) 100 kyr
1000 m
1000 m
Lobe 4
H) 112.5 kyr
1000 m
1000 m

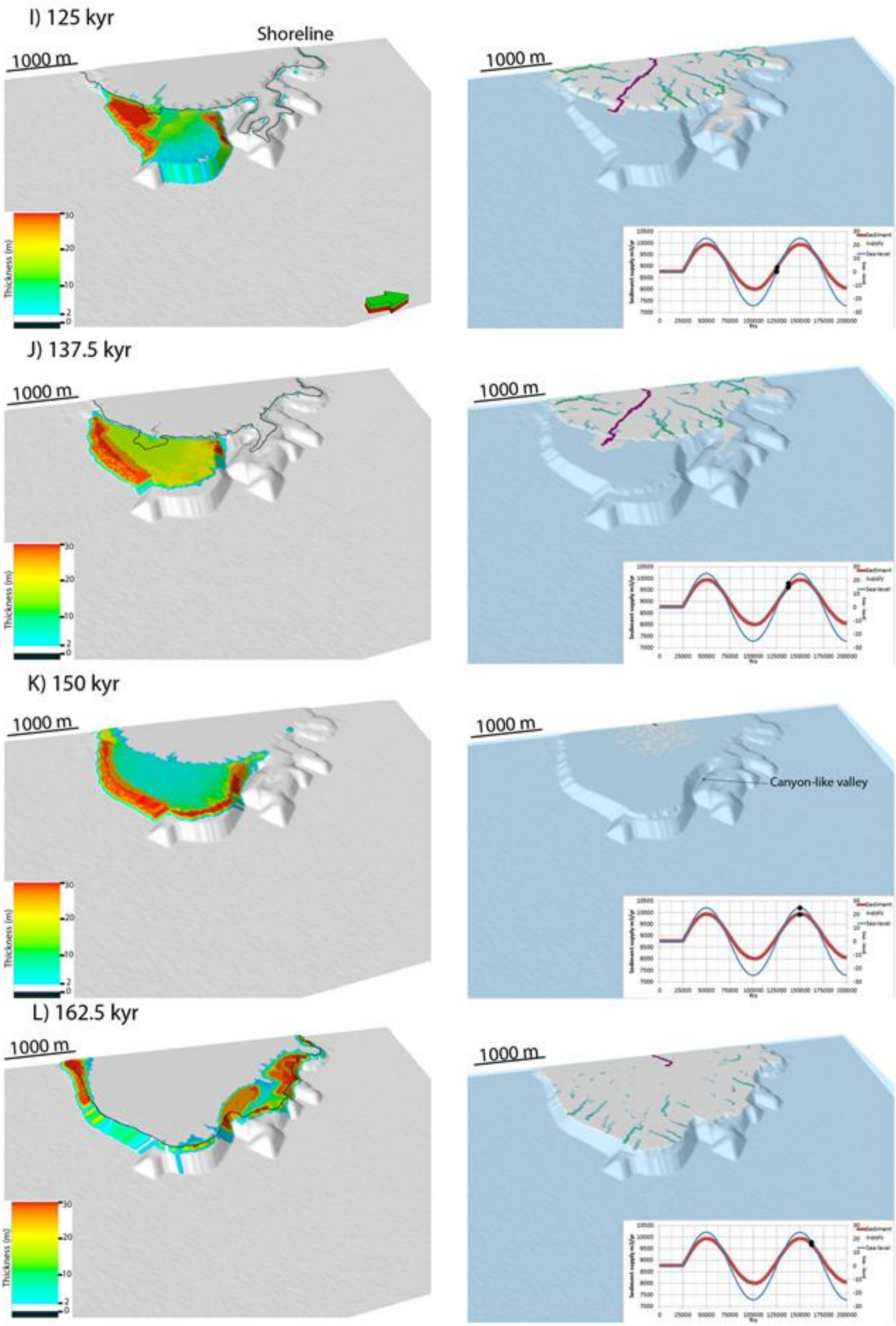
I) 125 kyr
Shoreline
1000 m
Thickness (m)
30
20
10
2
0
J) 137.5 kyr
K) 150 kyr
Canyon-like valley
L) 162.5 kyr

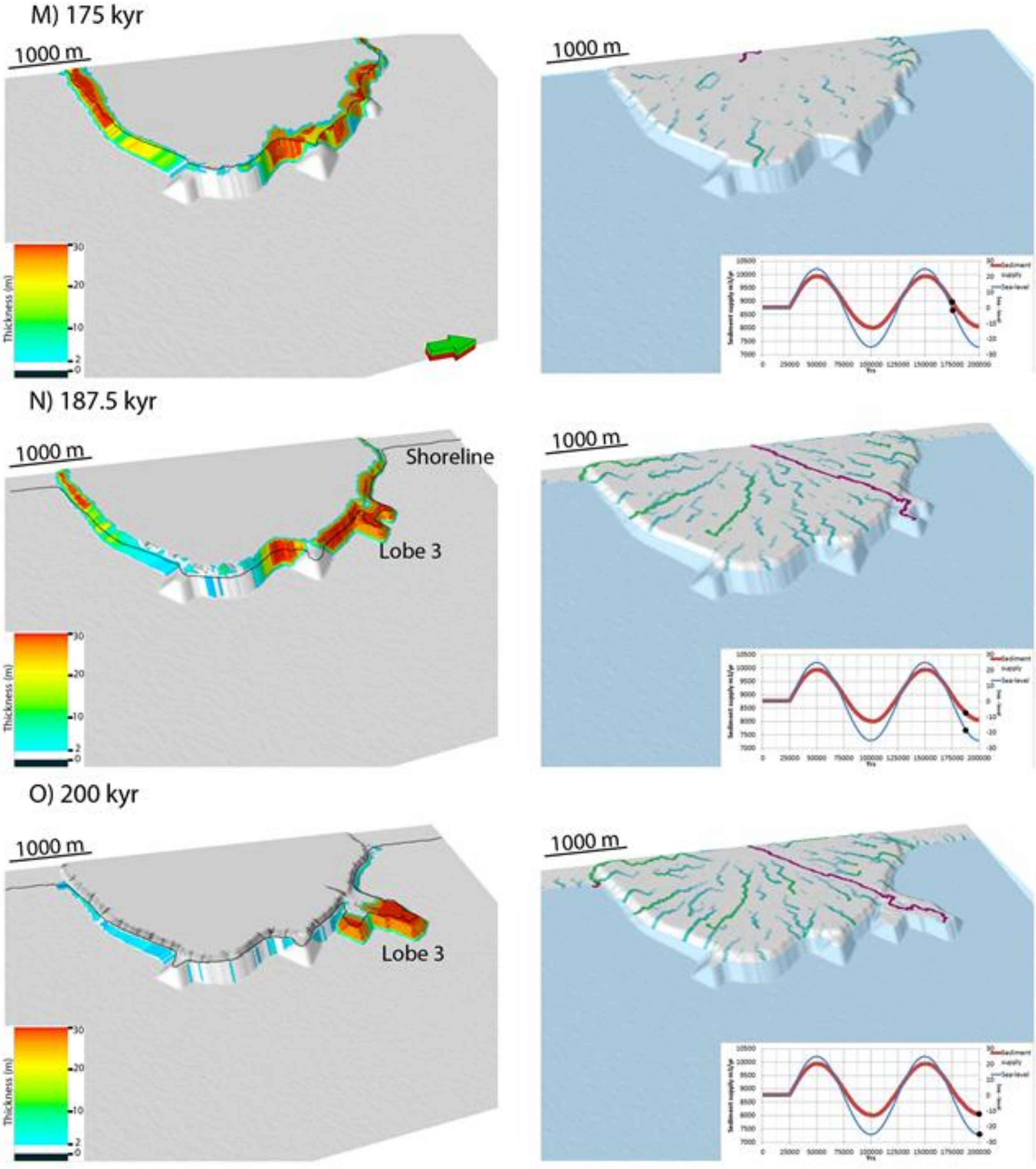

Fig. 35: Sequential evolution of the in-phase sediment supply model at intervals of 12.5 kyr. Left-hand side shows oblique view of the delta morphology an isopach for previous 12.5 kyr. Shoreline is marked by a black line. Right-hand side shows channel evolution and sea-level (same view as isopach). Vertical exaggeration 2:1.

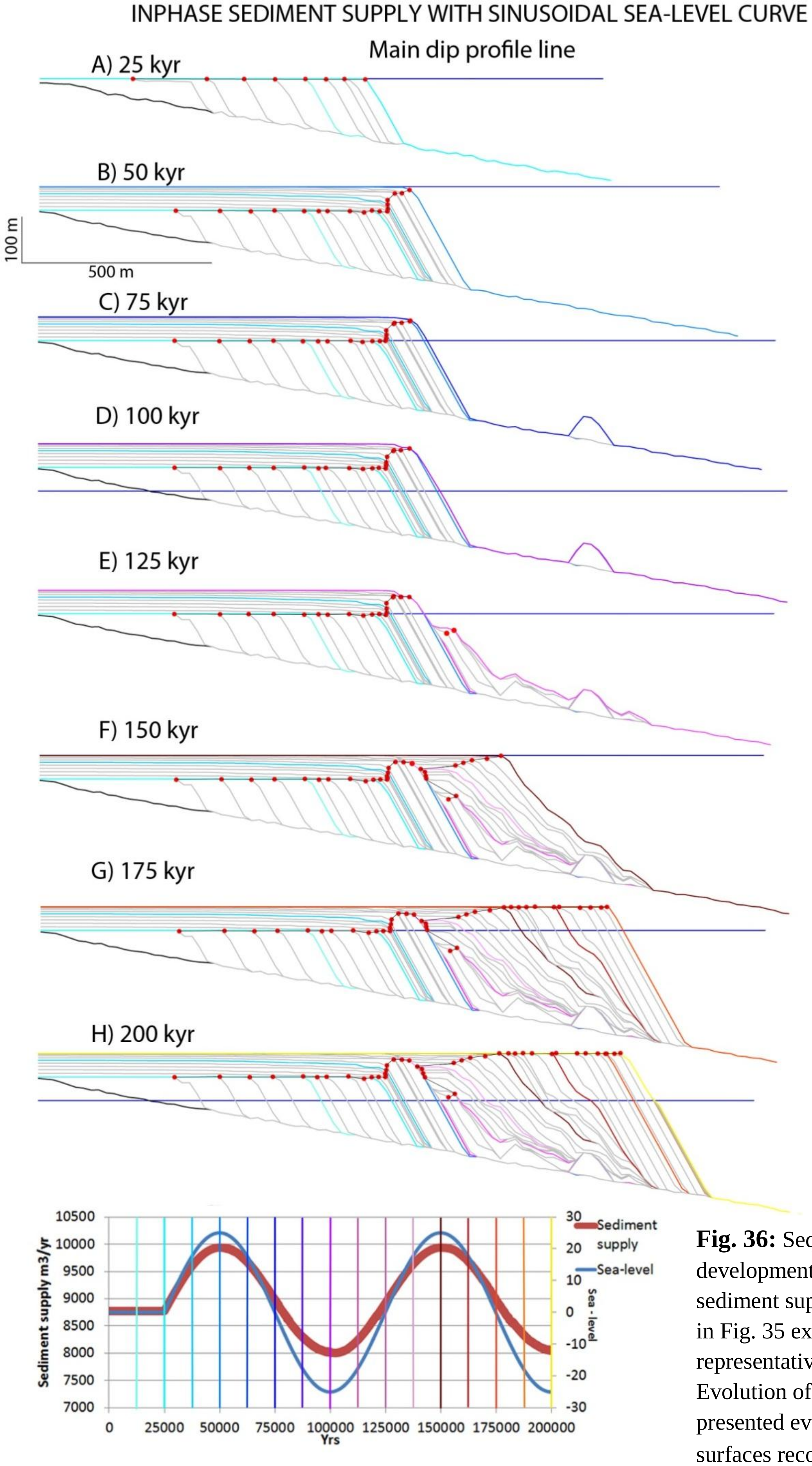

Fig. 36: Sequential development of the in-phase sediment supply model shown in Fig. 35 expressed in a representative dip section. Evolution of the delta is presented every 25 kyr, with surfaces recorded with a color every 12.5 kyr.

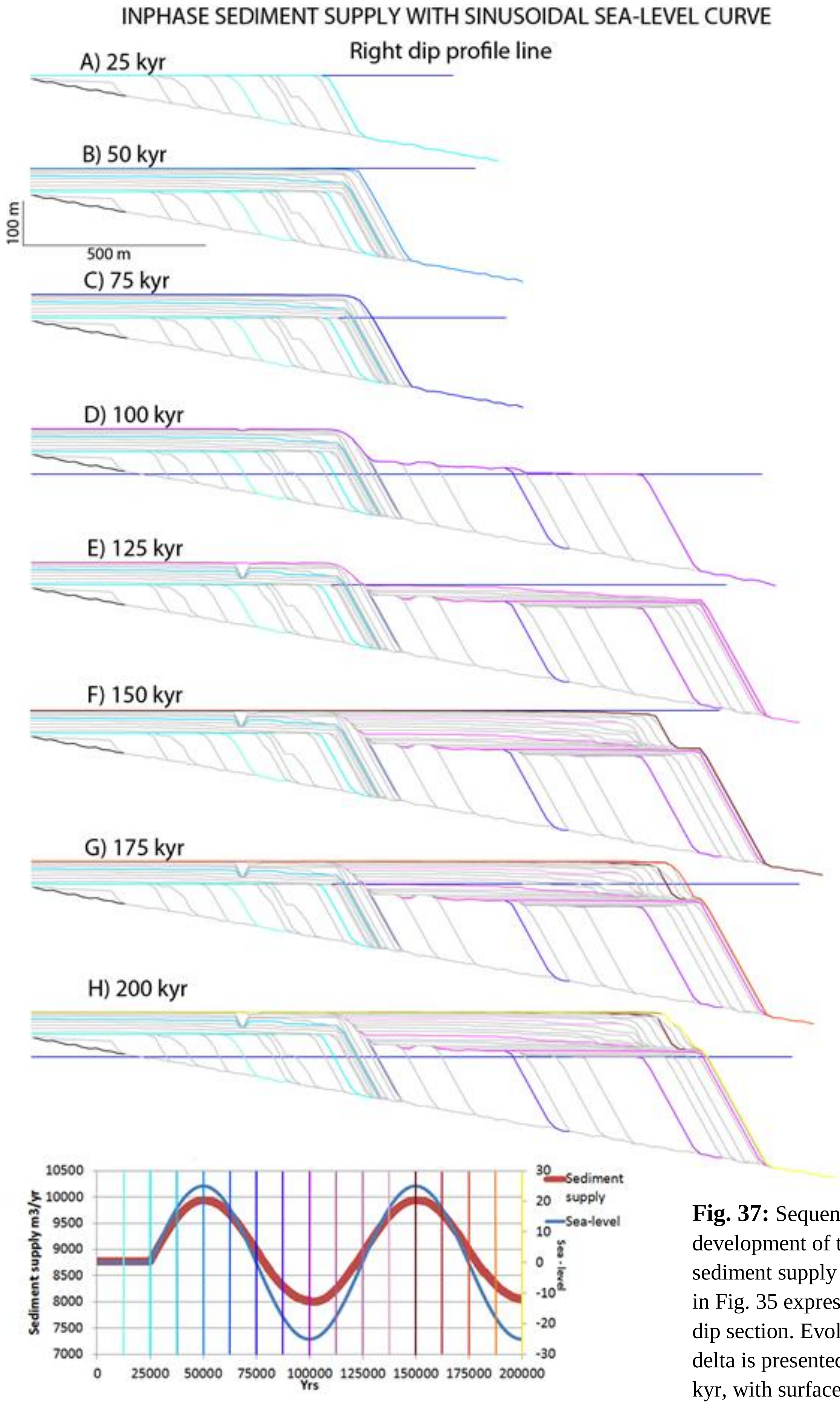

Fig. 37: Sequential development of the constant sediment supply model shown in Fig. 35 expressed in right dip section. Evolution of the delta is presented every 25 kyr, with surfaces recorded with a color every 12.5 kyr.

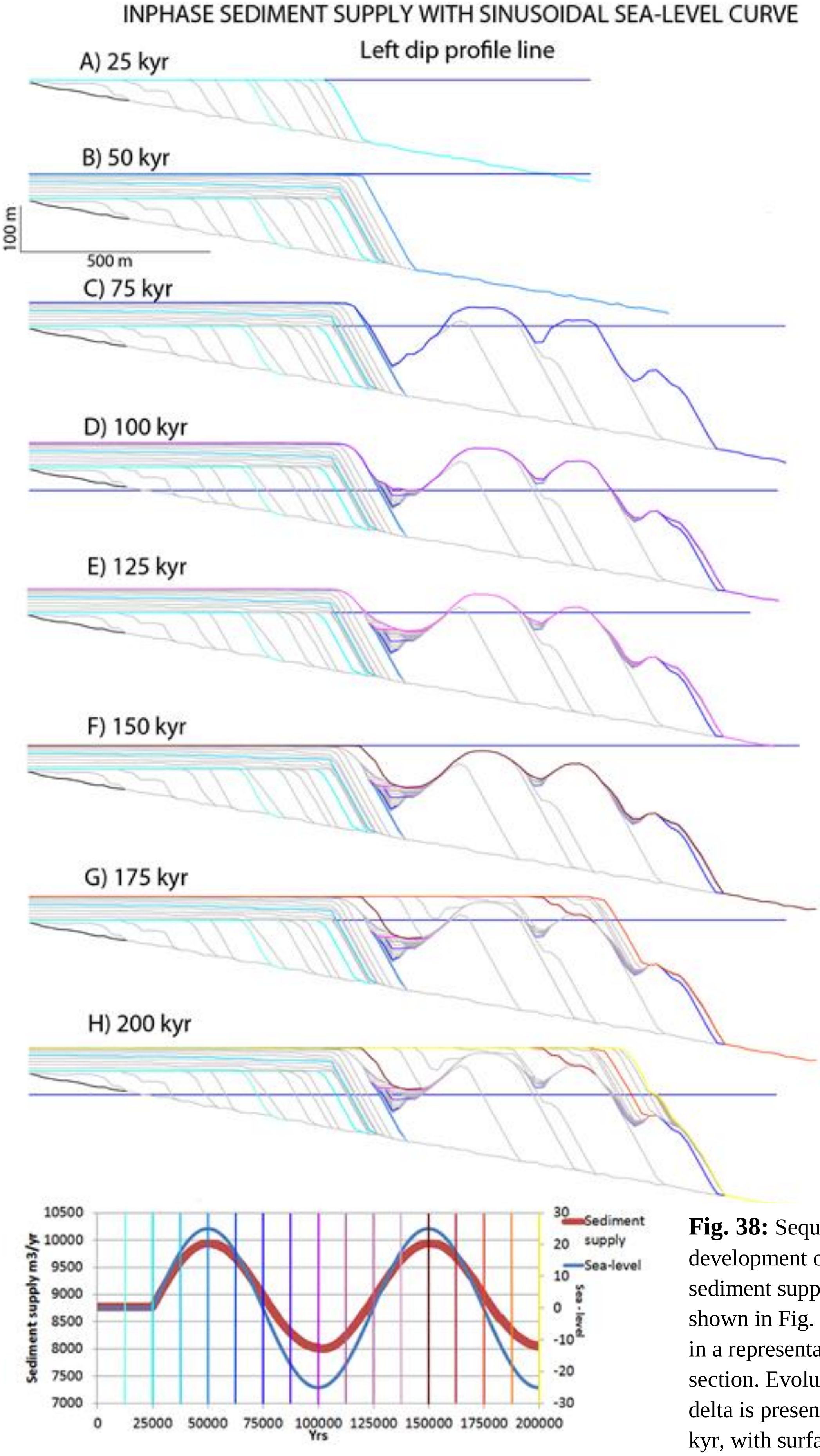

Fig. 38: Sequential development of the in-phase sediment supply model shown in Fig. 35 expressed in a representative dip section. Evolution of the delta is presented every 25 kyr, with surfaces recorded with a color every 12.5 kyr.

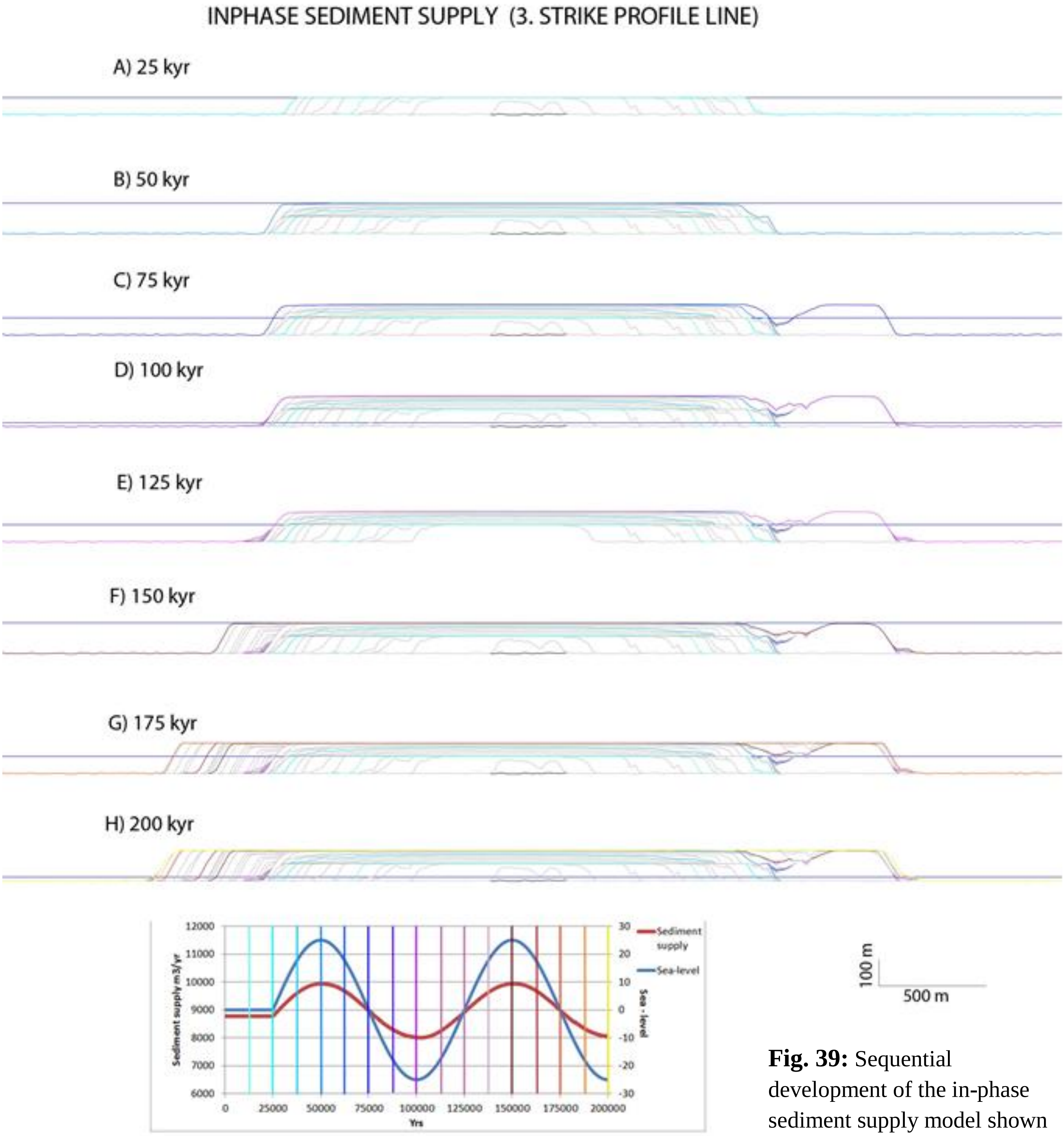

Fig. 39: Sequential development of the in-phase sediment supply model shown in Fig. 35 expressed in proximal strike section. Evolution of the delta is presented every 25 kyr, with surfaces recorded with a color every 12.5 kyr.

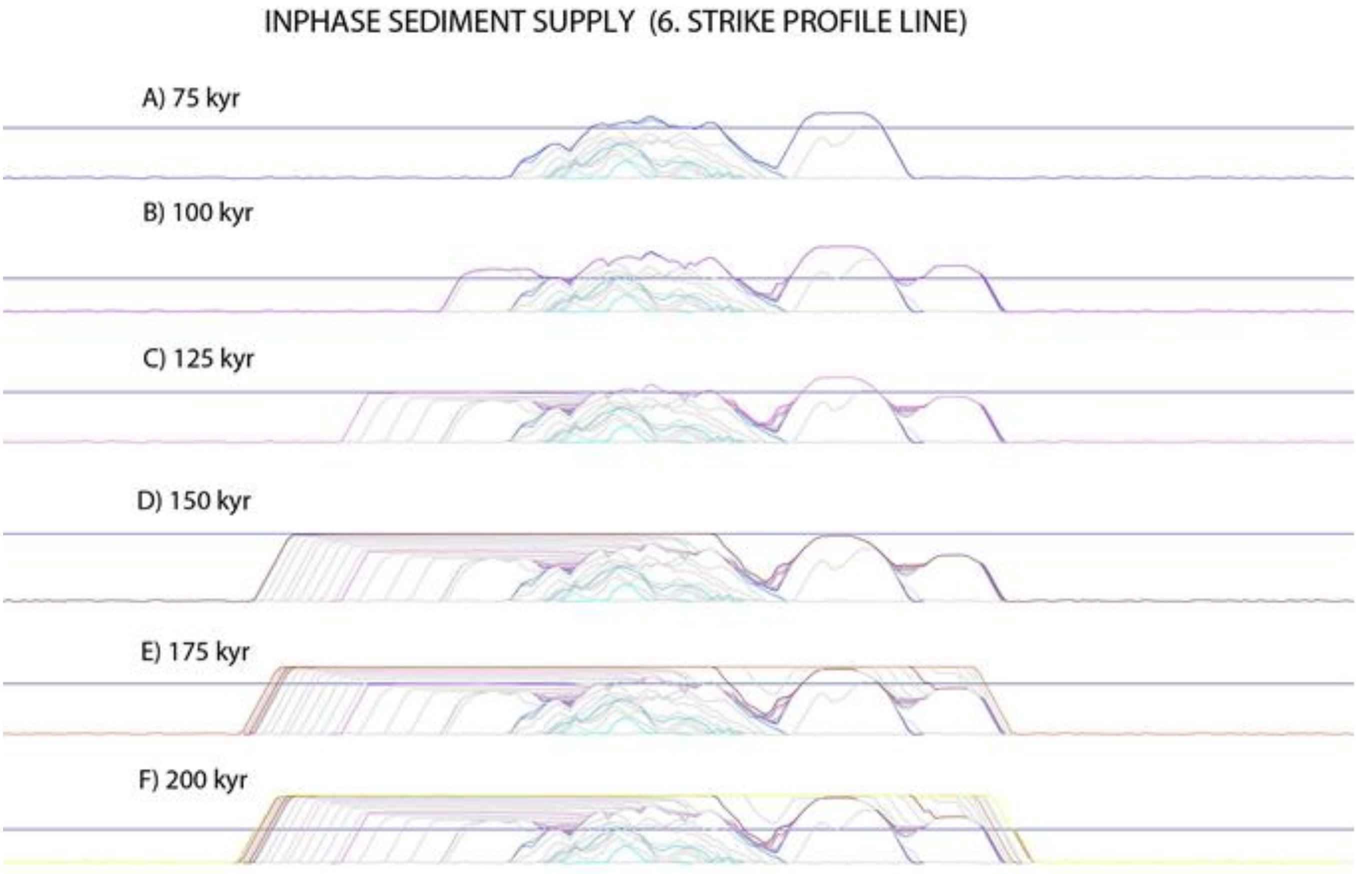

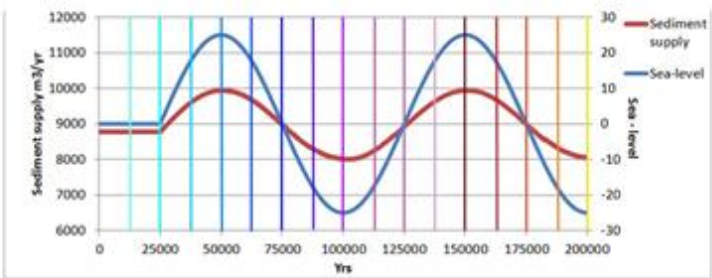

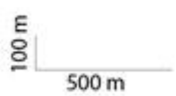

Fig. 40: Sequential development of the in-phase sediment supply model shown in Fig. 35 expressed in distal strike section. Evolution of the delta is presented every 25 kyr, with surfaces recorded with a color every 12.5 kyr.

5.3 Description for out-phase sediment supply model

From the first 25 kyr with constant sediment supply and sea-level, the deposition architecture at the out-phase sediment supply delta are similar to the two previous model run (constant sediment supply and in-phase sediment supply models), with deposition occurs as a continuous fringe along the delta front and with no topsets development (Fig. 41A). The basinward expansion and maximum thickness are also the same as latter models (Table. 16).

As the sea-level start rising from 25 kyr towards sea-level highstand, the sediment supply decreases along with the sea-level rise towards minimum sediment supply (6450 m^3/yr) at 50 kyr. During the time of sea-level rise, the out-phase delta have similar features as constant sediment supply and in-phase sediment supply models, with topset development and sediments deposited along the delta front and on the delta plain (Fig. 41B, C; Fig. 29B, C; 35B, C). Though break-point trajectory differs from the two latter models. Whereas constant- and in-phase sediment supply models have a progressively steeper basinward-climbing break-point trajectory (Fig. 30B, Fig. 36B), so change out-phase model from prograde basinward during the first 25 kyr to start climbing vertically as the sediment supply starts to decrease after 25 kyr (Fig. 42B). The system is aggraditional until sea-level highstand and minimum sediment supply at 50 kyr, where the delta forestep (Fig. 42B). At this time, the out-phase delta has prograded basinward by 44.6 m, which are 44.7 m lesser than constant sediment supply delta and 62.5 m lesser than the in-phase delta. The maximum thickness for out-phase model is also less than the two other models with its 185.7 m (Table. 16).

Between 50 and 100 kyr, sea-level falls by 50 m. During this time sediment supply increases from minimum sediment supply to it maximum sediment supply of 11100 m^3/yr (at 100 kyr). As sea-level starting to fall, channels begin to form and create lobes (labeled lobe 1). Isopach show at 62.5 kyr that there are two main depositional areas, while at 75 kyr, only lobe 1 is active and receive most of the sediments (Fig. 41D). The lobe is located on the right side of the delta and has a wedge-like form, lack topset development and have a basinward-falling break-point trajectory (Fig. 41C, D). There have been no deposition along the exposed delta front, and the delta front has started to get incised by the channels and undergoes erosion. As a result, the delta front has retreated landward by 17.8 m (Table. 16).

As sea-level fall continued towards lowstand at 100 kyr, the main channel changes avulsion from flowing towards lobe 1, to deposits sediment on both side of lobe 1, leaving lobe 1 inactive. As a result, Lobe 2 is created on the left side for lobe 1 (Fig. 41F). At 100 kyr, sea level reaches lowstand by -25 m and sediment supply has increased to its maximum by 11199 m^3/yr. The main channel has flow towards lobe 2 and on its way it has captured more flows and incise deeper into the exposed delta. Lobe 2 have between 87.5 and 100 kyr branched out to two fingerlike lobes (labeled 2a and 2b), and received most of the sediment, while the rest of the submarine delta front only get minor amounts of sediment (Fig. 41G). As the delta front exposed at the most and have thus been eroded, the out-phase delta have retreated landward 8.9 m (Table. 16).

Following maximum sediment supply at 100 kyr, sediment supply decreases until 150 kyr. During the early part of decreasing sediment supply (from 100 to 112.5 kyr), lobe 2 that developed during the preceding sea-level fall, continue to grow and lobe 2a and 2b get connected as infilling of the relict topography around the lobe (Fig. 41H). The lobe starting to develop topset, as the break-point trajectory has a gently upward-climbing break-point trajectory (Fig. 44E). The main channel incised increasingly deeper as the delta plain is still exposed, leaving a incised valley just behind lobe 2 (Fig. 41H). At 125 kyr, the lobe retrogrades as the sediments keep filling the relict topography around the lobe, with main deposition in the southern part of the lobe and expanding laterally towards south (Fig. 44E; Fig. 46C). In addition, the incised valley gets filled with sediments. As a result, the sediments accumulate ahead of the delta front and attach lobe 2 with the delta front, forming a basinward apron (Fig. 41I). This makes the delta front expanding 196.4 m (Table 16), with a basinward-falling break-point trajectory (Fig. 42E).

Thickness and height of foresets at the out-phase model

	Average foresets thickness (m)	Foresets height (m)	Topset height (m)
12.5 kyr	67	88.9	0
25 kyr	38.5	127.8	0
37.5 kyr	7	142.85	28,6
50 kyr	7,7	171.4	22,8
62.5 kyr	N/A	N/A	0
75 kyr	N/A	N/A	0
87.5 kyr	N/A	N/A	0
100 kyr	N/A	N/A	0
112.5 kyr	N/A	N/A	0
125 kyr	28	135.7	0
137.5 kyr	35.1	185.7	57.1
150 kyr	21	228.6	15,7
162.5 kyr	N/A	N/A	0
175 kyr	10,2	254.3	0
187.5 kyr	N/A	N/A	0
200 kyr	5,3	N/A	0

N/A; unable to measure

Table. 15: Results from measuring the forsets average thickness, height of the foresets and topsets height in the main dip profile line of the out-phase sediment supply model.

As the sea-level rise continues from 125 to 150 kyr, the accommodation space increases and the sediments keep filling the southern parts of the apron (Fig. 41J, K), making the break-point trajectory at the apron aggraditional (Fig. 44F), while the break-point trajectory at the delta front have an approximately 45° basinward-climbing trajectory (Fig. 42F). At minimum sediment supply and sea-level highstand at 150 kyr, the whole delta is drowned and the basinward expansion for the delta front has increased with 267.8 m, and maximum thickness has increased by 68.3 m (Table. 16).

Following sea-level highstand, sea-level falls 50 m until the end of the model run at 200 kyr. During the initial stage of sea-level fall, there is one prominent channel that avulse towards the left side of the delta and bringing the locus of deposition along. The isopach for 150 to 162.5 kyr shows (Fig. 41L) that deposition builds up a lobe, before sediments get deposited along the delta front and on the left side of the delta, which led to the deposition smoothed the lobe by 175 kyr (Fig. 41M). At his time, the delta front has expanded 62.5 m further basinward and increased its maximum thickness by 2.8 m (Table. 16). During the time of sea-level fall, no topset are developed and the break-point trajectory goes straight basinward (prograditional) (Fig. 42G).

Between 175 kyr and to the end of the model run (200 kyr), the sediment still increase its supply towards maximum, as sea-level continue to fall. A main channel has been formed between 175 and 187.5 kyr, and supplied a new lobe (labeled lobe 3), located left side of the delta with a southeast going direction. The main channel does not capture all sediments, as sediment also gets deposited along the delta front (Fig. 41N). By the time sea-level reaches lowstand and sediment supply is at its maximum at 200 kyr, the main channel have captured most of the sediments and have incise a valley just behind lobe 3 and deposits the majority of the sediments on the relict topography on the left side of lobe 3 (Fig. 41O). Lobe 3 itself get sediments by-passed as only the tip of the lobe get sediment accumulation. Throughout the model run (200 kyr), the out-phase delta front has expanded basinward by a total of 1428.6 m and has a maximum thickness at 257.1 m (Table. 16).

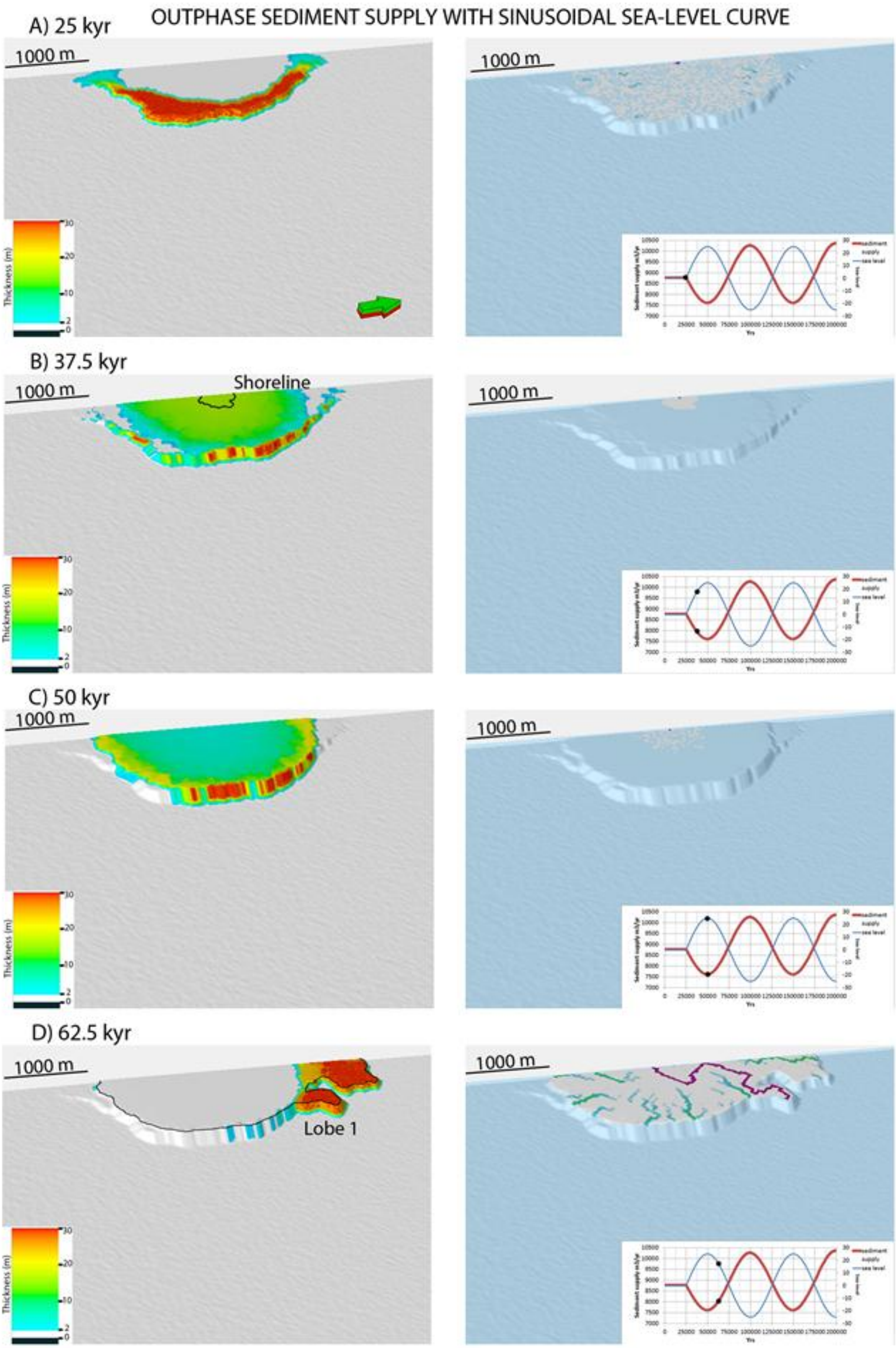
OUTPHASE SEDIMENT SUPPLY WITH SINUSOIDAL SEA-LEVEL CURVE
A) 25 kyr
B) 37.5 kyr
C) 50 kyr
D) 62.5 kyr
1000 m
Shoreline
Lobe 1
Thickness (m)
30
20
10
2
0

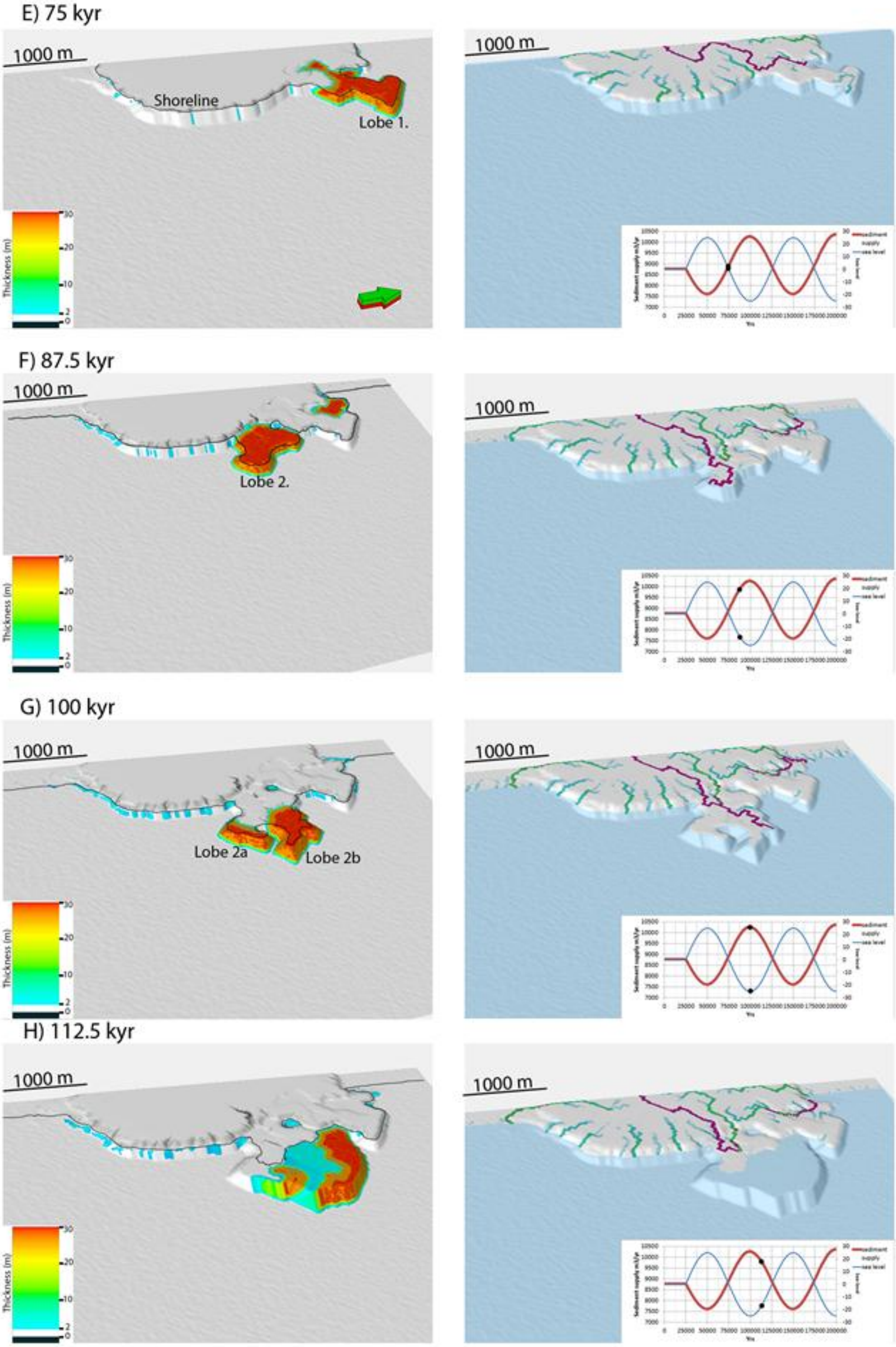
E) 75 kyr
1000 m
Shoreline
Lobe 1.
Thickness (m)
30
20
10
2
0
F) 87.5 kyr
Lobe 2.
G) 100 kyr
Lobe 2a
Lobe 2b
H) 112.5 kyr

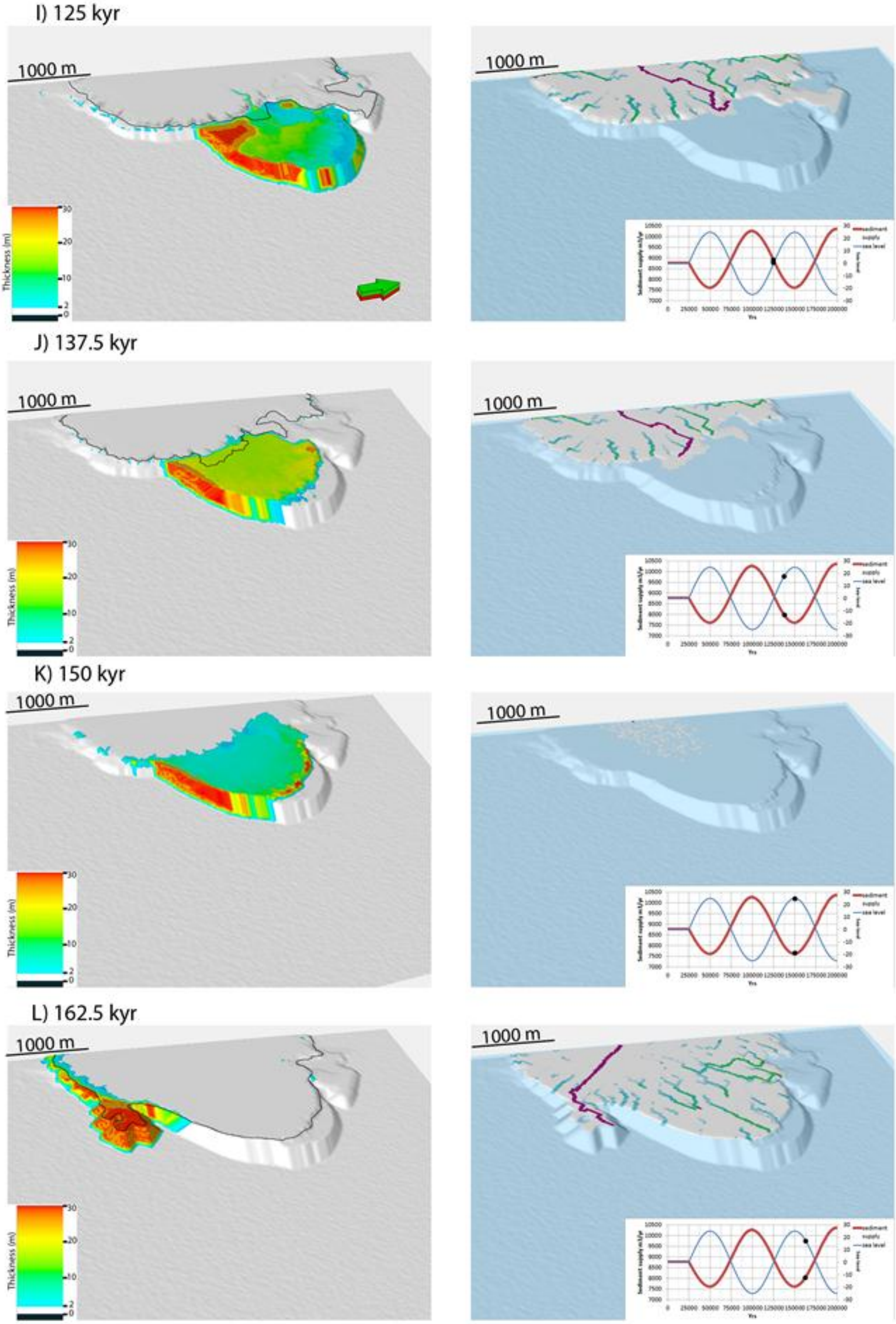
I) 125 kyr
1000 m
Thickness (m)
30
20
10
2
0
J) 137.5 kyr
K) 150 kyr
L) 162.5 kyr

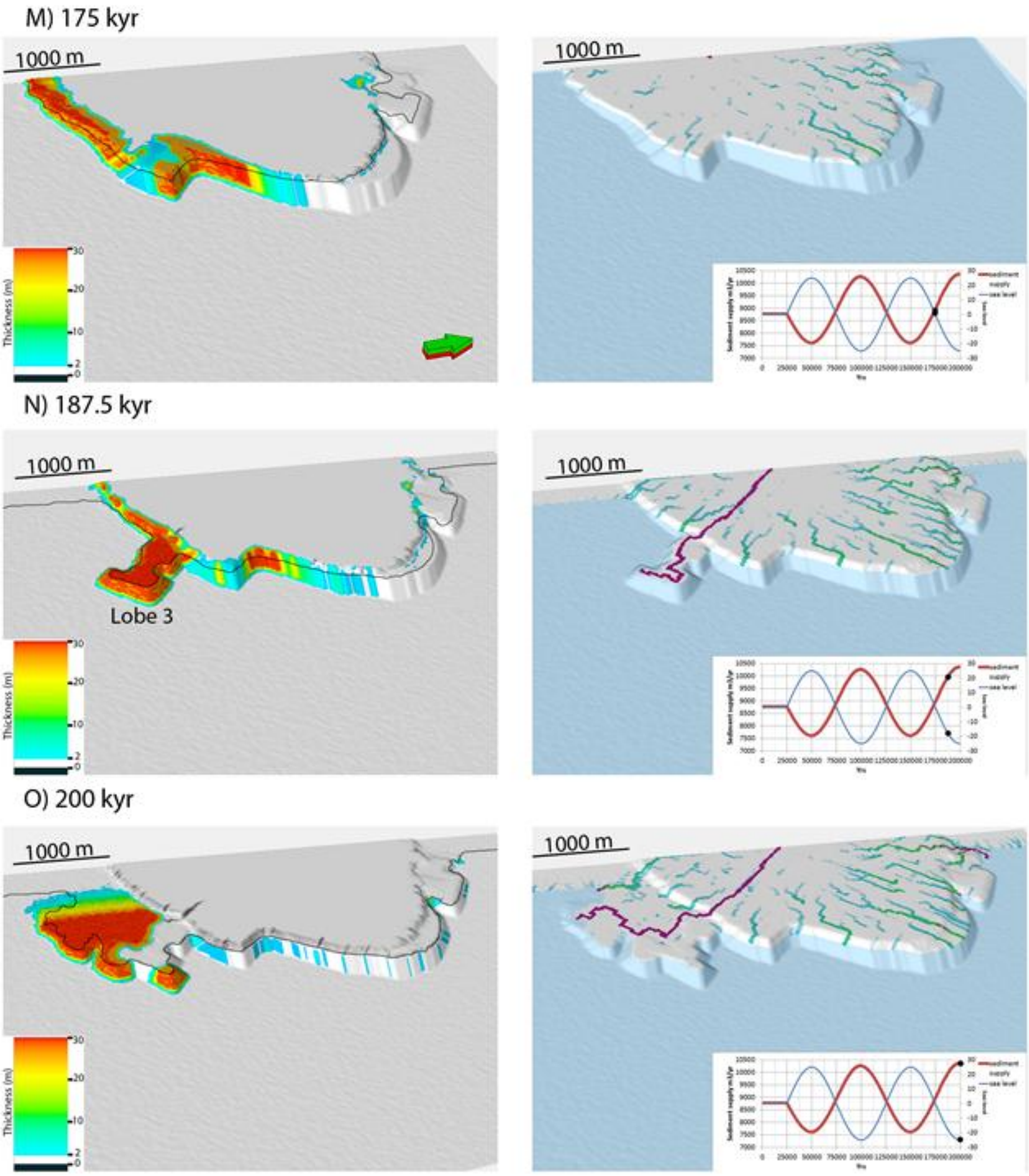

Fig. 41: Sequential evolution of the out-phase sediment supply model at intervals of 12.5 kyr. Left-hand side shows oblique view of the delta morphology an isopach for previous 12.5 kyr. Shoreline is marked by a black line. Right-hand side shows channel evolution and sea-level (same view as isopach). Vertical exaggeration 2:1.

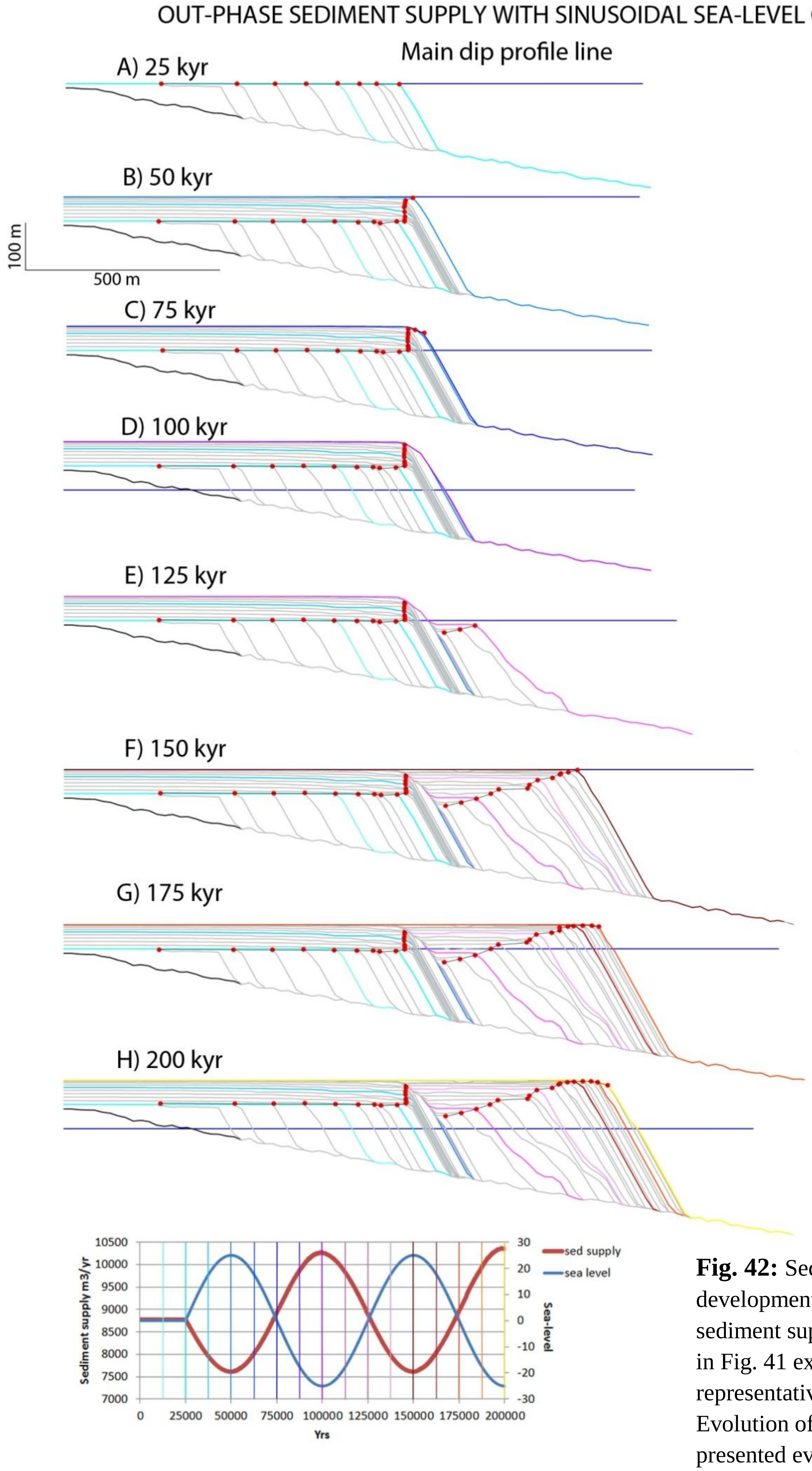

Fig. 42: Sequential development of the out-phase sediment supply model shown in Fig. 41 expressed in a representative dip section. Evolution of the delta is presented every 25 kyr, with surfaces recorded with a color every 12.5 kyr.

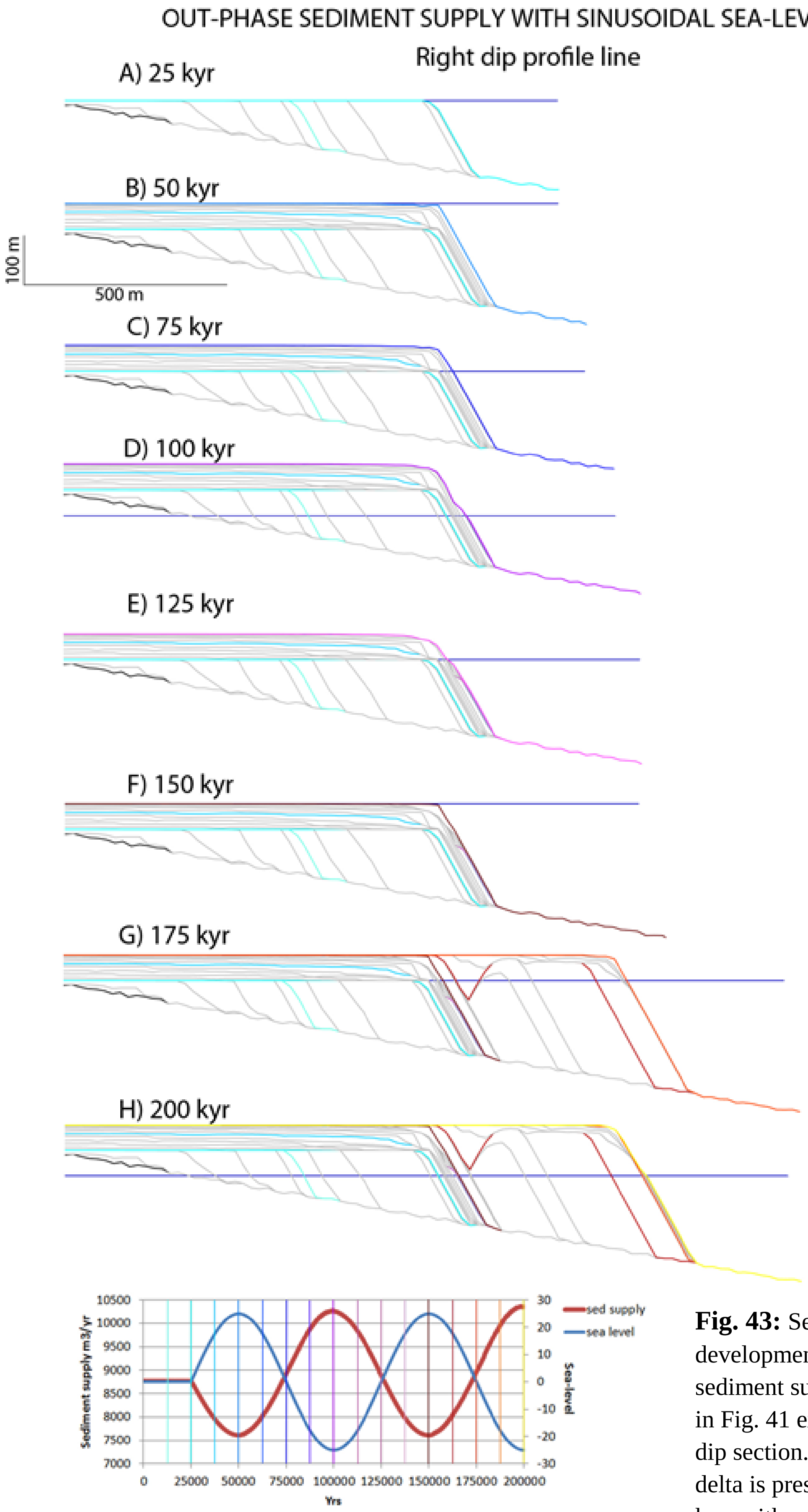

Fig. 43: Sequential development of the out-phase sediment supply model shown in Fig. 41 expressed in a right dip section. Evolution of the delta is presented every 25 kyr, with surfaces recorded with a color every 12.5 kyr.

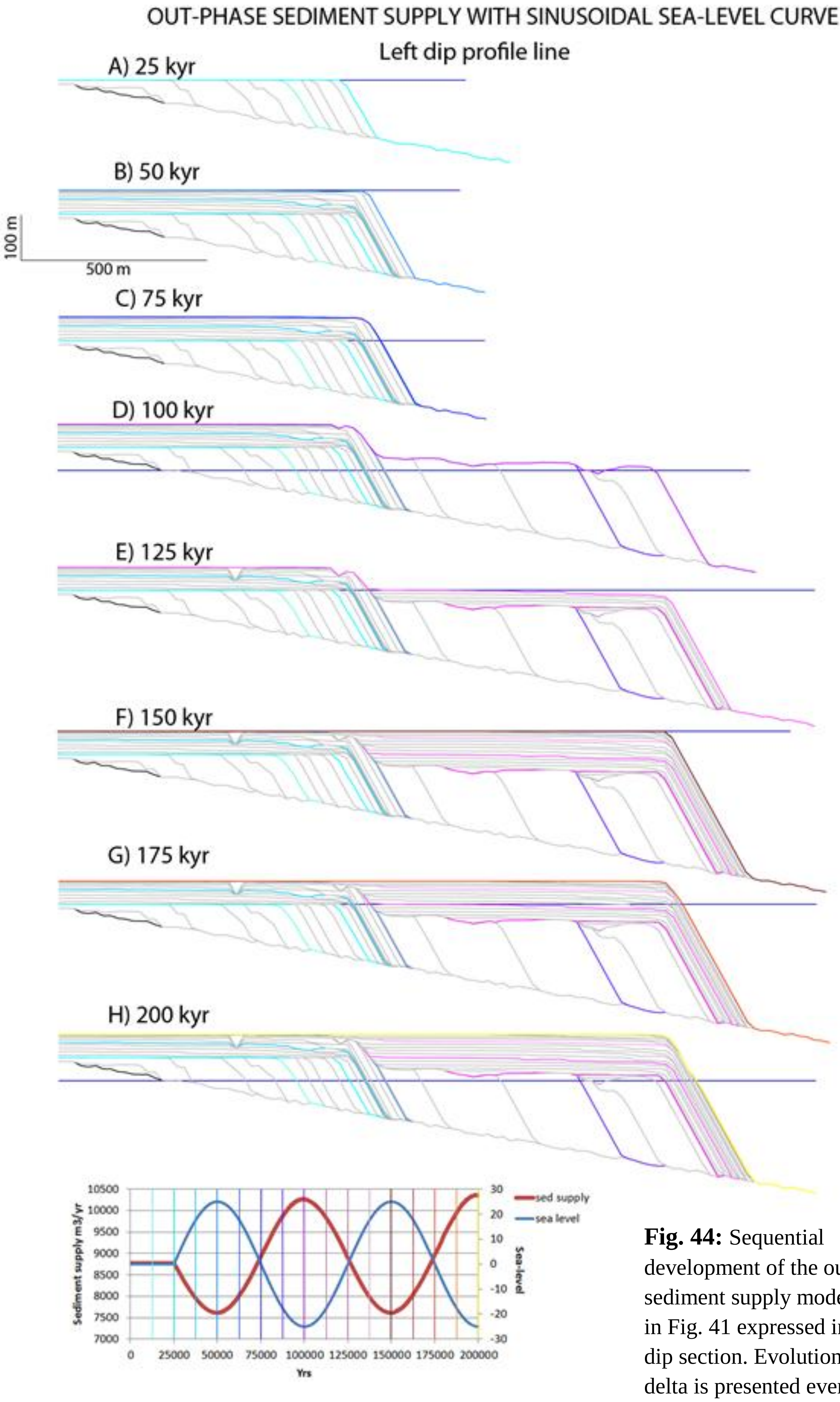

Fig. 44: Sequential development of the out-phase sediment supply model shown in Fig. 41 expressed in a left dip section. Evolution of the delta is presented every 25 kyr, with surfaces recorded with a color every 12.5 kyr.

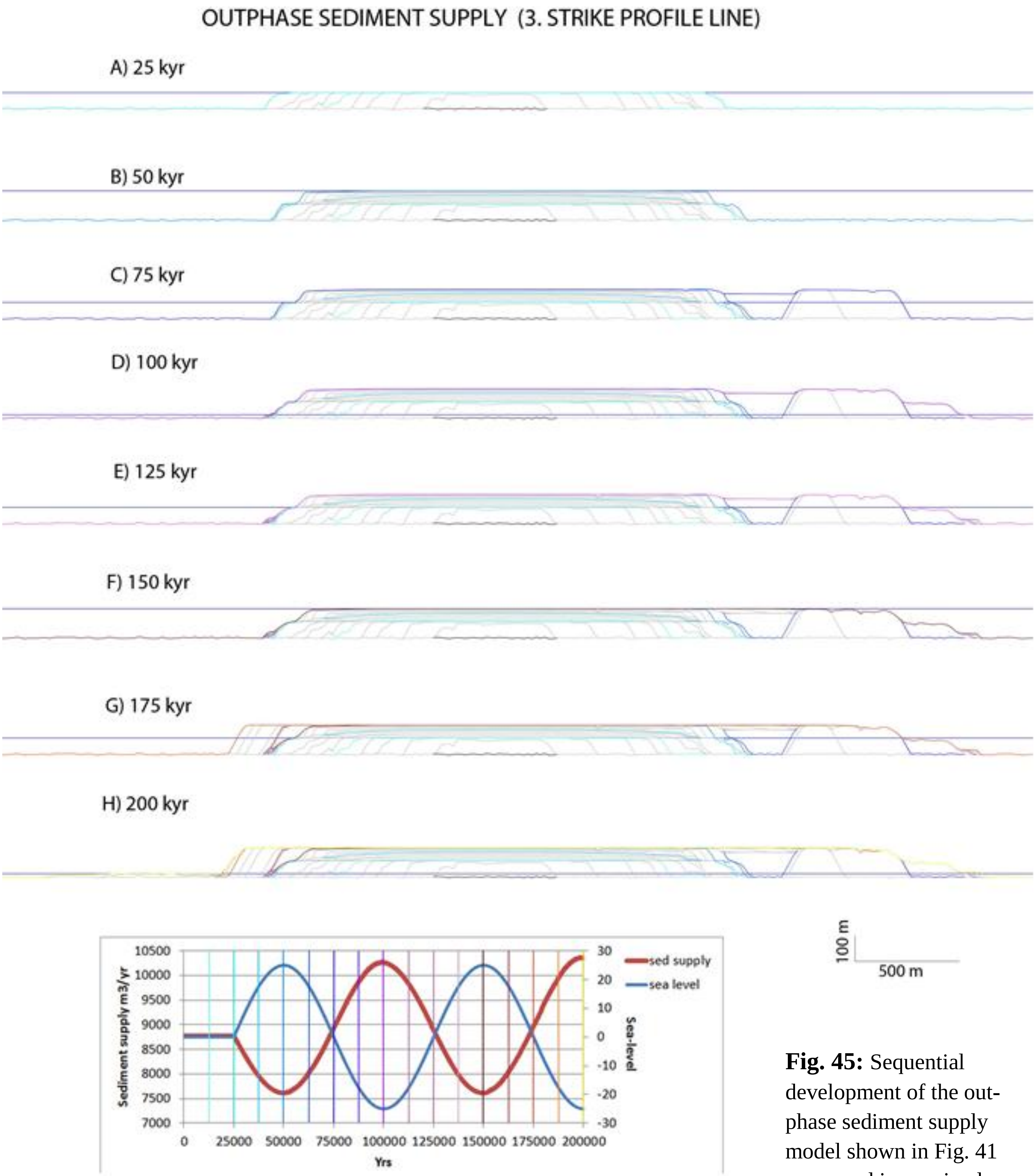

Fig. 45: Sequential development of the out-phase sediment supply model shown in Fig. 41 expressed in proximal strike section. Evolution of the delta is presented every 25 kyr, with surfaces recorded with a color every 12.5 kyr.

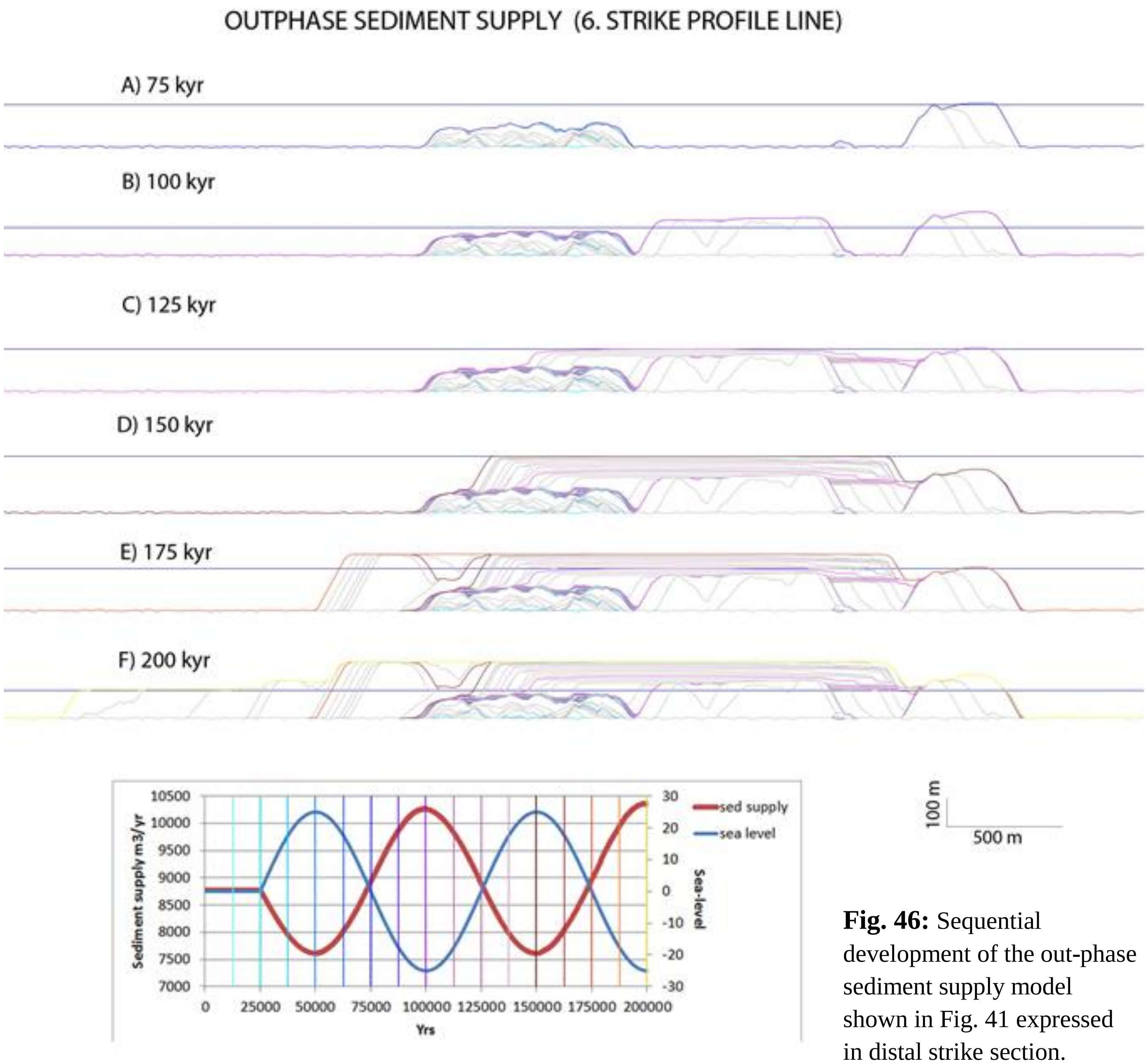

Fig. 46: Sequential development of the out-phase sediment supply model shown in Fig. 41 expressed in distal strike section. Evolution of the delta is presented every 25 kyr, with surfaces recorded with a color every 12.5 kyr.

Model:	25 kyr	50 kyr	75 kyr	100 kyr	125 kyr	150 kyr	175 kyr	200 kyr	Total amount sediment added
Constant sediment supply: Basinward expansion (m)	875	964,3	1026.8	1021.4	982.1	1053.6	1026.8	N/A	100 635 295 m3
Constant sediment supply: Maximum thickness (m)	137,4	192.8	200	200	192.8	214.3	207.1	N/A	
In-phase sediment supply: BE (m)	875	982.1	1000	1000	1000	1250	1535.7	1575	100 642 148 m3
In-phase sediment supply: MT (m)	137.4	200	200	200	194.3	235.7	278.6	285.7	
Out-phase sediment supply: BE (m)	875	919.6	901.8	892.9	1089.3	1357.1	1419.6	1428.6	88 117 068 m3
Out-phase sediment supply: MT (m)	137.4	185.7	185.7	185.7	185.7	254.3	257.1	257.1	

Table. 16: Overview of the three different models basinward expansion and their maximum thickness. In addition, an overview of how much sediment is supplied to the model during run time. *Note:* See section; 1.3 Approach and methodology for the description of measurements.

Chapter Six - Discussion and Conclusion

6.1 Effect of sediment supply control on 3D sequence development

The modeling results in this thesis illustrate the impact of sediment supply on the three-dimensional evolution of deltaic depositional sequences. Chapter four presented a series of experiments that investigated the stratigraphic response of deltas to sinusoidally varying sediment supply under condition of constant rate of sea level rise.

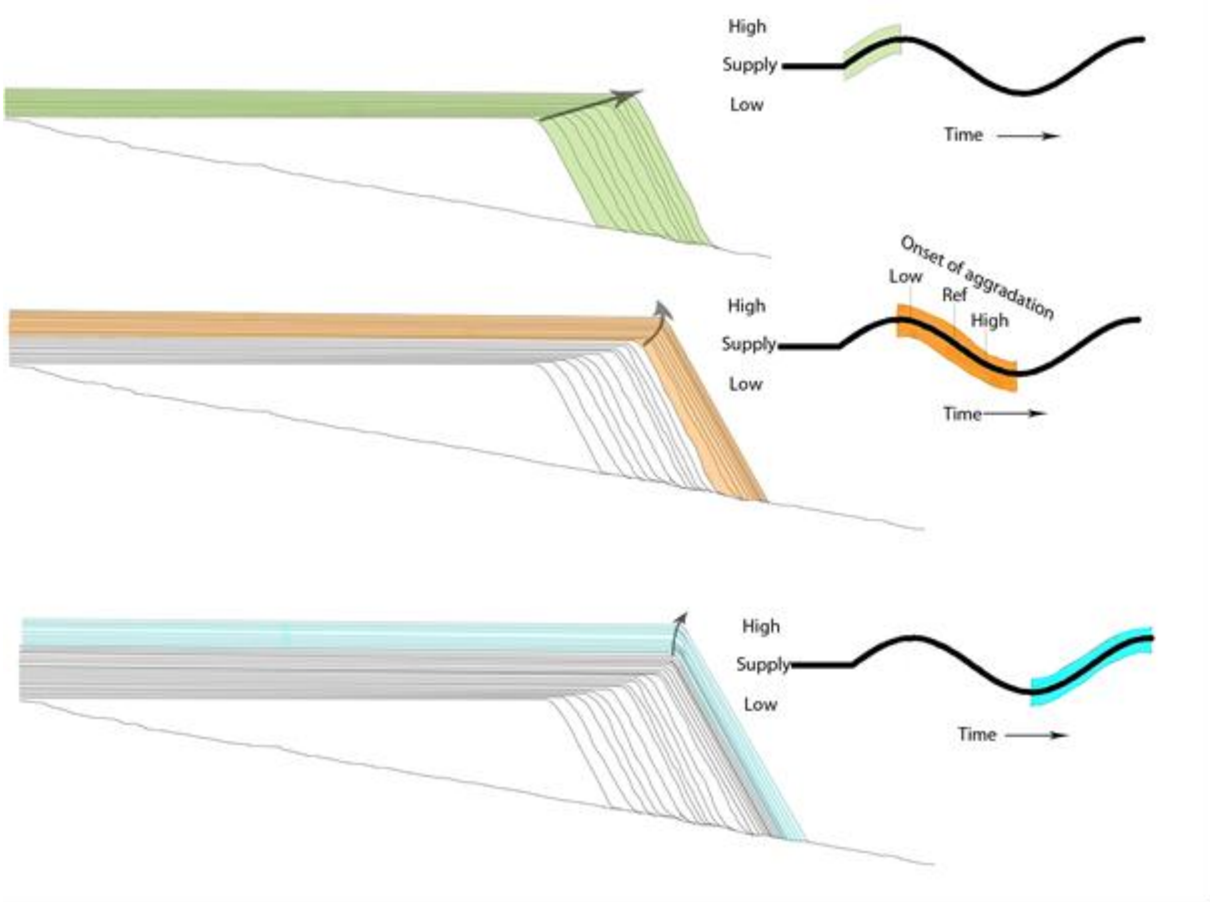

Fig. 47: Sketch illustrating how a delta response during sinusoidal variations in sediment supply under condition of linear sea-level rise. It is progradational-aggraditional during increase in the first increase (represented in green color) of sediment supply. Delta changes to aggraditional during decrease of sediment supply (illustrated with orange color), where onset of aggradation is controlled by the amount of sediment. At the second increase (light blue color), then either the delta remain aggraditional or if there is sufficient amount of sediment, the model can become aggraditional-progradational. Note the clustering of foresets as the sediment supply decreases.

During the initial part of the model run, sea-level starts rising and the sediment supply begin to increase towards maximum sediment supply. The three first models (reference, low-and high sediment supply models) have similar stratal geometries with progressively steepening of the break point trajectory (Fig. 12B; Fig. 15B; Fig. 16B) (Fig. 47). Comparisons with the three different models indicate a delay on the onset of aggradation associated with increasing sediment supply. In the low sediment supply model, the stratal geometry changes from progradational to aggradational to aggradational as soon as the sediment supply begins to decrease (at 50 kyr). Indicating that there is not enough sediment supplied to fill topset volume and also deliver sediment to foresets in order to prograde. As aggradation starts, the foresets clustered together (Fig. 15C). These features are characteristic for autoreatreat (Muto and Steel 1992; 1997). In contrast, in the reference model, onset of aggradation is delayed to maximum rate of decreasing sediment supply at the inflection point (at 75 kyr) (Fig. 12D), while the high sediment supply model, has a onset of aggradation when the rate of sediment supply slows towards minimum sediment supply (at 87.5 kyr)(Fig. 16D). As a result, high sediment supply has a delay of onset aggradation by 37.5 kyr. (Fig. 47)

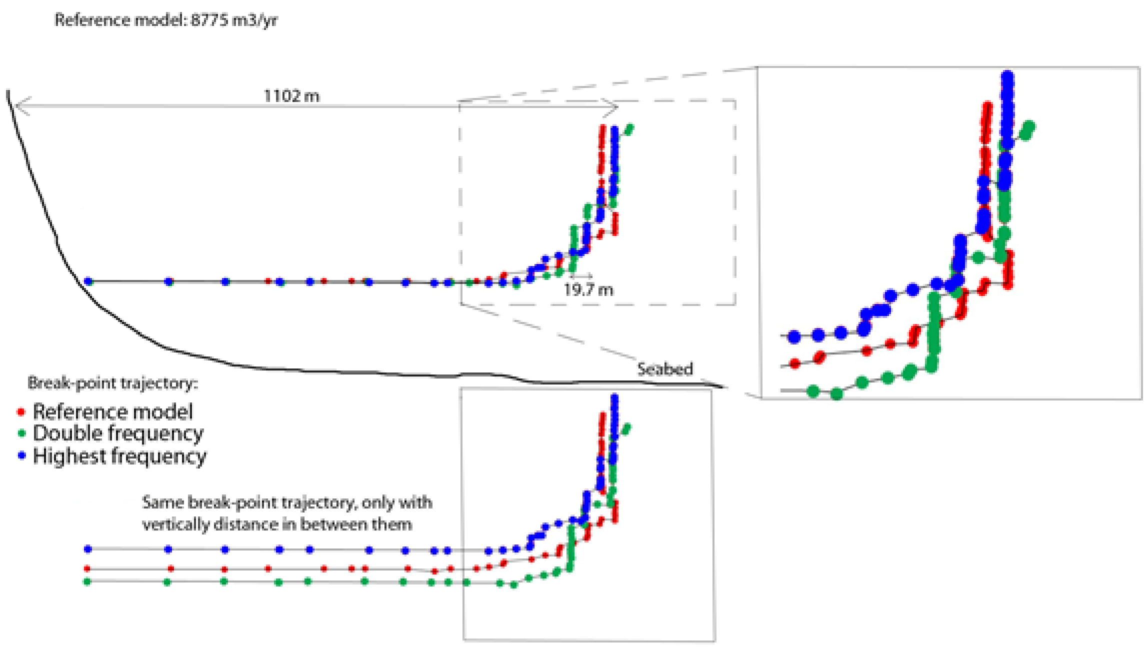

Fig. 48: Sketch with the actual break-point trajectories for the models with the same volume of sediment as a reference model. The three different trajectories (represented by different colors) illustrate the 19.7 m difference of onset of aggradation.

The stratal geometry in the models are characteristics of deposits of lowstand systems tract (LST), which display a combination of progradation and aggradation with increasingly aggradational break-point trajectory (Catuneanu et al.2009). These features are characteristic with a normal regression, which occur where sedimentation rates outpace the rate of new accommodation added due to sea-level rise at the shoreline (Catuneanu et al. 2009).

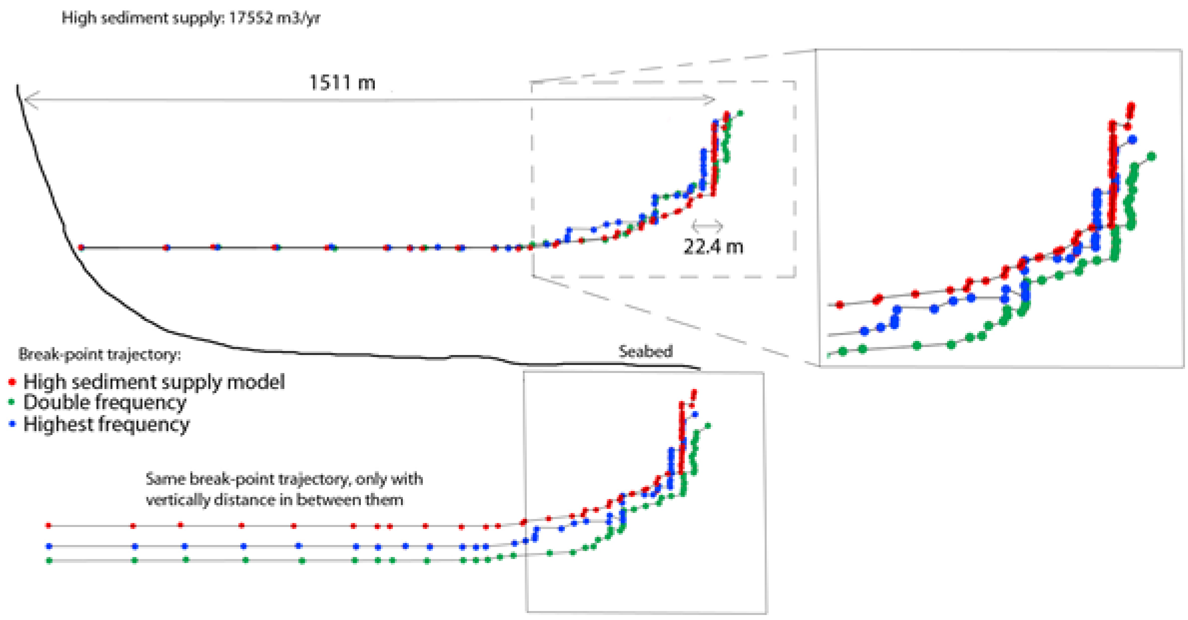

Fig. 49: Sketch with the actual break-point trajectories for the models with the same volume of sediment as high sediment supply model. The three different trajectories (represented by different colors) illustrates the 22.4 m difference of onset of aggradation.

The reference and high sediment supply models foresets clustering, starts at the maximum rate of decreasing sediment supply (Fig. 12C; Fig 16C) and is a good approximation for sediment supply cycles, but is only really resolvable in high supply situations. Variation in foreset spacing during model runs occurs in all models. The thickness, facies and foreset spacing are more complicated in natural systems where avulsion on the delta top will change where on the delta front sediment is supplied. Therefore, it will generate changes in forset thickness.

In the models where the frequency of sediment supply is higher, to a first approximation they have the same overall stratal evolution with progradation to aggradation (Fig. 19C; Fig. 20C). The onset of aggradation occurs in half wavelength model when sediment supply starts to decrease just after maximum sediment supply at 37.5 kyr (Fig. 19B). The one-fourth wavelength model becomes aggradational during maximum rate of decreasing sediment supply between 50 and 62.5 kyr (Fig. 20C).

Minor changes in trajectory with maximum supply intervals, leads to slight intervals with minor aggradation to progradation trajectory (Fig. 19D). The change to more progradational trajectory occurs shortly after an increase in sediment supply and becomes aggraditional again after decreasing sediment supply. These changes in trajectories are likely to changes within sediment volume. However, this is difficult to resolve as wavelength increases. Especially in one-fourth wavelength model where frequency between maximum and minimum sediment supply is short. The general trend is that one-fourth wavelength has a pulse of progradation (forestep) at maximum sediment supply, until sediment supply and water depth reaches equilibrium and becomes aggraditional.

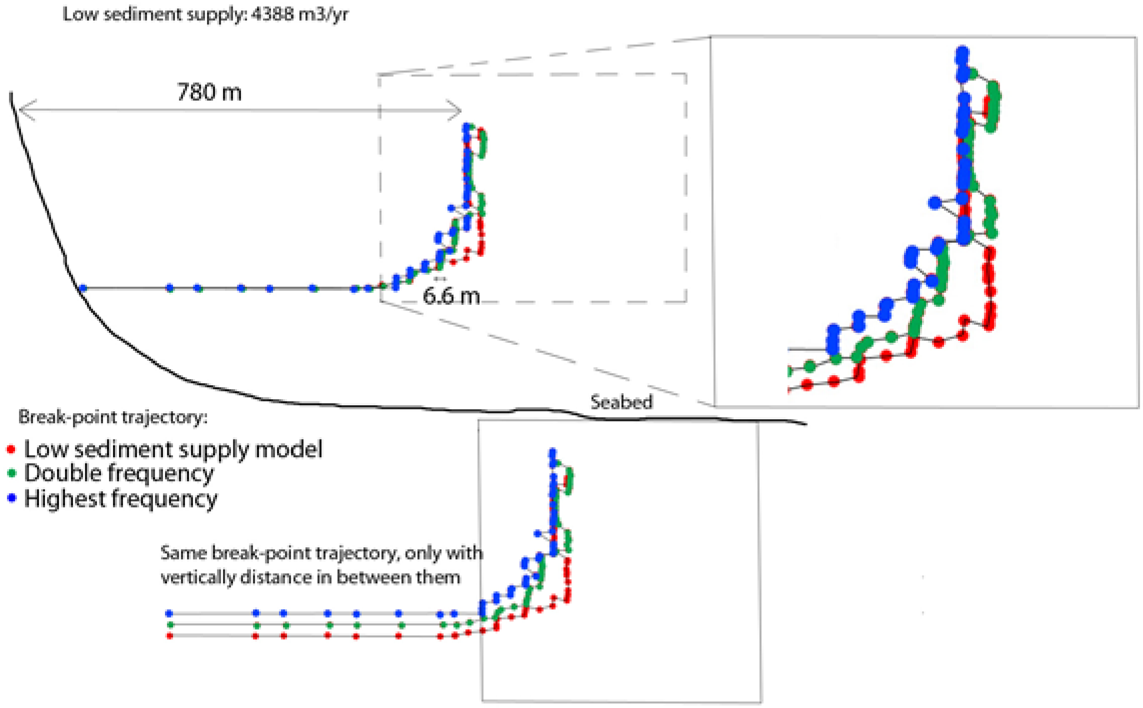

Fig. 50: Sketch with the actual break-point trajectories for the models with the same volume of sediment as low sediment supply model. The three different trajectories (represented by different colors) illustrate the 6.6 m difference of onset of aggradation.

By taking a look at all models and compare those with the onset of equilibrium between sediment supply and water depth, then there is a clear trend in terms of sediment volume between the different models. Initial sediment volume (reference, half-and one-fourth wavelength models) have a difference between each other at 19.7 m on the onset of aggradation (Table 12) (Fig. 48). The high sediment supply models have a difference of 22.4 m (Fig. 49), while low sediment supply models have a difference of 6.6 m on the onset of aggradation (Table 12) (Fig. 50). As a result, it seems that the point of aggradation is related to average sediment volume and not change of frequency.

In this section, it will be discussed similarities and differences in three-dimensional depositional sequence evolution on the basis of varying sediment supply with a sinusoidal sea-level cycle. At the three different models under conditions of sinusoidal sea-level change, the in-phase model sediment supply increases as sea-level rises towards the maximum sediment supply and sea-level highstand at 50 kyr. In contrast, the out-phase model initially has decreasing sediment supply during the same time interval. During the initial stages of sediment supply variations, all models start developing topsets due to sea-level rise. The in-phase model, which has increasing sediment supply, has enough sediment to fill all delta top. This is not the case at out-phase and constant sediment supply models. The constant sediment supply model initially backsteps on the left side of the delta as the sediment supply struggles to fill the topset accommodation (Fig. 26B, C; Fig. 32B, C). This lead to accumulation of sediment in the front and right side of the delta, while the left side of the delta gets starved of sediment and undergoes transgression (Fig. 26B, C), whereas the right side of delta, undergoes progradation (Fig. 27B; Fig. 29B).

In out-phase model, which has decreasing sediment volume as the sea-level starts to rise, also backsteps. As the delta gets drowned, the delta struggles to fill all the topset accommodation, leaving both left and right side of delta starved for sediments (Fig. 38B, C). The main dip profile line (Fig. 38B) shows aggradation stacking pattern from the previously deposits at 25 kyr. While the left and right dip profile lines (Fig. 39B; Fig. 40B) shows retrogradation with aggradation to progradation at the end of sea-level rise. The delta has undergone transgression during sea-level rise, with only minor regression towards the sea-level highstand. The constant sediment supply and in-phase models have the same overall stratal evolution at the main dip profile line with progressively steepening of break of slope and an aggraditional to progradational stacking pattern (Fig. 27B; Fig. 33B). This feature is characteristic of normal regression, where progradation is driven by sediment supply and sedimentation rate outpaces the rate of sea-level rise at the shoreline (e.g., Posamentier and Vail 1988; Helland-Hansen and Gjelberg 1994; Catuneanu et al. 2009). As sea-level approaches highstand, the deltas develop a subhorizontal delta top that passes basinward into smooth arcuate delta front (Fig. 26C; Fig. 32C; Fig. 38C).

During an early stage of sea-level fall, the deltas have a numerous poorly developed, shallowly incised channels. As the rate of sea-level fall increases, incised channels evolve and start to headwardly cut into the deltaic deposits formed earlier as they are exposed by continuing sea-level fall. As the incised channels cut deeper and back towards the sediment source, they capture more sediment and deposition becomes focused at incised channel mouths. Some of the incised channels become dominant, and capture other channels, leaving the captured channel mouths inactive (Fig. 26E, F; Fig. 32E, F; Fig. 38E, F). In constant sediment supply model, channels avulse until the maximum rate of sea level fall (at 75 kyr) where the elevation increases and a single channel becomes stable and transport all the sediment to the channel mouth (lobe 3). This also occurs in the in-phase model at maximum rate of sea-level fall (at 75 kyr) where the main channel shifts from flowing towards east (green arrow pointing north) to flowing in a southeasterly direction. In the out-phase model, lobes branch as the channel changes the position of the mouth. By the time in-phase model reaches its minimum sediment supply and the out-phase model its maximum sediment supply (at 100 kyr), delta fronts in all three models have become increasingly lobate and are dominated by incised channels that focus all sediments to forced regressive lobes at their mouths.

The break-point trajectory (in the main dip profile line) in the in-phase and constant sediment supply had a progressively steepening of breaking slope and an aggraditional to progradational stratal stacking pattern during sea-level rise (until 50 kyr, Fig. 27C; Fig. 33C; Fig. 39C). These features are characteristics of a highstand normal regression, which record a change from aggradation to progradation (Catuneanu et al. 2009).

However, deposition along the main dip profile line ceases at 50 kyr as the deposition during the sea-level fall was focused on the lobes. As a result, main dip profile line during sea-level fall is not representative and the dip profiles lines (Right and left dip profile lines) that represent deposits in lobes in all models therefore had to viewed (Fig. 28D; Fig. 34D, Fig 41D). These tell of basinward-falling break-point trajectory, together with deposition downstep and offlap. These features are characteristics of an accretionary forced regression (e.g. Hunt and Tucker 1992; Posamentier et al. 1992a; Posamentier et al. 1992b; Helland-Hansen and Gjelberg 1994). In all models, sediment supplied through incised channels is deposited in the forced regressive lobes.

During sea-level lowstand and early rise, sediment supply in the out-phase model begins to decrease, while in-phase it increases. Sediment transport in all models is still focused through the previously incised channels, and deposition is focused at their mouths. Sediment onlaps the previously exposed and incised top of the lobe and the lobes start to expand laterally and infill the relict topography around the lobe. As a result of infilling the relict topography around the lobes, it forms an apron in all models (Fig. 28E; Fig. 34E; Fig. 41E). Aprons have an aggraditional to progradiitional stacking pattern. In the initial part of the sea-level rise has out-phase and constant sediment supply models more sediment supplied than the in-phase model which has just begun to increase sediment supply after a minimum of sediment supply at sea level lowstand (at 100 kyr). As a result, the apron in out-phase and constant sediment supply models still building basinward as they fill the relict topography around the lobe. In contrast, in-phase model only fills the around the lobe and does not expand any further basinward.

At the time sea-level reaches sea-level highstand (at 150 kyr), out-phase model is at its minimum and in-phase at its maximum sediment supply again. The apron in all models has become more laterally extensive as the influence of the incised channels on sediment transport decreased. The apron in the in-phase and constant sediment supply models (Fig. 28F; Fig. 34F; Fig. 41F), have a break-point trajectory that have change from basinward-climbing to landward-climbing and sediments are deposited as a set of retrogradational units. In the in-phase model, the topsets-foresets transition has moved landward by approximately 110 m. In contrast, the out-phase model, which had a decreasing sediment supply, has an aggraditional stacking pattern with a break-point trajectory which climb vertically.
The landward-climbing break-point trajectory and the retrogradational stacking pattern in the in-phase and constant sediment supply models are characteristic of an accretionary transgression (Posamentier and Vail 1988; Helland-Hansen and Gjelberg 1994).

At sea-level highstand, the main dip profile line in the in-phase and out-phase models (Fig. 33F; Fig. 39F), have break-point trajectories with an upward-basinward climbing trajectory, as a result of accumulation of sediments in the delta front due to the laterally filling in relict topography around the apron during sea-level rise. During the time interval of sea-level rise, the in-phase model has poorly developed topsets and foresets is wavy as they onlaps on previous deposits. The out-phase model has more developed topsets, and more straight dipping foresets (Fig. 33F; Fig. 39F). The basinward climbing break-point trajectory, onlap and progradational-aggraditional stacking pattern are characteristic of lowstand systems tract (Posamentier and Vail 1998).

During sea-level highstand and early fall (from 150 kyr), sediment supply at the out-phase model begin to increase, while in-phase decreasing. During the initial decrease of sediment at in-phase model, there is a delay of forming incised valleys and lobes in the second fall. The sediments accumulate along the delta front forming a smooth arcuate delta front (Fig. 32L, M). The out-phase model got major avulsion as the deposits of sediment have changes from deposit sediment on the right side (during last sea-level fall) to the left side of the delta front, The break-point trajectory in both models have a downward basinward-climbing trajectory with no topsets and a progradational stacking pattern (Fig. 36G; Fig. 42G).
In contrast, constant sediment supply channels start avulsion to low area and develops forced regressive lobes and all sediment got accumulate to the lobe (Fig. 26L, M). As a result, the break-point trajectory is downward and basinward and deposits downstep. These features are associated with forced regression (Hunt and Tucker, 1992; Posamentier et al.1992a; Posamentier et al.1992b; Catuneanu et al. 2009). As the in- and out-phase models reach the maximum rate of sea-level fall with different degrees of supply of sediment supply (out-phase increasing, in-phase decreasing), lobes starts to evolve, creating a forced regressive apron, together with poorly developed, shallowly incised channels, (Fig. 32N, O; Fig. 38N, O).

At the end of model run, sea-level reaches lowstand at 200 kyr. Break-point trajectory in the in-and out-phase models have a basinward trajectory in both lobes deposits and along the main dip profile line (Fig. 33H; Fig 35H; Fig. 39H; Fig. 40H). The out-phase model, is at maximum sediment supply (at 200 kyr), and is more laterally extensive as it fills the relict topography around the lobe than in-phase model.
Constant sediment supply model have a downward basinward break-point trajectory and the associated deposits downstep and offlap (Fig. 30H; Fig 32H). These features are characteristics of forced regression (Catuneanu et al. 2009; Posamentier et al.1992a; Posamentier et al.1992b; Helland-Hansen and Gjelberg 1994).

Despite the varying sediment supply under conditions of sinusoidal sea level curve (last three models), it appears overall sea level is the driving mechanism controlling the stratigraphic evolution. In each model, the sea level shows a dynamic balance between erosion and deposition and sea-level in the models represents the highest level up to which a sedimentary succession can be build. In the last three models, with condition of sea level change, all models forms incised channels with varying head ward lobes, depending on the capture of incised channels, and eventually form a lobate delta front during sea level fall. At sea level rise, it fills all models relict topography around the lobes, and since the lobes expands laterally, it forming an apron. Varying sediment supply controls, to some degree, strike variations, basinward expansion (progradation vs. aggradation / retrogradation) and shoreline shifts (transgression and regression).

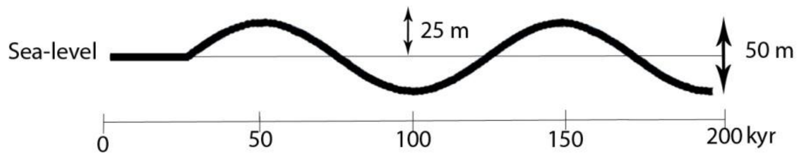

Fig. 51: Overview of the amplitude through time that was used in the sinusoidal sea-level cycle in chapter five. Amplitude through time is higher than the periods of greenhouse climate, but lower than Icehouse climatic periods.

During this study, the amplitude and the rate of sea level changes have been relatively high (Fig. 51) compared to greenhouse climate. With amplitude of 25 m, sediment supply has been able to keep up with the created / destroyed accommodation space during the models run. Greenhouse climate would have had a lower amplitude and rate of sea level changes, and thus would probably sediment supply influence been more important. Comparing the study with icehouse climate, the amplitude and the rate of sea level changes are much higher in icehouse climate. Quaternary ice caps may have forced a glacio-eustatic sea-level fall of approximately 120 m. Rate of sea level fall is proposed to be 1 cm/yr which is up to a thousand times faster than the average rate for tectono-sea-level fall (associated with tectonic processes) (Coe et al. 2005). Over the last 800 ka, have repeated slow growth and rapid melting of ice led to highly variable amplitudes in sea level. Glacio-eustatic sea-level fall of rates up to 5 m / ka, while a rapid marine transgression (during melting of ice) have rates up to 4 m/100 years (Ruddiman et al. 1989; Coe et al. 2005). At such amplitudes and rates of sea level changes during icehouse climate in the study results would probably have been different. Since icehouse climate gives large fluctuations in amplitude, stacking pattern and the break-point trajectory would probably been different. Especially during periods of rapid marine transgression, sediment supply to deltas in this study would not be able to fill the created accommodation space and stacking pattern would probably have landward detached parasequences.

6.1 Further Work

To get a better overview of the influence of sediment supply, it can be run simulations with different sea-level amplitude and frequency to see how sediment supply and sea level amplitude and rates interact. In addition to different sea-level changes (Greenhouse / Icehouse).

The interpretation of in-and out-phase models presented in this study can be further strengthened by more close investigation by simulating the phase shifts progressively between these two models.

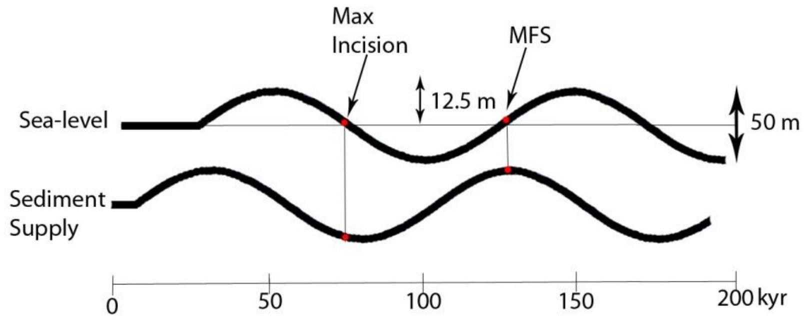

Fig. 52: An example of further work that illustrates the phase shift progressively between in-and out-phase models, which will provide insight into how the maximum flooding surface will behave under conditions of maximum sediment supply.

E.g. maximum rate of increase in sea level associated with maximum sediment supply (Fig. 52).

This example will give an insight into how the maximum flooding surface will behave under conditions of maximum sediment supply, and how the incision channel during maximum rate of sea-level fall behave under conditions of minimum sediment supply.

6.1 Conclusion

- The study was to investigate the role of sediment supply controlling the evolution of deltaic depositional system using 3D numerical model of sediment transport, deposition and erosion based on Ritchie et al. (1999).
- There is a delay on onset of aggradation associated with an increase in sediment supply volume.
- Point of aggradation is related to average sediment volume and not change of frequency.
- Foresets clustering is a good approximation for sediment supply cycles.
- Changes in sea level are the dominant control in evolution of deltaic depositional system.
- Further work is needed to get a better control over how the different sea-level changes and sediment supply interact.

References:

ALLEN, J.R.M., BRANDT, U., BRAUER, A., HUBBERTEN, H.W., HUNTLEY, B., KELLER, J., KRAML, M., MACKENSEN, A., MINGRAM, J., NEGENDANK, J.F.W., NOWACZYK, N.R., OBERHÄNSLI, H., WATTS, W.A., WULF, S. AND ZOLITSCHKA, B. 1999. Rapid environmental changes in southern Europe during the last glacial period. *Nature*, **400**, 740.

ATTAL, M., COWIE, P.A., WHITTAKER, A.C., HOBLEY, D., TUCKER, G.E. AND ROBERTS, G.P. 2011. Testing fluvial erosion models using the transient response of bedrock rivers to tectonic forcing in the Apennines, Italy. *Journal of Geophysical Research,* **116**, FO2005.

BACKERT, N., FORD, M AND MALARTRE, F. 2009. Architecture and sedimentology of the Kerinitis Gilbert-type fan delta, Corinth Rift, Greece. *Sedimentology,* **57**, 543-586.

BLUM, M.D. AND HATTIER-WOMACK, J. 2009. Climate change, sea-level change, and fluvial sediment supply to deepwater depositional systems. In: *External Controls on Deepwater Depositional Systems, SEPM Special Publication.* **92**, 15-39.

CATUNEANU, O. 2002. Sequence stratigraphy of clastic systems, concepts, merits, and pitfalls. *Journal of African Earth Sciences,* **35**, 1-43.

CATUNEANU, O., ABREU, V., BHATTACHARYA, J., BLUM, M., DALRYMPLE, R.W., ERIKSSON, P., FIELDING, C., FISHER, W., GALLOWAY, W., GIBLING, M.R., GILES, K., HOLBROOK, J., KENDALL, C.G., MACURDA, B., MARTINSEN, O., MIALL, A., NEAL, J., NUMMEDAL, D., POSAMENTIER, H.W., PRATT, B., SARG, R., SHANLEY, K., STEEL, R.J., STRASSER, A., TUCKER, M. AND WINKER, C. 2009. Towards the standardization of sequence stratigraphy. *Earth-Science Reviews,* **92,** pp. 1-33.

COE, A.L., BOESCENCE, D.W., CHURCH, K.D., FLINT, S.S., HOWELL, J.A. and WILSON, R.C. 2005, The sedimentary record of the sea-level change: *The Open University, Cambridge: Cambridge University Press*, 285 p.

COLLIER, R.E.L. AND GAWTHORPE, R.L. 1995. Neotectonics, drainage and sedimentation in central Greece: insights into coastal reservoir geometries in syn-rift sequences. In: *Hydrocarbon Habitat in Rift basins, Geological Society Special Publication*, **80**¸ pp. 165-181

COLLIER, R.E.L., LEEDER, M.R., TROUT, M., FERENTINOS, G., LYBERIS, E. AND PAPATHEODOROU, G. 2000. High sediment yields and cool, wet winters: Test of last glacial paleoclimates in the northern Mediterranean. *Geology,***28**, no.11; pp. 999.

GALLOWAY, W.E. 1989. Genetic Stratigraphic Sequences in Basin Analysis .1. Architecture and Genesis of Flooding-Surface Bounded Depositional Units. *American Association of Petroleum Geologists Bulletin*, **73,** 125-142.

GAWTHORPE, R.L., FRASER, A.J. AND COLLIER, R.E.L. 1994. Sequence stratigraphy in active extensional basins: implications for the interpretation of ancient basin-fills. *Marine and Petroleum Geology,* **11**, 6.

GUPTA, S., UNDERHILL, J.R., SHARP, I.R. AND GAWTHORPE, R.L. 1999. Role of fault interactions in controlling synrift sediment dispersal patterns: Miocene, Abu Alaqa Group, Suez Rift, Sinai, Egypt. *Basin Research,* **11**, pp. 167-189.

HELLAND-HANSEN, W. AND HAMPSON, G.J. 2009. Trajectory Analysis: Concepts and Applications. *Basin Research,* **21,** 454-483.

HELLAND-HANSEN, W. AND MARTINSEN, O.J. 1996. Shoreline trajectories and sequences: description of variable depositional-dip scenarios. *Journal of Sedimentary Research,* **66**, 670-688.

HENRIKSEN, S., HAMPSON, G.J., HELLAND-HANSEN, W., JOHANNESSEN, E.P. AND STEEL, R.J. 2009. Shelf edge and shoreline trajectories, a dynamic approach to stratigraphic analysis. *Basin Research,* **21**, 445-453.

HUGHES, P.D., WOODWARD, J.C. AND GIBBARD, P.L. 2005. Late Pleisticene glaciers and climate in the Mediterranean. *Global and Planetary Change,* **50**, 83.

HUGHES, P.D., WOODWARD, J.C. AND GIBBARD, P.L. 2006. Quaternary glacial history of the Mediterranean mountains. *Progress in Physical Geography,* **30**, 334.

HUNT, D. and TUCKER, M.E. 1992. Stranded parasequences and the forced regressive wegde systems tract: deposition during base-level fall. *Sedimentary Geology,* **81**, 1-9.

KIM, W. AND JEROLMACK, D.J. 2008. The Pulse of Calm Fan Deltas. *The journal of Geology,* **116**, pp. 315-330.

KIM, W., and PAOLA, C. 2007. Long-period cyclic sedimentation with constant tectonic forcing in an experimental relay ramp. *Geology,* **35**, 4, pp. 331-334.

KIM, W., DAI, A., MUTO, T. AND PARKER, G. 2009. Delta progradation driven by an advancing sediment source: Coupled theory and experiment describing the evolution of elongated deltas. *Water Resources Research,* **45**, W06428.

LEEDER, M.R., HARRIS, T. AND KIRKBY, M.J. 1998. Sediment supply and climate change: implications for basin stratigraphy. *Basin Research,* **10**, pp. 7-18.

LEEDER, M.R., MACK, G.H., BRASIER, A.T., PARRISH, R.R., MCINTOSH, W.C., ANDREWS, J.E. AND DUERMEIJER, C.E. 2008. Late-Pliocene timing of Corinth (Greece) rift-margin fault migration. *Earth and Planetary Science Letters*, **274**, pp. 132-141.

MORTIMER, E., GUPTA, S. AND COWIE, P. 2005. Clinoform nucleation and growth in coarse-grained deltas, Loreto basin, Baja California Sur, Mexico: a response to episodic accelerations in fault displacement. *Basin Research,* **17**, pp. 337-359.

MUTO, T. and STEEL, R.J. 1992. Retreat of the front in a prograding delta. *Geology,* **20**, 967-970.

MUTO, T. and STEEL, R.J. 2004. Autogenic response of fluvial deltas to steady sea-level fall: implications from flume-tank experiments. *Geology***, 32**, 401-404

POSAMENTIER, H.W. and ALLEN, G.P. 1999. Silisicalstic sequence stratigraphy: consepts and applications. *Consepts in Sedimentology and Palentology,* **7**, Society of Economic Paleontologists and Mineralogists (SEPM), pp 210.

POSAMENTIER, H.W. AND MORRIS, W.R. 2000. Aspects of the stratal architecture of forced regressive deposits. In: Sedimentary Responses to Forced Regressions (eds Hunt, D. and Gawthorpe, R.L.) *Geological Society of London Special Publication*. **172**, 19-46.

RITCHIE, B.D., GAWTHORPE, R.L. AND HARDY, S. 1999. Three-dimensional numerical modelling of coarse-grained clastic deposition in sedimentary basins. *Journal of Geophysical Research,* **104**, pp. 17,759 – 17,780.

RITCHIE, B.D., GAWTHORPE, R.L. AND HARDY, S. 2004. Three-Dimensional Numerical Modeling of Deltaic Depositional Sequences 1: Influence of the Rate and Magnitude of Sea-Level Change. *Journal of Sedimentary Research*, **74,** 203-220.

RITCHIE, B.D., GAWTHORPE, R.L. AND HARDY, S. 2004. Three-Dimensional Numerical Modeling of Deltaic Depositional Sequences 2: Influence of Local Controls. *Journal of Sedimentary Research*, **74,** 221-238.

SØMME, T.O., PIPER, D.J.W., DEPTUCK, M.E. AND HELLAND-HANSEN, W. 2011. Linking onshore-offshore sediment dispersal in the golo source-to-sink system (Corsica, France) during the late quaternary. *Journal of Sedimentary Research,* **81**, 118.

SWENSON, J.B. AND MUTO, T. 2006. Response of coastal plain rivers to falling relative sea-level: allogenic controls on the aggradational phase. *Sedimentology,* **54**, 207-221.

SYVITSKI, J.P.M. AND MILLIMAN, J.D. 2007. Geology, Geography, and Humans Battle for Dominance over the Delivery of Fluvial Sediment to the Coastal Ocean. *The Journal of Geology,* **115**, 1-19.

TUCKER, G.E., MCCOY, S.W., WHITTAKER, A.C., ROBERTS, G.P., LANCASTER, S.T. AND PHILLIPS, R. 2011. Geomorphic significance of postglacial bedrock scarps on normal-fault footwalls. *The Journal of Geology,* **116**, F01022

TZEDAKIS, P.C. 2005. Towards an understanding of response of southern European vegetation to orbital and suborbital climate variability. *Quaternary Science Reviews*, **24**, 1585.

TZEDAKIS, P.C. 2007. Seven ambiguities in the Mediterranean palaeoenvironmantal narrative. *Quaternary Science Reviews*, **26**, 2042.

UMHOEFER, P.J., DORSEY, R.J. AND RENNE, P. 1994. Tectonics of the Pliocene Loreto basin, Baja California Sur, Mexico, and evolution of the Gulf of California. *Geology*, **22**, p. 649-652.

VAN WAGONER, J.C., MITCHUM, R.M., POSAMENTIER, H.W. and VAIL, P.R. 1987. An overview of sequence stratigraphy and key definitions. In: Bally, A.W., *Atlas of Seismic Stratigraphy*, **1**, *Studies in Geology*, **27**, *American Association of Petroleum Geologists*, pp 11-14.

YOSHIDA, S., STEEL, R.J. AND DALRYMPLE, R.W. 2007. Changes in depositional processes – an ingredient in a new generation of sequence-stratigraphic models. *Journal of Sedimentary Research*, **77**, 447-460.

Appendix I, II & III:

Background work

Appendix I – Background for sediment supply values

In order to identify the amount of sediment that would supplied to the models, it needed a catchment area. The basis for the catchment area was Tor Sømme collection of data of catchment areas of the Gulf of Corinth. It was calculated an average catchment area of 146 km2. This was used as a starting point to find the amount of sediment supply that was supplied to the model.

In the search of sediment volume to the models, it was tested four different ways. The first test was based on Collier et al. 2000 that had looked on the sediment discharge rates (m^3/yr) from the last glacial lowstand and the last interglacial high stand deposits from the Alkyonides Gulf, Greece. Here was the catchment area of between 280 and 305 km^2. In last Glacial lowstand, the sediment discharge rate was 22,200 m^3/yr, while the last inter glacial highstand the sediment discharge rate was 12,900 m^3/yr.
Another way was to look at Leeder et al. 1998 work in which two different fan was studied (a Holocene fan in Leidy Creek, Nevada and a late Quaternary fan from the Millner Creek fan). The Holocene fan had a catchment area of 60.3 km^2 and had a sediment discharge rate of 17820 m^3/yr. The late Quaternary fan had a catchment area of 35.5 and sediment discharge rate of 2460 m^3yr.

Tucker et al. 2011 had worked Holocene bedrock fault scarps in Central Apennines, Italy. In the paper it was decided on an erosion rate of 0.25 mm/yr, which was used to multiply by the drainage area of 146 km2 used in the model (taken from Tor Sømme data in the Gulf of Corinth) (Erosion rate by catchment area). The calculation resulted in a sediment discharge rate of 365000 m^3/yr.

The last option that were tested to obtain sediment supply volume models were Syvitski and Milliman et al. 2007 work on BQART formula. This formula was developed further after Syvitski (2003) ART formula. Here, the average relief from Tor Sømme catchment area in the Gulf of Corinth used (1.3 km). Two tests at different temperatures were tested. The first test that was based on the temperature from modern Lake Ioannina, northern Mediterranean (Leeder et al.1998) had an average temperature of 14.4 °C. Calculation of the test gave 1109.6 m^3/yr. The second test was based also on Lake Ioannina, northern Mediterranean, where the average temperature from glacial maximum (Prentice et al. 1992) was 11.9°C. From the calculations, a sediment discharge rate of 917 m^3/yr was given. The density of the sediment that were used during calculations was 1.922 g/cm^3 (wet sand density).

The calculations have not taken into account for the possibility of different bedrock lithology.

After several modeling tests with different sediment delivery volumes, the choice fell down on Collier et al. 2000.

Appendix II – Background for modeling parameters

In order to achieve the best possible results from 3D numerical modeling, several tests were run which include changing erodibillity of the delta, Diffusion coefficient (alpha), delta hardness (m), shear limit and random seed (Fig. 53). See the figure below for a glimpse of independently selected test images. These images are taken at lowstand of sea level at 75 kyr in order to see how the models behave during high – and lowstand sea-level and maximum and minimum sediment supply. The values that gave the best results were 0.0000075 for erodibillity, 2.0 for diffusion coefficient, 0.4 for delta hardness, 2.0for shearlimit and 61 in random seed. These values were used in all models in the thesis.

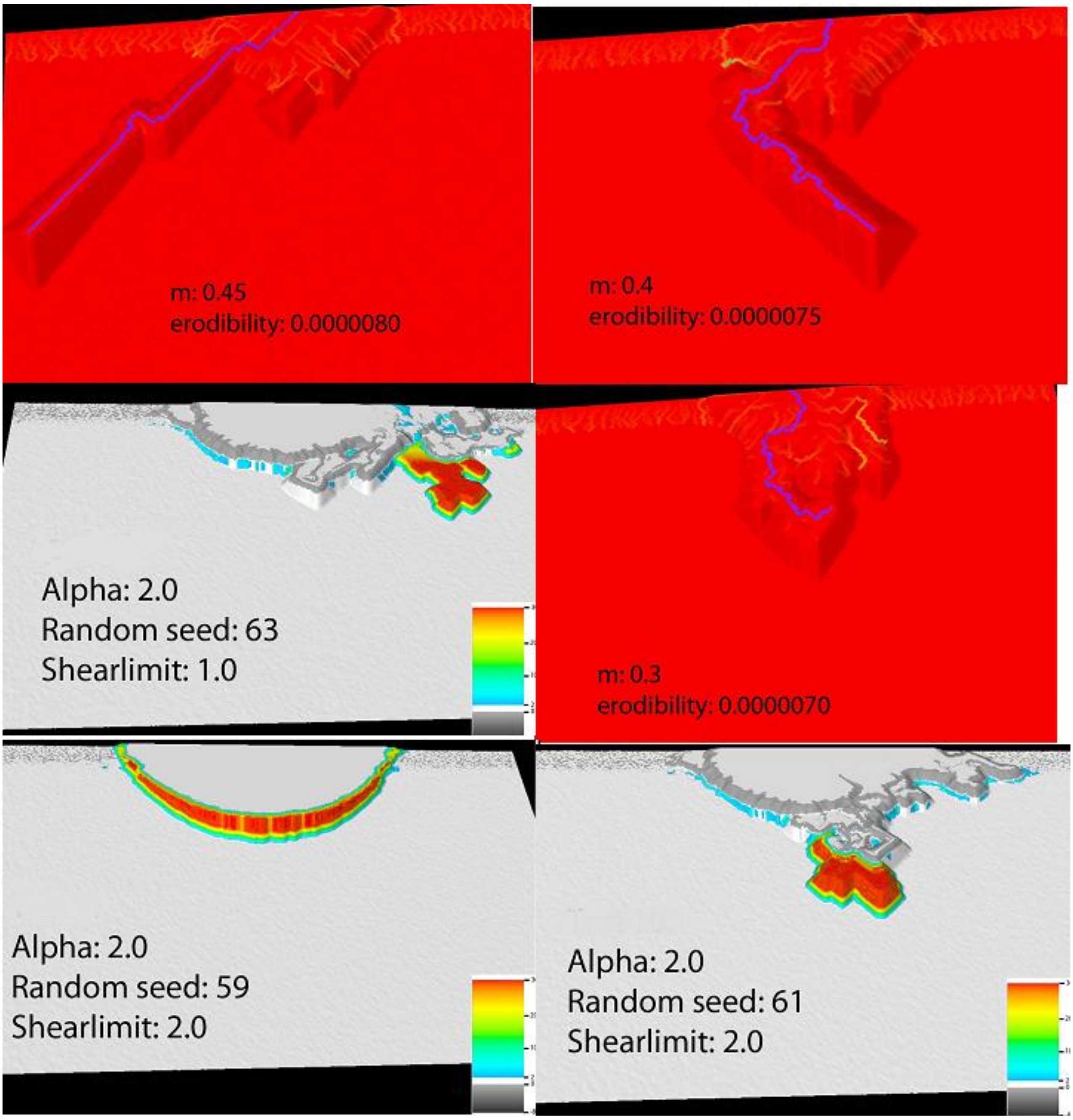

Fig. 53: Independently selected test images in order to find the parameters to be used at the different models.

These values were plotted in an input file like this (see Fig. 54). Below is a brief and basic description of the main parameters in the input file.

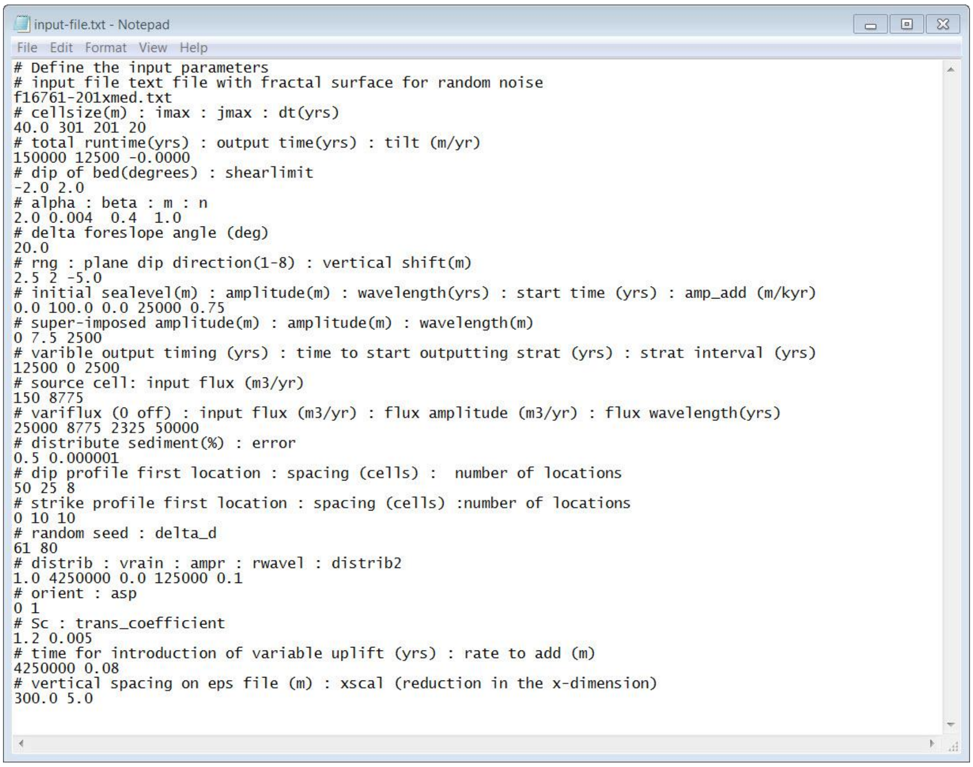

```
input-file.txt - Notepad
File  Edit  Format  View  Help
# Define the input parameters
# input file text file with fractal surface for random noise
f16761-201xmed.txt
# cellsize(m) : imax : jmax : dt(yrs)
40.0 301 201 20
# total runtime(yrs) : output time(yrs) : tilt (m/yr)
150000 12500 -0.0000
# dip of bed(degrees) : shearlimit
-2.0 2.0
# alpha : beta : m : n
2.0 0.004  0.4  1.0
# delta foreslope angle (deg)
20.0
# rng : plane dip direction(1-8) : vertical shift(m)
2.5 2 -5.0
# initial sealevel(m) : amplitude(m) : wavelength(yrs) : start time (yrs) : amp_add (m/kyr)
0.0 100.0 0.0 25000 0.75
# super-imposed amplitude(m) : amplitude(m) : wavelength(m)
0 7.5 2500
# varible output timing (yrs) : time to start outputting strat (yrs) : strat interval (yrs)
12500 0 2500
# source cell: input flux (m3/yr)
150 8775
# variflux (0 off) : input flux (m3/yr) : flux amplitude (m3/yr) : flux wavelength(yrs)
25000 8775 2325 50000
# distribute sediment(%) : error
0.5 0.000001
# dip profile first location : spacing (cells) :  number of locations
50 25 8
# strike profile first location : spacing (cells) :number of locations
0 10 10
# random seed : delta_d
61 80
# distrib : vrain : ampr : rwavel : distrib2
1.0 4250000 0.0 125000 0.1
# orient : asp
0 1
# Sc : trans_coefficient
1.2 0.005
# time for introduction of variable uplift (yrs) : rate to add (m)
4250000 0.08
# vertical spacing on eps file (m) : xscal (reduction in the x-dimension)
300.0 5.0
```

Fig. 54: Image of how the input-file for the reference model looks like. All the different parameters in the models were change by changing the parameters in the input-file.

Cellsize (m) - Size in meters for each cell in the model

Imax 301 and Jmax 201 - Scale of the model (x,y)

Dt(yrs) - Temporal evolution of the model that obtain information each dt years

Total runtime (yrs) 175000 – How many years the model are running.

Output time (yrs) - Time of the model provides a picture into Petrel

Tilt (m/yr) - How much tilt there is in the model

Shearlimit - Amount of stress on the sediments before erosion occurs

Dip of bed (degrees) - Gives the initial basin physiography dip

Alpha -Beta - This is the diffusion rate on the foreslope

M - Delta hardness, erodability to the delta

Delta foreslope angle (deg) – Degree of the slope failure

Rng - Gives the height in m of the noise on the initial surface

Initial sea-level (m) - Sea-level value in height at the start of the model.

Amplitude (m) - Cycles of sea-level change

Wavelength (yrs) - Wavelength in yrs of the cycle of sea-level change

Start time (yrs) – When the sea level cycles starts

Amp_add (m/kyr) – Subsidence/ uplift

Super-imposed amplitude – In order to add Milankovitch cycles

Variable output timing (yrs) – Can reduce or increase the output time later in the modeling (This means that it can have constant sea-level for the time you given (for instance in the first 25 000 years), before the variation starts)

Strat interval (yrs) – Time you want it to output dip and strike profile image. This year you have to multiple with 10 to get the right year of outputting the images.

Source cell - The cell to be the source of sediment supply. (Imax tells how many cells there are in the width of the model. If imax have 300 cells, will a source cell at 150 provide an entry of sediment in the middle of the model)

Input flux (m^3/yr) - Amount of sediment added to the model (providing a constant sediment supply)

Variflux - Providing a cycle of sediment delivering

Variflux -> input flux (m^3/yr) - Amount of sediment added to the model (providing a varying sediment supply)

Variflux -> flux amplitude (m^3/yr) - Cycles of sediment supply

Variflux -> flux wavelength (yrs) - Frequency in yrs of the cycle of sediment supply change

Random seed - This gives a different choice when running the models, the random location at which it starts delivering sediments. (This value is the same for all experiments in order to be able to compared the results)

Appendix III – Right and Left dip profile line in Chapter Four:

In Chapter Four the break-point trajectory measured from the main dip profile line. To verify that the trajectory of main dip line profile is representative of the whole model, then both right and left-hand dip line profile has been compared (Fig. 55) with respect to the pulses of progradation / retrogradation (forestep / backstep). This gave varied results, particularly in the back-stepping events in right and left-hand dip line profile at low sediment supply models gave a clear indication that retrogradation occurred

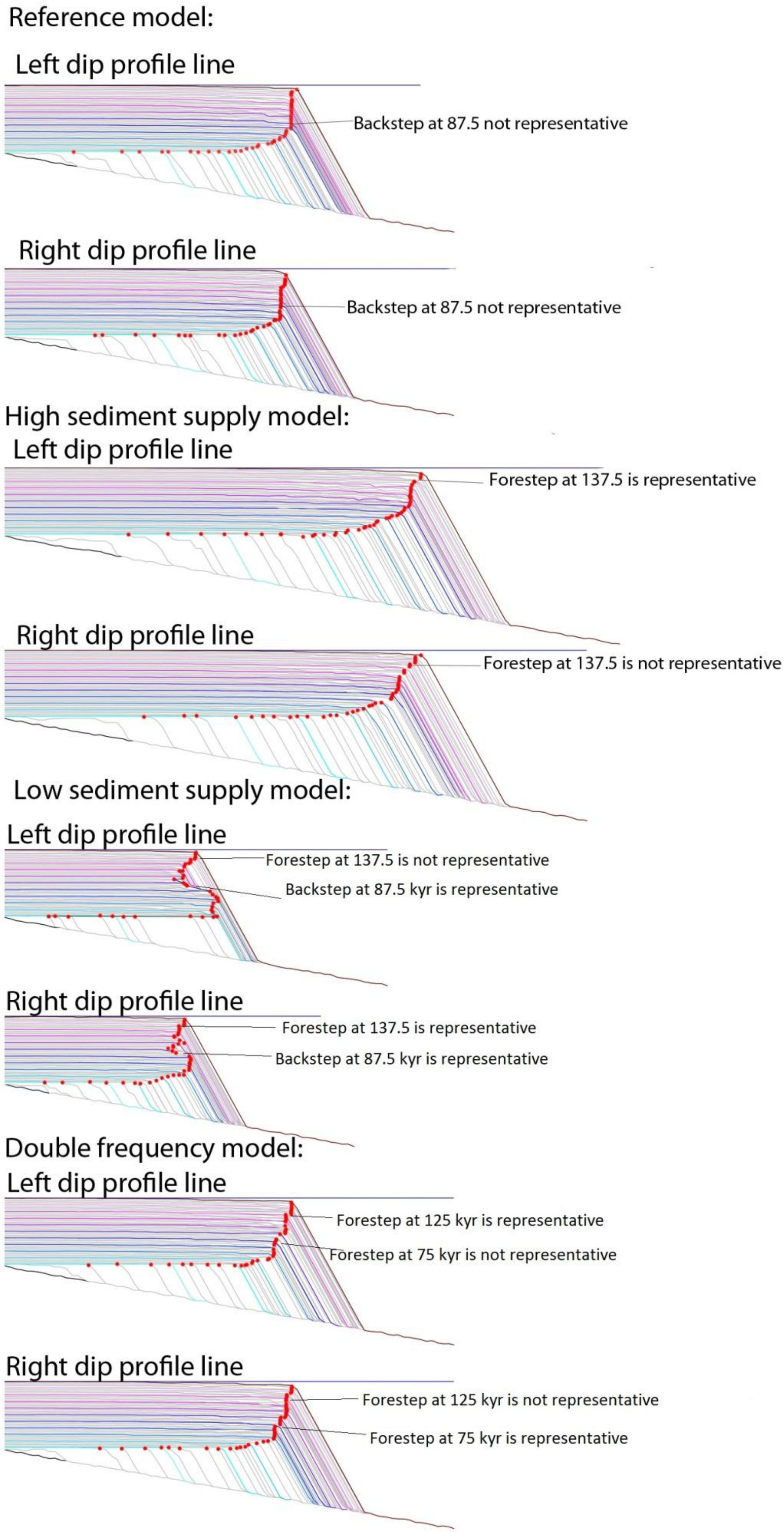

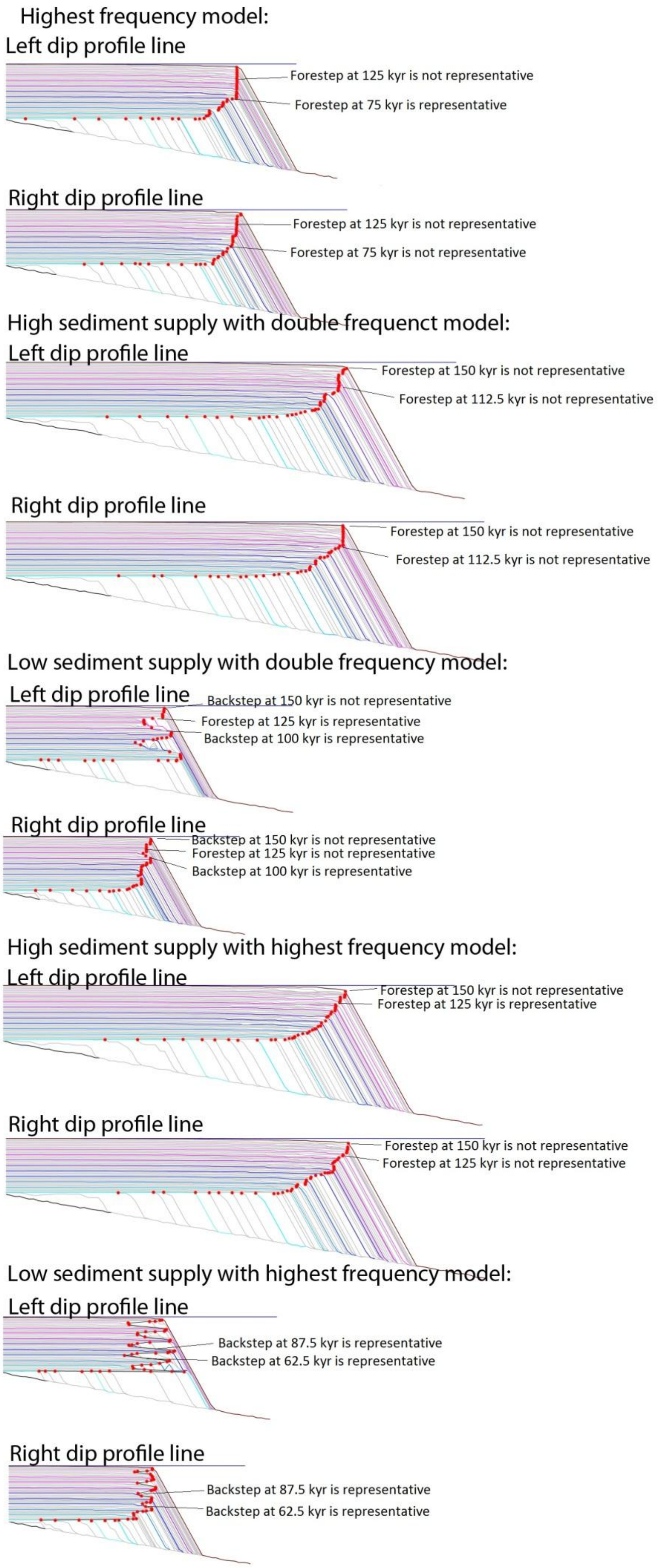

Fig. 55: Images of the right and left dip profile line for the models in chapter four. These show an overview about the different pulses of progradation / retrogradation in main dip line profile is representative of the entire delta.